2015-04-15

Yeast Upf1 Associates With RibosomesTranslating mRNA Coding Sequences Upstream of Normal Termination Codons: A Dissertation

Ei Ei Min
University of Massachusetts Medical School

YEAST Upf1 ASSOCIATES WITH RIBOSOMES TRANSLATING mRNA CODING SEQUENCES UPSTREAM OF NORMAL TERMINATION CODONS

A Dissertation Presented By

Ei Ei Min

The signatures of the Dissertation Committee signify completion and approval as to style and content of the Dissertation.

_____

Allan Jacobson, Ph.D., Thesis Advisor

_____

David Bedwell, Ph.D., Member of Committee

_____

Andrei Korostelev, Ph.D., Member of Committee

_____

Dannel McCollum, Ph.D., Member of Committee

_____

Sean Ryder, Ph.D., Member of Committee

The signature of the Chair of the Committee signifies that the written dissertation meets the requirements of the Dissertation Committee.

_____

Melissa Moore, Ph.D., Chair of Committee

The signature of the Dean of the Graduate School of Biomedical Sciences signifies that the student has met all graduation requirements of the School.

_____

Anthony Carruthers, Ph.D.,

Dean of the Graduate School of Biomedical Sciences

Interdisciplinary Graduate Program

April 15, 2015

Dedication

I would like to dedicate my thesis to my dearest parents

(U Min Din and Daw Than Than Yee).

Acknowledgements

I would like to take this opportunity to thank people who gave me different kinds of support during my time in graduate school.

First, I would like to thank my advisor, Allan, for his continuous support and advice, and most of all, giving me the opportunity to perform exciting research projects at his lab. I have learned so much from him how to do science as well as non-science (or nonsense). I will always be grateful for his support and generosity.

I would like to acknowledge the critical impact that my committee members (Melissa, Sean, Andrei, Dan and Craig) have had on my progress in the Ph.D program here at UMass. I would like to specially thank Melissa for her advice and helpful criticism. I would not have reached this point without your help. I would also like to offer thanks to David Bedwell who served as my outside committee member, and who has increased my understanding of my thesis work.

I would also like to thank previous and current members of the Jacobson Laboratory (Feng, Nadia, Marcus, Shuby, Bijoyita, Phyllis, Deb, Dave, Robin, and Alper). Their expertise, suggestions and kindness have been crucial for my accomplishments from the beginning to the end of my Ph.D journey. Especially Bijoyita for being a great colleague and friend.

I would like to thank my dear friends (Sneha, Kanti, Astha, Neesha, Ritu, and Hewan), who have made my time outside lab fun and exciting. Especially Sneha, who is my classmate and best friend, and we have gone through together many ups and downs during our years at UMass.

Finally, I would like to thank my family who have been with me at every step of the way, and has been my greatest supporter. I feel most fortunate to have them in my life. My parents (U Min Din and Daw Than Than Yee) for their unending love and support for whatever I choose to do in life. My baby sisters (Nilar Min and Poe Ei Min) who have been an inspiration for my goals. My husband, Kaung Zin Htoo, for his support and understanding my passion and goals.

Abstract

Nonsense-mediated mRNA decay (NMD) specifically targets mRNAs with premature translation termination codons for rapid degradation. NMD is a highly conserved translation-dependent mRNA decay pathway, and its core Upf factors are thought to be recruited to prematurely terminating mRNP complexes, possibly through the release factors that orchestrate translation termination. Upf1 is the central regulator of NMD and recent studies have challenged the notion that this protein is specifically targeted to aberrant, nonsense-containing mRNAs. Rather, it has been proposed that Upf1 binds to most mRNAs in a translation-independent manner. In this thesis, I investigated the nature of Upf1 association with its substrates in the yeast *Saccharomyces cerevisiae*. Using biochemical and genetic approaches, the basis for Upf1 interaction with ribosomes was evaluated to determine the specificity of Upf1 association with ribosomes, and the extent to which such binding is dependent on prior association of Upf1's interacting partners. I discovered that Upf1 is specifically associated with Rps26 of the 40S ribosomal subunit, and that this association requires the N-terminal Upf1 CH domain. In addition, using selective ribosome profiling, I investigated when during translation Upf1 associates with ribosomes and showed that Upf1 binding was not limited to polyribosomes that were engaged in translating NMD substrate mRNAs. Rather, Upf1 associated with translating ribosomes on most mRNAs, binding preferentially as ribosomes approached the 3' ends of open reading frames. Collectively, these studies provide new mechanistic insights into NMD and the dynamics of Upf1 during translation.

Table of Contents

List of Tables

List of Figures

List of Abbreviations

mRNA	Messenger RNA
NMD	Nonsense-mediated mRNA decay
PTC	Premature termination codon
UPF	Up-frameshift
Pab	Poly(A) binding protein
ORF	Open reading frame
uORF	Upstream open reading frame
eRF 1 and 3	Eukaryotic release factor 1 and 3
eIF3, eIF4G, eIF4AIII	Eukaryotic translation initiation factors
EJC	Exon junction complex
UTR	Untranslated region
SMG	Suppressor with morphological effect on genitalia
Rps	Small ribosomal protein
Rpl	Large ribosome protein
RRP	Relative Ribosome Position

Preface

Copyright information

Results presented in Chapter II has appeared in the publication below:

Min E*, Roy B*, Amrani N, He F, and Jacobson A. (2013). (**Co-first authors*) Yeast Upf1 CH domain interacts with Rps26 of the 40s ribosomal subunit. RNA**19**:1005-15.

List of Third Party Copyrighted Material

Declaration of figure/table contributions by co-authors on publications listed in the previous section:

Chapter II

Figure 2.1 was contributed by Nadia Amrani

Figure 2.7, 2.8, 2.9, and 2.10 were contributed by Bijoyita Roy

CHAPTER 1

General Introduction

Introduction

Nonsense-mediated mRNA decay is a translation-dependent post-transcriptional regulator of gene expression

Gene expression involves the transfer of information from DNA through messenger RNA (mRNA) to protein. It is a highly accurate and well-controlled process, allowing approximately one incorrect amino acid per 10,000 inserted (Kurland, 1992; Zaher and Green, 2009). Not surprisingly, the accuracy of gene expression is regulated by several quality control mechanisms operating at multiple steps of the process. Three translation-coupled mRNA surveillance pathways that check the fidelity of the translation process and degrade defective cytoplasmic mRNAs have been identified in eukaryotes. Non-stop decay (NSD) targets mRNAs lacking a termination codon; no-go decay (NGD) acts on mRNAs containing ribosome-stalling elements; and nonsense-mediated decay (NMD), the subject of this thesis, recognizes and degrades mRNAs harboring a premature translation termination codon (PTC) (Kervestin and Jacobson, 2012; Lykke-Andersen and Bennett, 2014; Shoemaker and Green, 2012).

The accelerated degradation of mRNAs derived from genes harboring nonsense mutations was first recognized with *URA3* transcripts of *Saccharomyces cerevisiae* (Losson and Lacroute, 1979). Related studies in human cells revealed that transcripts of β-globin nonsense alleles had reduced abundance (Chang and Kan, 1979; Maquat et al., 1981). Comparable phenomena were later observed in other eukaryotic organisms (Belgrader and

Maquat, 1994; Chang et al., 2007; Gatfield et al., 2003; Stalder and Muhlemann, 2008; Wittkopp et al., 2009; Yoine et al., 2006).

NMD is translation-dependent, with nonsense codon recognition by the translation apparatus required for triggering the degradation of substrate mRNAs (Kervestin and Jacobson, 2012). Consistent with this notion, interference with any step of translation abrogates NMD and causes stabilization of PTC-containing transcripts. Such effectors include suppressor tRNAs that antagonize termination and antibiotics such as anisomycin, cycloheximide, and puromycin, which inhibit translation by distinct mechanisms (Belgrader et al., 1993; Gozalbo and Hohmann, 1990; Losson and Lacroute, 1979).

Since approximately 15-20% of all known mutations causing inherited disorders result from nonsense mutations (Mort et al., 2008), NMD is of substantial clinical significance and general biological importance (Linde and Kerem, 2008). The synthesis of C-terminally truncated proteins encoded by PTC-containing mRNAs is markedly reduced in cells because NMD reduces mRNA abundance, frequently resulting in haploinsufficiency phenotypes. Potential therapeutic approaches to diseases caused by nonsense mutations have been investigated in cells, animal models, and human clinical trials, with most efforts focused on restoring function for a variety of different nonsense-containing mRNAs by promoting nonsense codon readthrough (Keeling et al., 2014; Peltz et al., 2013).

NMD has a post-transcriptional regulatory function in gene expression beyond mRNA surveillance. In addition to its role in degrading aberrant

transcripts, NMD also regulates many normal mRNAs encoding functional full-length proteins. Accordingly, NMD function is linked to diverse biological processes, such as embryonic development and differentiation (Bruno et al., 2011; Gong et al., 2009; Wittkopp et al., 2009), cell proliferation (Lou et al., 2014; Weischenfeldt et al., 2008), and cellular immunity (Balistreri et al., 2014; Gloggnitzer et al., 2014; Riehs-Kearnan et al., 2012). NMD components are not essential for viability in *S. cerevisiae* (Jacobson and Peltz, 1996), whereas deletion or mutation of NMD factors causes defects in larval development in *D. melanogaster* (Metzstein and Krasnow, 2006), brain development in *D. rerio* (Wittkopp et al., 2009), pleiotropic effects in *A. thaliana* (Yoine et al., 2006), and embryonic lethality in *M. musculus* (Medghalchi et al., 2001).

Characterization of factors involved in controlling NMD

Genes encoding factors that regulate NMD were identified in genetic screens in the yeast *S. cerevisiae* and the worm *C. elegans.* (Cui et al., 1996; Culbertson et al., 1980; He and Jacobson, 1995; Lee and Culbertson, 1995; Leeds et al., 1991; Peltz et al., 1993b). The worm genes *SMG2*, *SMG3*, and *SMG4* (Smg=suppressor with morphognetic effect on genitalia) are orthologues of yeast *UPF1, UPF2,* and *UPF3,* respectively, and these genes encode the three core factors of the NMD pathway (Hodgkin et al., 1989; Pulak and Anderson, 1993). Inactivation of these highly conserved genes stabilizes nonsense-containing mRNAs while having no significant effects on the

abundance and stability of most wild-type transcripts (Leeds et al., 1991; Peltz et al., 1993b; Yun and Sherman, 1995)

Among the Upf factors, Upf1 is the most conserved protein (amino acid sequence identities for Upf proteins between human and yeast are 48.5%, 20.8%, and 16.8% for Upf1, Upf2, and Upf3, respectively) (Culbertson and Leeds, 2003). Upf1 belongs to helicase superfamily I (SF1) with two RecA-like domains in tandem at its C-terminus and a cysteine- and histidine-rich Zn^{2+}-finger domain (CH domain) at N-terminus (Chakrabarti et al., 2011; Clerici et al., 2009; Leeds et al., 1992). Purified Upf1 has ATP- and RNA- binding activities, and possesses RNA-dependent ATPase and RNA helicase activities (Bhattacharya et al., 2000; Czaplinski et al., 1995). Upf1's ATP-binding and hydrolysis activities are required for NMD activity, as mutations eliminating these activities inhibit NMD (Weng et al., 1996, 1998). Upf2 is an acidic protein with multiple MIF4G domains (structures comparable to the middle domain of eukaryotic initiation factor eIF4G) in its N-terminal two-thirds (Clerici et al., 2014; Kadlec et al., 2004; Ponting, 2000). Upf3, a basic protein with an RNP-type RNA binding domain (RBD), (Bhattacharay et al., 2000, He et al., 1996; He et al., 1997). Upf1 and Upf2 are predominantly cytoplasmic whereas Upf3 is a nucleo-cytoplasmic shuttling protein (Kim et al., 2001; Lykke-Andersen et al., 2000; Serin et al., 2001). Upf factors were shown to interact with each other from biochemical and yeast two-hybrid studies (Clerici et al., 2009; He et al., 1996) (Figure 1.1). The CH domain of Upf1 interacts with a C-terminal domain of Upf2

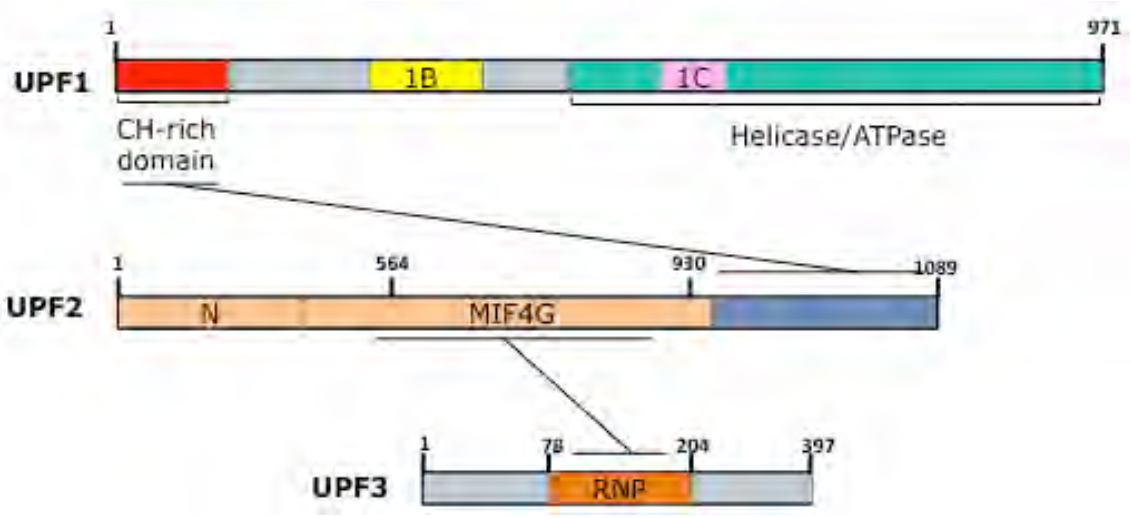

Figure 1.1 – Upf proteins interact with each other.

Amino acid numbering defines the interaction domains and the size of individual proteins in yeast.

CH = cysteine- and histidine-rich zinc-finger domain

1B, 1C = additional regulatory domains

MIF4G = middle portion of eIF4G

RNP = putative ribonucleoprotein domain

(Clerici et al., 2009; He et al., 1996). In turn, a MIF4G domain in the most C-terminal of Upf2 binds to the RBD of Upf3 (Kadlec et al., 2004; Serin et al., 2001). A recent crystal structure (Kadlec et al., 2004) of the complex between the human Upf2 and Upf3b proteins demonstrates that the complex, as well as hUpf2 alone, has RNA-binding activity, whereas the RBD domain of hUpf3b has no intrinsic RNA binding activity, but that domain is involved in binding to hUpf2. Overexpression of Upf1 can compensate for mutations in Upf2 and Upf3, but not *vice versa* (Maderazo et al., 2000), and the maximal *in vitro* activation of the Upf1 ATPase and helicase activities requires both Upf2 and Upf3 (Chamieh et al., 2008). These observations implied that Upf1 is the key effector of NMD, whereas Upf2 and Upf3 are likely to be regulators of Upf1 function. Structural studies showed that Upf1 exists in a closed conformation in which the CH domain interacts with its helicase domain, resulting in an increase in RNA binding and a decrease in ATPase and helicase activities. Upon Upf2 binding, the structure of Upf1 is rearranged to an open conformation, thereby alleviating the inhibitory effect of the CH domain on ATP hydrolysis and RNA unwinding capability (Chakrabarti et al., 2011; Chamieh et al., 2008).

In addition to its core Upf proteins, NMD in higher eukaryotes involves additional Smg factors (Kervestin and Jacobson, 2012; Schweingruber et al., 2013). Smg factors regulate phosphorylation/dephosphorylation cycles of multiple serine or threonine [S/TQ] residues in the N- and C-terminal regions of metazoan Upf1 (Grimson et al., 2004; Ohnishi et al., 2003a; Okada-Katsuhata et al., 2012; Yamashita et al., 2001). Upf1 is phosphorylated by Smg-1, a

phosphatidylinositol 3-kinase-related kinase (Yamashita et al., 2001). Phosphorylated-Upf1 creates two independent binding sites for Smg5, Smg6, and Smg7. Smg-6, a PIN (PilT N-Terminus) domain endonuclease, binds to the N-terminal region of phosphorylated Upf1 (Chakrabarti et al., 2014; Glavan et al., 2006; Okada-Katsuhata et al., 2012). Smg5 and Smg7 bind phosphorylated residues in the C-terminus of Upf1 as a heterodimer (Chakrabarti et al., 2014; Okada-Katsuhata et al., 2012), and the resulting Smg5-Smg7 complex dephosphorylates Upf1 through Smg5 interaction with the structural and catalytic subunits of the PP2A phosphatase (Ohnishi et al., 2003b; Page et al., 1999; Yamashita, 2013). Regulation of the phosphorylation/dephosphorylation state of Upf1 is important for NMD function in metazoans. Deletion or mutation of the *SMG5*, *6*, or *7* genes inhibits NMD and leads to accumulation of phosphorylated Upf1 (Kashima et al., 2006; Page et al., 1999; Paillusson et al., 2005; Pulak and Anderson, 1993). Upf1 phosphorylation is also observed in yeast cells (Lasalde et al., 2014; Wang et al., 2006). However, there are no apparent Smg1 and Smg5-Smg7 orthologs in *S. cerevisiase,* and no direct evidence that Upf1 phosphorylation regulates NMD in yeast (Lasalde et al., 2014; Wang et al., 2006).

Other interacting partners of Upf proteins include the release factors eRF1 and eRF3 and the exon-junction complex (EJC), a dynamic structure deposited by spliceosomes 20-24 nucleotides upstream of exon-exon junctions during splicing. The EJC core complex is formed by eIF4AIII, Y14, MAGOH, and MLN51 (Bono and Gehring, 2011). The C-terminal domain of Upf3 binds to a composite

surface formed by eIF4AIII, Y14, and MAGOH (Buchwald et al., 2010; Gehring et al., 2003). Upf1 interacts with eRF1 and eRF3 (Czaplinski et al., 1998; Ivanov et al., 2008; Kashima et al., 2006) and in human cells this leads to assembly of the Smg1-Upf1-eRF1-eRF3 (SURF) complex on the ribosome (Kashima et al., 2006; Yamashita et al., 2009).

Multiple classes of transcripts are endogenous substrates of NMD

Gene expression studies employing microarray analysis or RNA-Seq with mRNAs of yeast, fly, or human cells showed that 3–10% of cellular transcripts (including both PTC-containing and apparently wild-type transcripts) are up-regulated upon NMD inactivation (Guan et al., 2006; He et al., 2003; Lelivelt and Culbertson, 1999; Mendell et al., 2004; Ramani et al., 2009; Tani et al., 2012; Wittmann et al., 2006; Yepiskoposyan et al., 2011). These transcripts include: (i) PTC-containing mRNAs generated from genomic mutations (He et al., 2003), (ii) inefficiently spliced pre-mRNAs that enter the cytoplasm with intact introns (He et al., 1993), (iii) mRNAs that contain upstream open reading frames (uORFs) (Arribere and Gilbert, 2013; Gaba et al., 2005; He et al., 2003; Nyiko et al., 2009; Vilela et al., 1999), (iv) mRNAs in which the ribosome has bypassed the initiator AUG codon and commenced translation in an alternative reading frame (Welch and Jacobson, 1999), (v) transcripts of pseudogenes (He et al., 2003; McGlincy and Smith, 2008), (vi) transcripts with abnormally long 3´-UTRs (Das et al., 2000; Kebaara and Atkin, 2009; Kertesz et al., 2006; Muhlrad and Parker, 1999a; Pulak and Anderson, 1993), (vii) mRNAs that are subject to frameshifting (He et al.,

2003), (viii) unproductively spliced transcripts (Ge and Porse, 2014; Lykke-Andersen et al., 2014; Weischenfeldt et al., 2012), and (ix) non-coding RNAs (ncRNAs) (Kurihara et al., 2009; Lykke-Andersen et al., 2014; Tani et al., 2013).

Despite extensive identification of transcripts targeted by NMD, our understanding of the mechanism of NMD on substrate selection is very limited. A common feature in most of the endogenous transcripts susceptible to NMD is the occurrence of aberrant translation termination events, such as premature translation termination or a termination event that is not equivalent to normal termination (Kervestin and Jacobson, 2012; Schweingruber et al., 2013). To understand the mechanism of NMD, it is important to identify the unique molecular features or events that distinguish premature termination from normal termination.

Mechanistic differences between premature and normal termination

Translation termination entails binding of the release factors eRF1 and eRF3 to the ribosomal A-site upon in response to the presence of a stop codon (UAA, UAG, or UGA) (Alkalaeva et al., 2006; Jackson et al., 2012). eRF1 recognizes stop codons and its conserved Gly-Gly-GLn motif activates the peptidyl transferase center of the ribosome to mediate peptide release (Cheng et al., 2009; Song et al., 2000). eRF3 is a GTPase whose activity is stimulated by ribosome-bound eRF1 and it links eRF1 recognition of stop codons to hydrolysis of the polypeptide chain (Frolova et al., 1996; Salas-Marco and Bedwell, 2004). After peptide release, eRF3 is dissociated from the ribosome and eRF1 recruits

the ribosome-recycling factor ABCE1 (the ATP-binding cassette protein) (Barthelme et al., 2011; Becker et al., 2012; Pisarev et al., 2010). Dissociation and recycling of ribosomal subunits is triggered by ABCE1 and the translation initiation factors eIF3, eIF1, eIF1A, and eIF3j (Becker et al., 2012; Khoshnevis et al., 2010; Pisarev et al., 2007a; Pisarev et al., 2010). Other factors, including poly(A)-binding protein (Pab1) have been shown to have possible roles in translation termination (Cosson et al., 2002; Hoshino et al., 1999; Ivanov et al., 2008). Pab1 may promote the formation of an mRNP complex favorable to normal translation termination (Amrani et al., 2006b; Fatscher et al., 2014; Hilleren and Parker, 1999).

Premature termination appears to be mechanistically different from normal termination. Toeprint analyses of the position of ribosomes on mRNA failed to detect any toeprinting signals from ribosomes at normal stop codons in *S. cerevisiase* cell extracts unless translation termination was compromised by inactivation of eRF1 function with a temperature-sensitive mutation. By contrast, ribosomes at premature termination codons (PTCs) yielded toeprinting signals consistent with A-site occupancy without eRF1 inactivation (Amrani et al., 2004). Similarly, human β-globin mRNA with a nonsense mutation at codon 39 was found to yield a toeprint signal for prematurely terminating ribosomes, whereas the normal β-globin mRNA failed to manifest a toeprint at its normal termination codon (NTC) (Peixeiro et al., 2012). These data indicate that translation termination at NMD-inducing premature stop codons is less efficient than normal termination, and may cause pausing of ribosomes at PTCs. Additional evidence

for mechanistic differences between premature and normal termination has been drawn from experiments addressing nonsense suppression (or nonsense codon readthrough). Although nonsense suppression can occur at some NTCs (Dunn et al., 2013; Goodenough et al., 2014), it occurs more frequently at PTCs (Keeling et al., 2014; Peltz et al., 2013; Welch et al., 2007), with the basal level of readthrough occurring at a frequency of <0.1% at normal stop codons and <1% at premature stop codons (Keeling et al., 2014). Collectively, these results suggest that although both premature and normal translation termination begin when a stop codon occupies the ribosomal A-site, subsequent steps at the respective termination events appear to be mechanistically different.

Activation of NMD and associated events

Upf1 promotes the rapid decay of nonsense-containing mRNAs by interacting with components of general mRNA degradation pathways. In yeast cells, NMD-targeted mRNAs are degraded predominantly through accelerated decapping, followed by Xrn1-mediated 5'-3′ decay or by exosome-mediated 3'-5' decay (He and Jacobson, 2001; Muhlrad et al., 1994). In yeast and human cells, Upf1 interacts with the decapping enzyme Dcp2 (He and Jacobson, 1995; Loh et al., 2013; Unterholzner and Izaurralde, 2004). Such association probably takes place while the mRNAs are still associated with polyribosomes because Upf1 co-sediments with polyribosomes in yeast (Atkin et al., 1995), and phosphorylated hUpf1 is mainly present in the polysome fraction in mammalian cells (Pal et al., 2001). Moreover, in yeast, decapped nonsense-containing mRNAs are

associated with polyribosomes (Hu et al., 2010). In higher eukaryotes, rapid decay of nonsense-containing mRNA can be initiated by both endonucleolytic and exonucleolytic decay pathways by virtue of interactions between phosphorylated Upf1 with either Smg6 or the Smg5-Smg7 complex. The Smg6 endonuclease activity cleaves NMD-targeted mRNAs in the vicinity of PTCs and the resulting 5' and 3' fragments are subsequent degraded by the exosome and Xrn1, respectively (Eberle et al., 2009; Huntzinger et al., 2008; Lykke-Andersen et al., 2014; Schmidt et al., 2014). The Smg5-Smg7 heterodimer also recruits the CCR4-NOT deadenylase to NMD substrates by interaction with Pop2, and decay intermediates are subjected to decapping and to 5'-3' degradation by Xrn1 (Loh et al., 2013; Unterholzner and Izaurralde, 2004).

Upf1 functions not only in activating rapid decay of NMD-targeted mRNAs, but also in other related processes that accompany recognition of a PTC. These events include degradation of the nascent polypeptide, translational repression of the mRNA, and disassembly of the prematurely terminating mRNP complex and recycling of the components of the translation apparatus (Kervestin and Jacobson, 2012). In yeast, Upf1 functions in the degradation of nascent polypeptides encoded by PTC-containing mRNAs by promoting the ubiquitin-mediated proteasomal degradation of the C-terminally truncated polypeptides (Kuroha et al., 2009; Takahashi et al., 2008). Upf1 might play a role as an E3 ubiquitin ligase because the Upf1 N-terminal CH domain is similar to E3 RING finger domains, and directly interacts with the E2 component Ubc3. Upf1 can

also self-ubiquitinate *in vitro* in a Upf3-dependent manner (Takahashi et al., 2008).

Nonsense-containing mRNAs are thought to be translationally repressed before their degradation. Upf1 association with a nonsense-containing mRNA leads to decreased translation efficiency (Isken et al., 2008; Muhlrad and Parker, 1999b) and Upf1 appears to target nonsense-containing mRNAs to cytosolic P-bodies, which are cytoplasmic foci that are enriched in decapping enzymes and the 5'- to 3' degradation machinery (Durand et al., 2007; Fillman and Lykke-Andersen, 2005; Sheth and Parker, 2006; Stalder and Muhlemann, 2009). In mammalian cells, phosphorylated Upf1 interacts with eIF3 of the 43S pre-initiation complex at the initiation codon of an NMD target and interferes with 60S ribosomal subunit joining, thereby repressing translation (Isken et al., 2008)

In addition to promoting accelerated mRNA decay, the Upf1 ATPase and helicase activities appear to have a role in disassembling an otherwise poorly dissociable ribosome and mRNP complex subsequent to peptide hydrolysis (Kervestin and Jacobson, 2012). For example, in human cells expressing ATPase-deficient Upf1, endonucleolytically cleaved and partially degraded nonsense-containing β-globin mRNA accumulates (Franks et al., 2010) and, in yeast: (i) translational reinitiation after premature termination is markedly reduced *in vivo* or *in vitro* when any one of the three yeast Upf proteins is absent (Amrani et al., 2004; Ghosh et al., 2010) and (ii) extracts from yeast lacking Upf1 manifest a ribosome recycling defect that can be complemented by purified Upf1 (Ghosh et al., 2010).

Current models for NMD activation by premature termination

Three prevalent models have been proposed to explain the mechanism of NMD activation. All three models take into account Upf factor association in an abnormal mRNP environment ((Kervestin and Jacobson, 2012) ; Figure 1.2).

The *faux* UTR model conceives that the 3'-UTR created by a PTC is deficient in termination regulatory factors that are normally present on an authentic 3'-UTR (Amrani et al., 2004; Amrani et al., 2006b; Kervestin and Jacobson, 2012). In this model, proper termination of translation is postulated to depend on effective interactions between termination release factors and proteins bound to the "normal" 3'-UTR. By contrast, the abnormal context of a *faux* UTR created by a PTC is thought to favor the recruitment of the Upf proteins to the prematurely terminating ribosome, most likely due to the absence of proximal interaction between eRF3 and Pab1 (Kervestin and Jacobson, 2012). Consistent with this model, bringing the normal 3'-UTR in close spatial proximity to the PTC by deleting the coding region downstream of a PTC or by folding the poly(A) tail back to the vicinity of the PTC suppresses NMD (Buhler et al., 2006; Eberle et al., 2008; Hagan et al., 1995; Peltz et al., 1993a). In addition, mimicking normal termination by artificial tethering of factors such as eRF3 or Pab1 rescues NMD substrates from rapid degradation (Amrani et al., 2004; Behm-Ansmant et al., 2007; Eberle et al., 2008; Fatscher et al., 2014; Joncourt et al., 2014). However, the *faux* UTR model is questioned by studies reporting that mRNAs that contain PTCs and lack poly(A) tails are still subject to NMD, and yeast cells

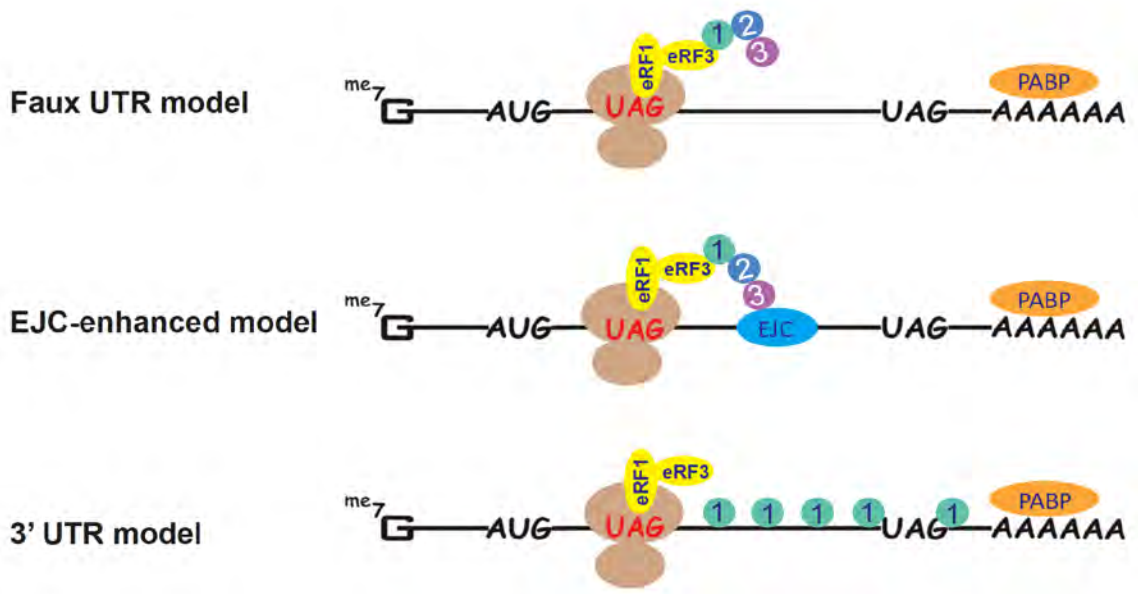

Figure 1.2 – Current models for NMD activation by premature termination.

The *faux* UTR model takes into account the lack of proximity between the premature stop codon and the poly(A) tail, which in turn disrupts interaction between eRF3 and PABP and creates an abnormal translation termination context.

The EJC-enhanced model requires EJC factors to bridge Upf1 bound by the termination factors and Upf2 and Upf3 associated with an EJC.

The 3′ UTR model postulates that the extended length of the 3-′ UTR formed between the premature stop codon and the poly(A) tail creates a binding platform for Upf1.

Shaded brown ovals = ribosomal subunits; Black line = mRNA; 1,2, and 3 represent Upf1, Upf2, and Upf3 respectively.

lacking Pab1 can still elicit degradation of NMD-targeted mRNAs (Meaux et al., 2008).

The EJC-enhanced model proposes that NMD in metazoans depends on the presence of an exon-junction complex (EJC) 3' to a PTC (Isken and Maquat, 2007; Nagy and Maquat, 1998; Zhang et al., 1998). In this model, elongating ribosomes strip off the EJCs or any other RNA-binding proteins located within the open reading frame of transcripts during normal translation. However, if translation terminates prematurely, the EJC downstream of a terminating ribosome serves as an anchoring point for the assembly of an NMD complex, thereby enhancing NMD (Kervestin and Jacobson, 2012; Lejeune and Maquat, 2005). In support of this model, tethering one of the EJC components to the 3′-UTR of mRNAs triggers NMD (Gehring et al., 2005; Gehring et al., 2003; Lykke-Andersen et al., 2001) and deletion of the ECJ core proteins (Y14, eIF4A3 or Barentsz/MLN51) selectively stabilizes the PTC-containing mRNAs (Ferraiuolo et al., 2004; Gehring et al., 2003; Palacios et al., 2004; Shibuya et al., 2004). However, the EJC-enhanced model fails to explain how NMD targets mRNAs derived from intron-less precursors or mRNAs that have not undergone proper splicing (Kertesz et al., 2006; LeBlanc and Beemon, 2004; Quek and Beemon, 2014; Rajavel and Neufeld, 2001). This model is further complicated by recent reports demonstrating that approximately 20% of splicing events do not assemble EJCs on exon-exon junctions, and about 40-50% of the detected EJCs bind to non-canonical positions on mRNAs (Buchwald et al., 2010; Sauliere et al., 2012; Singh et al., 2012). Further, data indicating that EJCs stimulate translation

(Chazal et al., 2013; Ma et al., 2008; Nott et al., 2004) imply that the effect of EJCs on NMD may be indirect.

The 3′-UTR model, which is a variation of the *faux* UTR model, posits that 3'-UTR length is a major determinant for NMD activation. In general, long 3′-UTRs mimic the extended distance between the stop codon and Pab1 on poly(A) tails seen in premature translation termination. In this model, an abnormally long 3′-UTR, resulting from the presence of a PTC, provides a binding platform for RNA binding proteins like Upf1, which in turn can recruit Upf2/Upf3, thereby activating NMD. This model is supported by identification of long 3'-UTRs as a conserved NMD-inducing feature in yeast, flies, worms, plants, and mammals (Kebaara and Atkin, 2009; Kertesz et al., 2006; Longman et al., 2007; Muhlrad and Parker, 1999a; Pulak and Anderson, 1993; Schwartz et al., 2006; Yepiskoposyan et al., 2011). Additional support for this model came from recent studies demonstrating Upf1 binding to mRNA 3'-UTRs (Gregersen et al., 2014; Hurt et al., 2013; Zund et al., 2013) in what appears to be a length-dependent relationship (Hogg and Goff, 2010). However, a recent study from the Jacquier lab reported that a large number of transcripts that have long 3′-UTRs are not subject to NMD in *S. cerevisiae*. They showed that only mRNAs with short ORFs are subjected to NMD, whereas mRNAs with long open reading frames escape NMD despite the presence of long 3'-UTRs (Decourty et al., 2014).

NMD activation models suggest that PTC-mRNAs are distinguished from normal mRNAs by aberrant mRNP structures due to the presence of NMD-enhancing factors or abnormal distance between the PTC and the 3' end of

mRNA. However, each model has caveats and discrepancies with available data. In all three situations, the aberrant mRNP is thought to enhance Upf1 association with the eRFs and ribosomes, promoting subsequent binding of the Upf2-Upf3 complex to Upf1 and the activation of mRNA decay.

Upf1 recruitment to mRNP complexes

In the past 20 years, studies in multiple experimental models have sought to elucidate the mechanism of Upf1 targeting to prematurely terminating mRNPs. RNA immunoprecipitation (RIP) experiments showed that Upf1 preferentially associates with *bona fide* NMD substrates in yeast, worms, and mammalian cells (Decourty et al., 2014; Johansson et al., 2007; Johns et al., 2007; Kurosaki et al., 2014). Other studies in mammalian cells showed that Upf1 could bind to PTC-containing reporter mRNAs in a translation-dependent manner (Kurosaki and Maquat, 2013).

According to current NMD activation models, Upf1 is thought to be selectively recruited to NMD-targeted mRNAs during translation, most likely through interactions with the release factors eRF1 and eRF3 located on prematurely terminating ribosomes. Consistent with this notion, Upf1 interacts with the release factors and ribosomes (Czaplinski et al., 1998; Wang et al., 2001). In human cells, Upf1 associates with eRF-bound ribosomes forming the SURF (Smg-1-Upf1-Release Factors) complex, and a downstream EJC bound by Upf2 and Upf3 activates Upf1 function (Kashima et al., 2006; Yamashita et al., 2009). However, recent transcriptome-wide Upf1 binding studies suggested that

instead of binding directly to the ribosomes, Upf1 might occupy translationally active mRNAs, and then to be activated when a ribosome encounters a PTC. In mammalian cells, *in vivo* UV crosslinking and immunoprecipitation followed by high-throughput sequencing (CLIP-Seq) studies suggested promiscuous Upf1 binding to 3'-UTRs, i.e., Upf1 targets both NMD-sensitive and NMD-insensitive transcripts. Upon translation inhibition with puromycin or cycloheximide, the relative distribution of Upf1 was seen to shift to mRNA coding sequences (CDS) (Gregersen et al., 2014; Hurt et al., 2013). This led to the notion that, during normal translation, elongating ribosomes would displace Upf1 from the CDS, thereby restricting detectable Upf1 binding to 3'-UTRs (Gregersen et al., 2014; Hurt et al., 2013; Kurosaki and Maquat, 2013; Shigeoka et al., 2012). However, translation-dependent recruitment of Upf1 to mRNAs contradicts another study demonstrating translation-independent binding of Upf1 to 3'-UTRs (Hogg and Goff, 2010). By purifying tagged reporter mRNAs, Hogg and Goff demonstrated that Upf1 binding to mRNAs occurred in a 3'-UTR length-dependent manner, even when translation was inhibited. Translation-independent association of Upf1 with mRNA is difficult to reconcile with the requirement for ongoing translation as a trigger for NMD (Kervestin and Jacobson, 2012).

In conclusion, there is some uncertainty about the timing and specificity of Upf1 interaction with mRNPs. Some results indicate that mechanistic distinctions between premature and normal termination lead to preferential association of Upf1 with prematurely terminating mRNPs. Other data suggest that Upf1 associates with all translationally active mRNAs, possibly through ribosomes.

Clearly, we have yet to understand the step of translation during which Upf1 associates with ribosomes, and whether such association is limited to PTC-containing mRNAs or all translationally active mRNAs.

SPECIFIC AIMS FOR THIS THESIS:

The main objective of this thesis is to elucidate when and where during translation Upf1 targets mRNP complexes in the yeast *Saccharomyces cerevisiae*. The experiments and data have been organized into two chapters. Data in Chapter II addresses whether Upf1 binds directly to ribosomes and, if so, where. To pursue biochemical analyses, I optimized a ribosome purification system yielding intact rRNAs and proteins and sought to determine whether Upf factors co-purified with specific ribosomal subunits. These studies were complemented by genetic analyses of Upf1 interactors. In Chapter III, I determined the timing of Upf1 binding to translating ribosomes and assessed whether Upf1 is selectively recruited at prematurely terminating ribosomes. Selective ribosome profiling was utilized to determine whether mRNA footprints protected by Upf1-bound ribosomes reflected preferential Upf1 association with a subset of such footprints.

CHAPTER II

Upf1 CH domain interacts with Rps26 of the 40S ribosomal subunit

This work presented in this chapter has been published as:

Min E, Roy B, Amrani N, He F, and Jacobson A. (2013). Yeast Upf1 CH domain interacts with Rps26 of the 40s ribosomal subunit. RNA**19**:1005-15.

My contribution to this chapter: Figures 2.2, 2.3, 2.4, 2.5, 2.6

Summary

The central nonsense-mediated mRNA decay (NMD) regulator, Upf1, selectively targets nonsense-containing mRNAs for rapid degradation. In yeast, Upf1 preferentially associates with mRNAs that are NMD substrates, but the mechanism of its selective retention on these mRNAs has yet to be elucidated. Previously, we demonstrated that Upf1 associates with 40S ribosomal subunits. Here, we define more precisely the nature of this association using conventional and affinity-based purification of ribosomal subunits, and a two-hybrid screen to identify Upf1-interacting ribosomal proteins. Upf1 coimmunoprecipitates specifically with epitope-tagged 40S ribosomal subunits, and Upf1 association with high-salt washed or puromycin-released 40S subunits was found to occur without simultaneous eRF1, eRF3, Upf2, or Upf3 association. Two-hybrid analyses and in vitro binding assays identified a specific interaction between Upf1 and Rps26. Using mutations in domains of *UPF1* known to be crucial for its function, we found that Upf1:40S association is modulated by ATP, and Upf1:Rps26 interaction is dependent on the N-terminal Upf1 CH domain. The specific association of Upf1 with the 40S subunit is consistent with the notion that this RNA helicase not only triggers rapid decay of nonsense-containing mRNAs, but may also have an important role in dissociation of the premature termination complex.

Introduction

Nonsense-mediated mRNA decay (NMD), a cytoplasmic mRNA surveillance pathway, targets transcripts harboring a premature translation termination codon (PTC) or a termination codon in a context characteristic of premature termination (Jacobson and Izaurralde, 2007; Kervestin and Jacobson, 2012; Kervestin et al., 2012). In part, NMD ensures that the potentially toxic polypeptide products of its substrate mRNAs do not accumulate in the cell (Jacobson and Izaurralde, 2007; Kervestin and Jacobson, 2012; Kervestin et al., 2012). Factors that regulate NMD include Upf1, Upf2, and Upf3, the principal regulators in all eukaryotes, as well as Smg-1 and Smg-5 through -9, proteins that play additional regulatory roles in metazoans (Kervestin and Jacobson, 2012; Kervestin et al., 2012; Schoenberg and Maquat, 2012). The three Upf proteins form a complex with Upf2 acting as a bridge between Upf1 and Upf3 (Chamieh et al., 2008; He et al., 1997; Serin et al., 2001). Single or multiple deletions of the *UPF* genes have similar mRNA decay phenotypes, suggesting that these proteins function in a common pathway (He et al., 1997; He et al., 2003; Maderazo et al., 2000; Wang et al., 2001), albeit one that may be branched under some circumstances (Chan et al., 2007; Huang et al., 2011).

Upf1, the key effector of NMD, has a cysteine- and histidine-rich zinc-finger domain (CH domain) at its N-terminus and a helicase domain comprised of twelve conserved motifs common to the members of helicase superfamily I (SF1) (Fairman-Williams et al., 2010). Upf1 shows RNA-dependent ATPase and 5′-to-3′ RNA helicase activities, both of which while critical for NMD

(Czaplinski et al., 1998; Wang et al., 2001), have unresolved roles in the process. In yeast, ATPase-deficient Upf1 accumulates with NMD substrates in cytoplasmic processing bodies (Sheth and Parker, 2006) and, in human cells, ATPase- or helicase-deficient Upf1 leads to the accumulation of partially degraded 3′ decay intermediates (Franks et al., 2010). These reports, and others (Ghosh et al., 2010), suggest a role for Upf1 in disassembling post-termination mRNPs in a mechanism that requires its ATPase and helicase activities. Notably, the maximal activation of these activities is stimulated by a complex of Upf2 and Upf3 (Chakrabarti et al., 2011; Chamieh et al., 2008).

Numerous studies have shown that NMD is inhibited by drugs, mutations, or mRNA structures that inhibit translation (Jacobson and Izaurralde, 2007), or by suppressor tRNAs (Belgrader et al., 1993; Gozalbo and Hohmann, 1990; Losson and Lacroute, 1979), indicating that a premature stop codon must be recognized by translating ribosomes for NMD to occur. This conclusion is reinforced by experiments demonstrating a direct correlation between the extent of ribosome occupancy at a PTC and the degree to which NMD is activated (Gaba et al., 2005). Additional links between translation and NMD include the observations that decapping and degradation of nonsense-containing transcripts occur while the transcript is associated with polyribosomes (Hu et al., 2010; Mangus and Jacobson, 1999) and that the Upf factors colocalize with polyribosomes, 80S ribosomes, and ribosomal subunits (Atkin et al., 1995; Atkin et al., 1997; Ghosh et al., 2010; Mangus and Jacobson, 1999; Peltz et al., 1993a). Consistent with a dependence of NMD on translation termination, Upf1 interacts with the release

factors eRF1 and eRF3 in humans and yeast, possibly to function in termination events using its helicase and RNA binding activities (Czaplinski et al., 1998; Ghosh et al., 2010; Wang et al., 2001). In vertebrates, Upf1 and its regulator Smg-1 interact with the release factors forming the SURF (Smg-1-Upf1-Release factors) complex and this SURF-associated Upf1 appears to be able to interact with Upf2-Upf3 bound to the exon junction complex (Kashima et al., 2010; Yamashita et al., 2009).

While nonsense codon recognition by the ribosome, and Upf1 interaction with the release factors, are steps that are incorporated into most models of NMD (Kervestin and Jacobson, 2012) there is some uncertainty about the timing and specificity of Upf1 interaction with terminating mRNPs. Some models and some experimental results indicate that mechanistic distinctions between premature and normal termination lead to preferential association of Upf1 with mRNPs undergoing premature termination (Amrani et al., 2006a; Amrani et al., 2004; Buhler et al., 2006; Johansson et al., 2007; Kervestin and Jacobson, 2012; Kervestin et al., 2012). Other models, and other data, suggest that Upf1 associates with all terminating ribosomes and that specificity for premature termination events is achieved by subsequent Upf1 interactions with factors that could only remain mRNA-associated if termination had occurred upstream of its normal site (Le Hir et al., 2000; Peltz et al., 1993a; Sun and Maquat, 2000). Additional studies imply that specificity for hUpf1 is imparted by mRNA 3'-UTR length (Hogg and Goff, 2010). Here, we address the Upf1 localization problem by providing biochemical and genetic evidence for the association of Upf1 with

ribosomal subunits in the budding yeast *Saccharomyces cerevisiae*. First, we utilized independent approaches to confirm our earlier observations of Upf1 association with the 40S ribosomal subunit (Ghosh et al., 2010). Having confirmed such interactions, we then defined the domains of Upf1 on which they depend as well as a specific ribosomal protein with which Upf1 interacts.

Results

Upf1 binds to affinity-purified 40S ribosomal subunits

Our previous experiments demonstrated that yeast Upf1 associates with purified 40S ribosomal subunits (Ghosh et al., 2010). We have now explored this interaction further by testing whether Upf1 is retained by an alternative method of ribosome isolation, namely affinity purification. We constructed yeast strains harboring epitope-tagged Rps13 or Rpl25 (Table 2.1), which would be incorporated into 40S or 60S ribosomal subunits, respectively. These proteins were selected for modification based on their accessibility on the solvent side of the ribosome (Ben-Shem et al., 2011; Inada et al., 2002; Spahn et al., 2001). We inserted an HA tag at the C-terminus of Rps13 and a c-Myc tag at the C-terminus of Rpl25. The tags did not appear to disrupt the functions of the respective proteins since the tagged strains exhibited growth characteristics comparable to those of untagged strains in liquid YEPD culture at 25°C (Figure 2.1.A) or on multiple solid media at 25°C or 30°C (Figure 2.1.B).

Immunoprecipitations with antibodies targeting the HA or c-Myc epitopes showed efficient capture of the corresponding ribosomal protein from cell extracts (Figures 2.2.A and 2.2.B, compare lane 5 in top panels). Importantly, we found Upf1 to be present in these immunoprecipitates, but absent in immunoprecipitates from untagged strains (Figures 2.2.A and 2.2.B, bottom panels, compare lane 5 to lane 2). These results demonstrate that Upf1 is also associated with a ribosomal complex using extraction conditions that differ from those used in our original experiments (Ghosh et al., 2010). Cell-free extracts

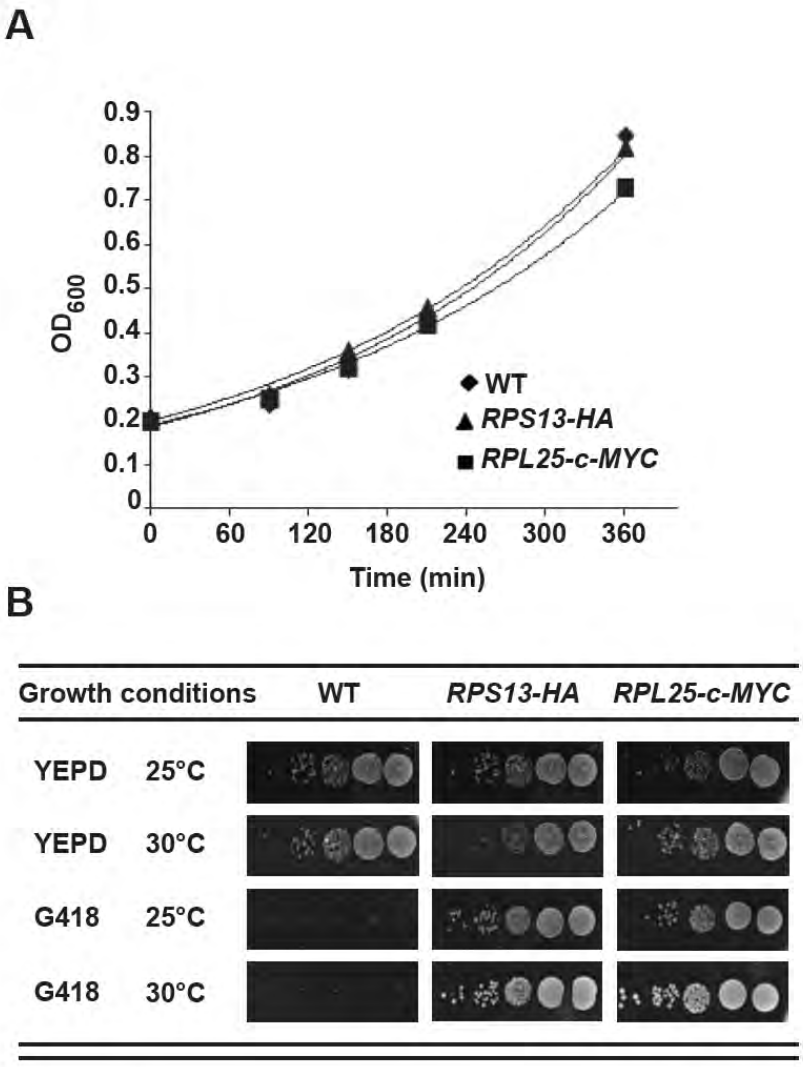

Figure 2.1 – Yeast strains harboring HA- or c-Myc-tagged *RPS13 or RPL25* genes grow at wild-type rates.

(A) Growth curves for yeast strains in liquid YPD medium at 25°C. Symbols: wild-type [WT] (♦), *RPS13-HA* (▲), and *RPL25-c-Myc* (■). (B) Liquid cultures of yeast strains WT, *RPS13-HA* and *RPL25-c-Myc* were serially diluted and incubated on YEPD plates, and plates containing G418, at the temperatures shown.

treated with puromycin to promote ribosome dissociation (Algire et al., 2002; Azzam and Algranati, 1973; Lawford, 1969) allowed for a test of the subunit-specific association of Upf1 (Figures 2.2.A and 2.2.B). Under these conditions, we observed significant enrichment of Upf1 in the HA-specific immunoprecipitates (targeting Rps13-HA) (Figure 2.2.A, bottom panel, lane 8), but not in the c-Myc-specific immunoprecipitates (targeting Rpl25-c-Myc) (Figure 2.2.B, bottom panel, lane 8). These results demonstrate that, in an independent assay, Upf1 still associates with 40S ribosomal subunits and not with 60S subunits.

To determine whether this association was mediated indirectly by Upf1 interaction with mRNA, cell lysates were treated with micrococcal nuclease prior to ribosome immunoprecipitation. These experiments showed significant retention of Upf1 in the immunoprecipitates (Figure 2.3, lane 6), implying that Upf1 is associated directly with ribosomes. The absence of poly(A)-binding protein (Pab1), a factor known to be associated with the mRNA 3' poly(A) tail (Sachs and Davis, 1989), in the immunoprecipitates further supported the idea that Upf1 is associated with ribosomes.

Upf1 association with 40S ribosomal subunits requires its ATPase activity, but not its ATP-binding or RNA-binding activities, or the functions of the other NMD factors

To further understand the basis of Upf1 association with 40S ribosomal subunits we employed domain-specific mutations to determine whether some of

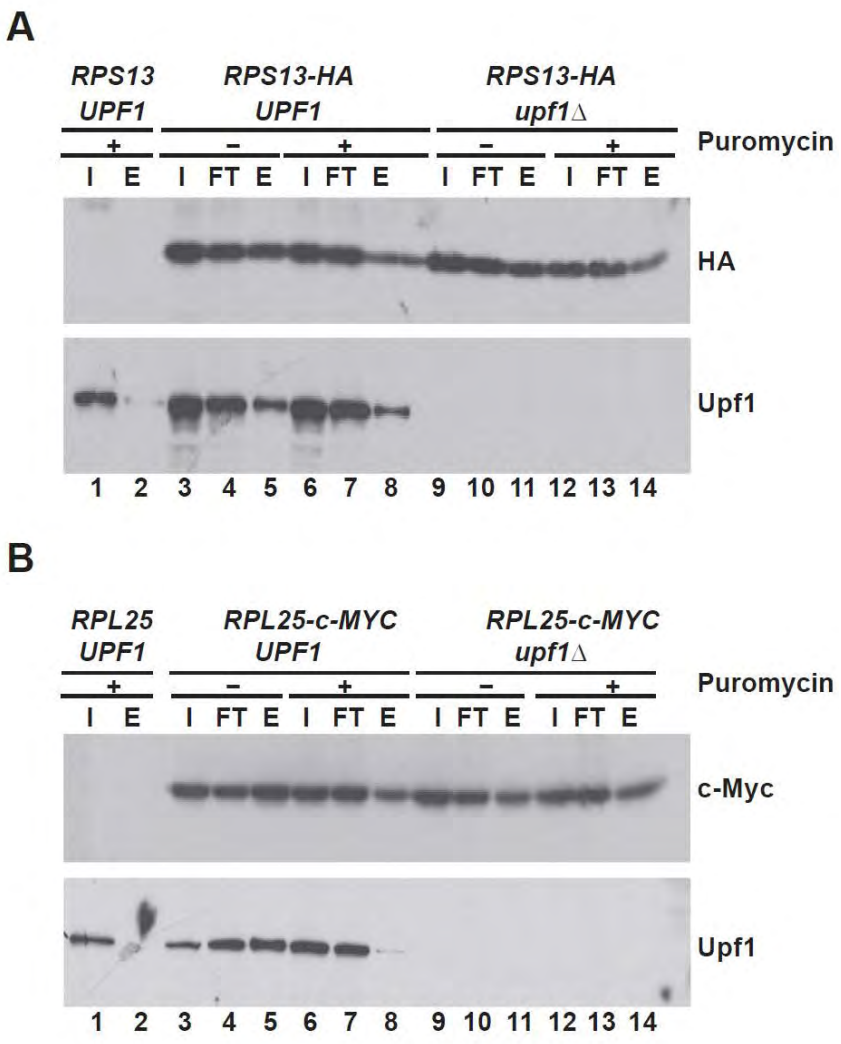

Figure 2.2 – Treatment with puromycin diminishes co-immunoprecipitation of Upf1 with Rpl25-c-Myc, but not with Rps13-HA.

Lysates from yeast WT, *RPS13-HA-WT, and RPS13-HA-upf1*Δ (A), and WT, *RPL25-c-MYC*-WT, and *RPL25-c-MYC-upf1*Δ (B) prepared with (+) or without (-) puromycin treatment were immunoprecipitated with anti-HA antibody or anti-c-Myc antibody, respectively. Input (I), flowthrough (FT), and eluate (E) were analyzed by western blotting for the presence of Rps13-HA, Rpl25-c-Myc, or Upf1 with specific antibodies. One-tenth of input and flowthrough samples were loaded for SDS-PAGE analysis.

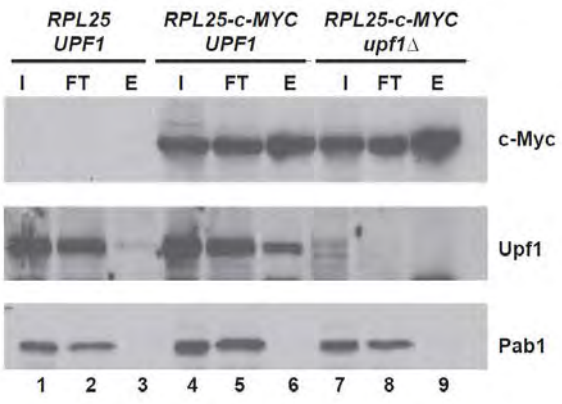

Figure 2.3 – Micrococcal nuclease treatment does not diminish co-immunoprecipitation of Upf1 with c-Myc-Rpl25.

Micrococcal nuclease-treated lysates from yeast WT, *RPL25-c-Myc-WT*, and *RPL25-c-Myc-upf1*Δ were immunoprecipitated with α-c-Myc antibodies. Input (I), flowthrough (FT), and eluate (E) were analyzed by western blotting for the presence of c-Myc-Rpl25, Upf1, or Pab1 with specific antibodies. One-tenth of input and flowthrough samples were loaded for SDS-PAGE analysis.

the biochemical activities known to be associated with those Upf1 domains might be required for this interaction. High-salt washed 40S and 60S ribosomal subunits were purified with or without prior puromycin release from cells harboring wild-type *UPF1,* or different *upf1* alleles (Figure 2.4.A), and tested for Upf1:40S association by western blotting. The concurrent retention of Rps6 in the purified ribosomal subunits served as a control for 40S subunit integrity and 60S subunit purification. As shown in Figure 2.4.B, neither the C62Y or C84S mutations in the N-terminal CH domain, nor the K436E or RR973AA mutations in the C-terminal helicase domain (that respectively inactivate ATP binding or RNA binding) had any significant effect on the association of Upf1 with high-salt washed 40S subunits prepared with or without puromycin-mediated release. In contrast, Upf1 derived from the *upf1* DE572AA ATP hydrolysis mutant failed to associate to any significant extent with 40S subunits even though Rps6 was amply recovered and Upf1 from the DE572AA mutant was expressed at levels comparable to wild-type Upf1 (Figure 2.4.C). Wild-type Upf1, analyzed in the same manner as the three mutant versions of the protein, retained its preference for 40S subunit association (Figure 2.4.B).

Additional insight into the determinants of Upf1 association with 40S subunits was obtained by evaluating whether the other two UPF proteins were required for this association. High-salt washed 40S and 60S ribosomal subunits were purified with or without prior puromycin treatment from cells lacking Upf2, Upf3, or both proteins, and then assayed by western blotting for retention of Upf1 (Figure 2.5). These experiments showed that Upf1 co-purified predominantly with

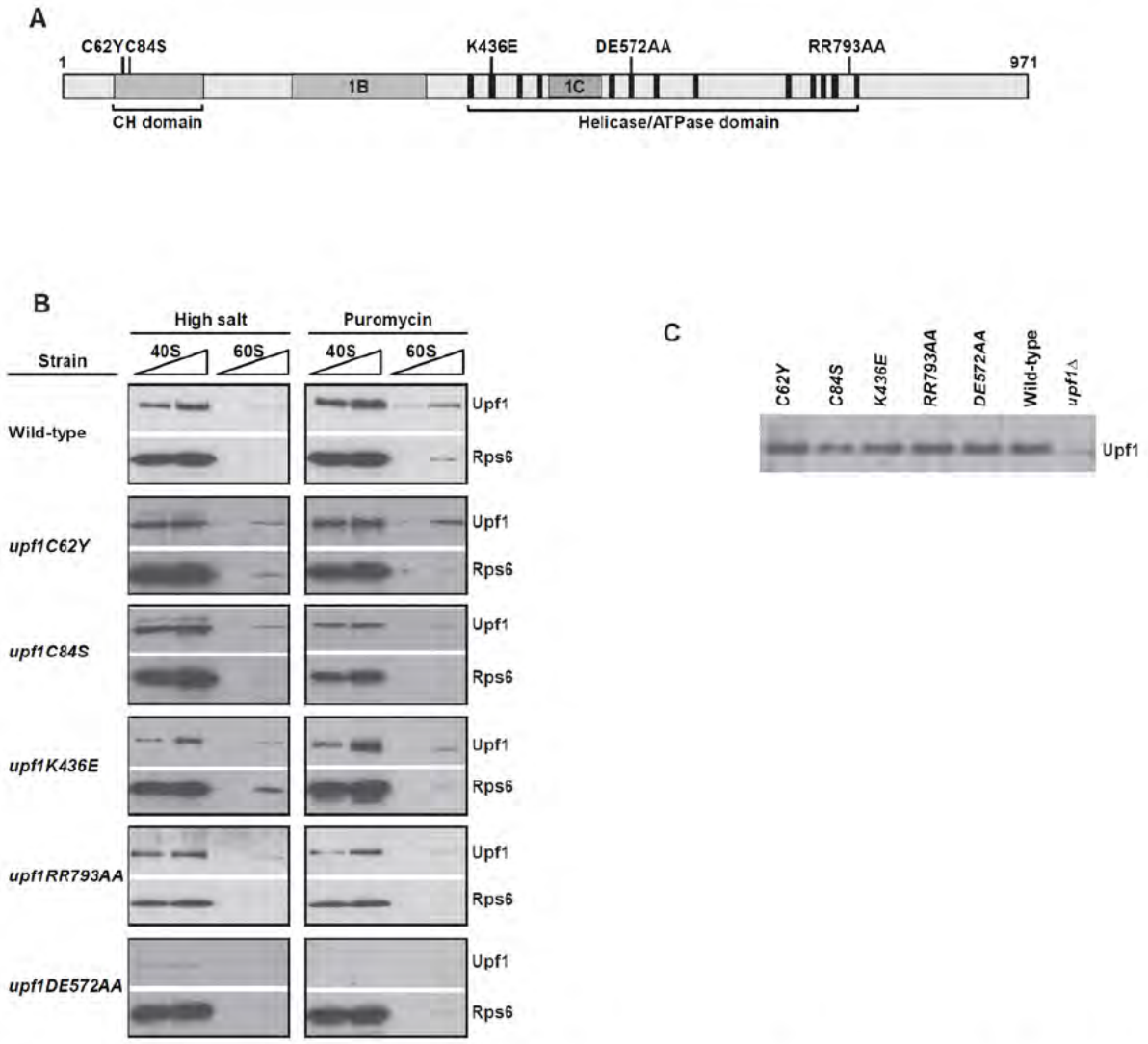

Figure 2.4 – Upf1:40S ribosomal subunit association is modulated by ATP. (A) Schematic representation of amino acid substitutions in the functional domains of Upf1. (B) Ribosomal subunits were prepared under high salt conditions with or without prior puromycin treatment from strains harboring different *upf1* alleles. Increasing amounts (5 µg and 10 µg) of purified subunits were analyzed by SDS-PAGE and western blots were probed with specific antibodies. (C) Western blot for Upf1 from equal amounts of cell lysates of the indicated genotypes.

40S ribosomal subunits in *upf2Δ*, *upf3Δ,* and *upf2Δupf3Δ* strains, similar to the results observed in wild-type strains and consistent with earlier studies showing that polysome-association of Upf1 is independent of the other NMD factors (Atkin et al., 1997). In several of the strains analyzed, a modest amount of Upf1 association with 60S subunits was observed; however, as monitored by Rps6 recovery, this appeared to reflect 40S subunit contamination in the 60S subunit preparations (Figure 2.5). Collectively, these data indicate that the association of Upf1 with 40S ribosomal subunits is neither bridged by, nor dependent on Upf2 or Upf3.

Several reports of experiments done in yeast and mammalian cells have indicated that Upf1 association with a prematurely terminating ribosome may be attributable to direct interactions with the release factors, eRF1 and eRF3 (Czaplinski et al., 1998; Ivanov et al., 2008; Kashima et al., 2006; Singh et al., 2008). Since we observed Upf1 association with 40S subunits purified after puromycin release (Figures. 2.4.B and 2.5) it seemed unlikely that maintenance of Upf1:40S interaction depended on the eRFs. Nevertheless, we tested directly whether either of the release factors was present in the purified 40S ribosomal subunits. Western blotting analyses showed that the same subunit preparations that had substantial bound Upf1 were devoid of detectable levels of Sup45/eRF1 or Sup35/eRF3 (Figure 2.6), indicating that Upf1 can maintain an association with 40S ribosomal subunits independent of the two release factors. However,

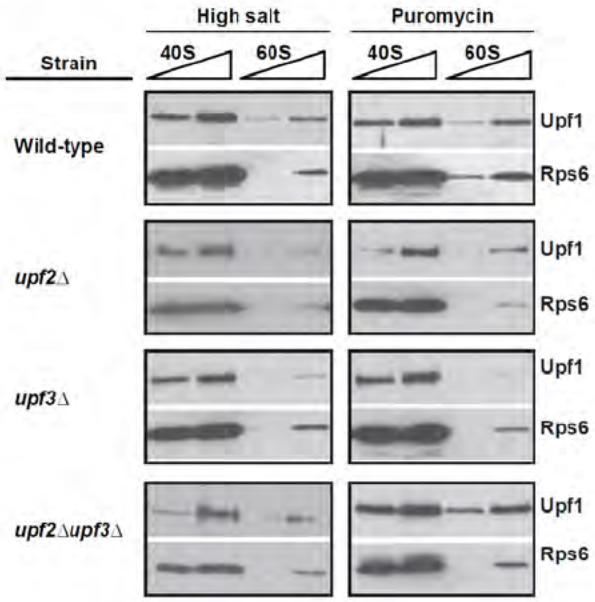

Figure 2.5 – Upf1:40S ribosomal subunit association is independent of Upf2 and Upf3.

Ribosomal subunits were prepared under high salt conditions with or without prior puromycin treatment from yeast strains harboring *upf2*Δ, *upf3*Δ, or *upf2*Δ*upf3*Δ mutations. Increasing amounts (5 μg and 10 μg) of purified subunits were analyzed by SDS-PAGE and western blots were probed with specific antibodies.

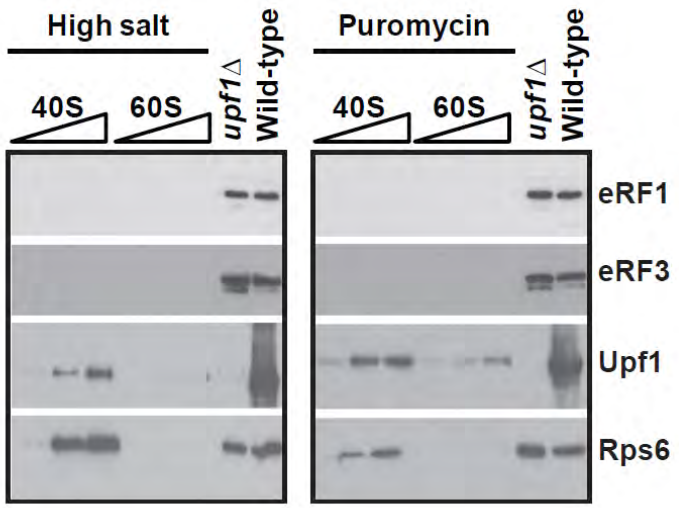

Figure 2.6 – Upf1:40S ribosomal subunit association is independent of the release factors eRF1/Sup45 and eRF3/Sup35. Ribosomal subunits were prepared under high salt conditions with or without prior puromycin treatment from wild-type cells. Increasing amounts (5 μg and 10 μg) of purified subunits were analyzed by SDS-PAGE and western blots were probed with specific antibodies. Lanes marked *upf1Δ* or wild-type are lysates from the respective cells.

whether Upf1's initial association with the 40S subunits depended on these factors remains to be ascertained.

Upf1 interacts with specific 40S ribosomal proteins

Upf1 association with 40S ribosomal subunits suggests two possible types of interactions that may mediate this association: protein-protein and/or protein-rRNA. Evidence for Upf1:ribosomal protein association has been obtained from co-immunoprecipitation experiments in higher eukaryotes (Yamashita et al., 2009). This precedent, and our observation that Upf1's RNA-binding activity was dispensable for 40S subunit association (Figure 2.4), led us to test for Upf1 interaction with specific small subunit ribosomal proteins using a directed yeast two-hybrid screen. Using full-length Upf1 as bait (fused to the *GAL4* DNA binding domain) and thirty-two 40S ribosomal proteins as prey (fused to the *GAL4* activation domain) (He et al., 1996; Valasek et al., 2003), bait and prey plasmids were co-transformed into a *S. cerevisiae* GGY1::171 strain that contains an integrated *GAL1-lacZ* reporter construct. In these strains the expression of the reporter is directly related to the extent of interaction of the bait and prey proteins. With a *GAL4-UPF2* fusion serving as a positive control for two-hybrid interaction, five ribosomal proteins were found to manifest significant *lacZ* expression, indicating an interaction with Upf1 (Figure 2.7, left panel). In both qualitative plate-based and quantitative liquid β-galactosidase assays, the strongest interactions were observed with Rps26. Significantly, the Upf1:Rps26 interaction was as strong qualitatively and quantitatively as the well characterized

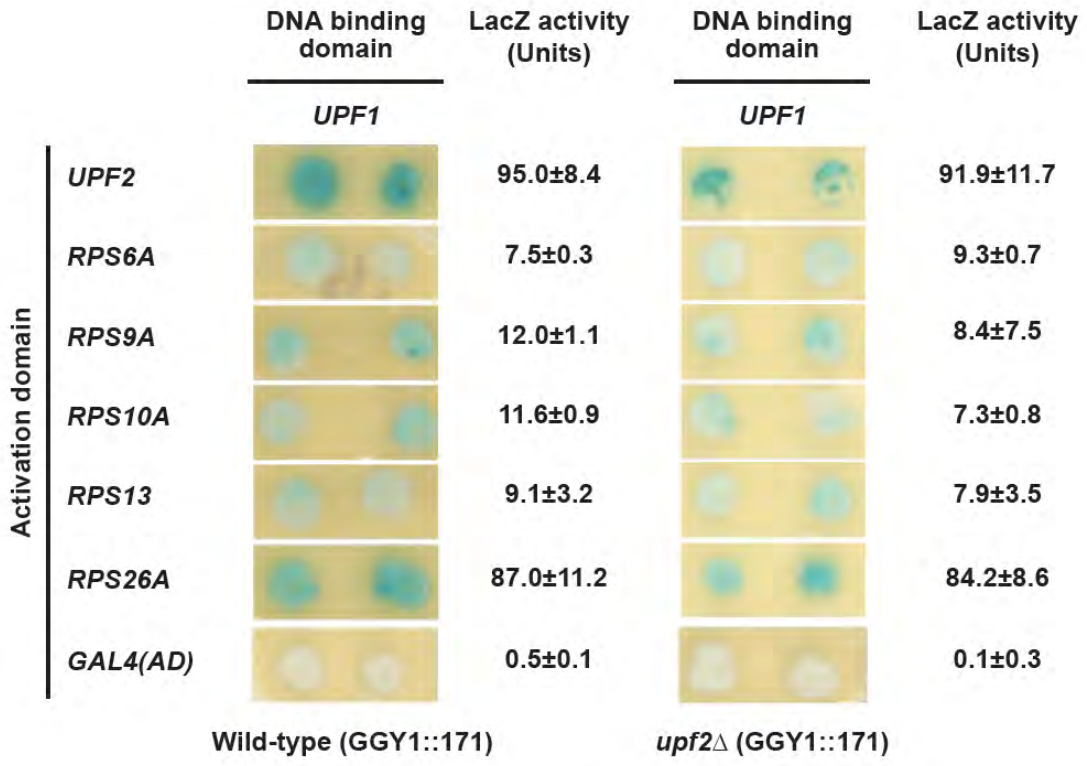

Figure 2.7 – Upf1 interacts with 40S ribosomal proteins. Directed yeast two-hybrid assays were performed using *UPF1-GAL4* (DNA-binding domain) as bait and a library of *RPS-GAL4* (activation domain) fusion proteins as prey. Individual transformants were assayed for β-galatosidase activity qualitatively on plates and quantitatively in liquid assays. Interactions were tested in GGY1::171 wild-type (left panel) and GGY1::171 *upf2Δ* (right panel) strains. Values for β-galatosidase assays represent mean ± standard deviation for three independent experiments performed on cultures from independent transformants.

Upf1:Upf2 interaction (Figure 2.7, left panel) (He et al., 1996; He and Jacobson, 1995). Weaker Upf1 interactions were observed with Rps6, Rps9, Rps10, and Rps13 (Figure 2.7, left panel).

Although our experiments with purified subunits show that Upf1 association with the 40S subunit is independent of Upf2 and Upf3, we tested if the two-hybrid interactions with the individual ribosomal proteins were mediated by either of these NMD factors, or by some aspect of Upf1 multimerization. We assayed the interactions between Upf1 and the candidate ribosomal proteins in two-hybrid yeast strains harboring deletions of *UPF1*, *UPF2,* or *UPF3* and found no change in the interactions between Upf1 and the candidate ribosomal proteins in any of these strains (Figure 2.7, right panel, and data not shown). These results indicate that Upf1:40S ribosomal protein interactions are not bridged by other NMD factors and are likely to be direct.

Point mutations in the CH domain of Upf1 alter its interaction with Rps26

To gain further insight into the Upf1 domain that interacts with Rps26, its strongest 40S ribosomal protein interactor, we analyzed Upf1:Rps26 interaction using five full-length *upf1* loss of function alleles (Figure 2.4.A). Figure 2.8.B shows that two-hybrid interaction between Upf1 and Rps26 was lost completely in strains harboring the C62Y or C84S mutations. The K436E mutation showed a modest decrease in *lacZ* expression, whereas the DE572AA and RR793AA mutants did not exhibit any change in two-hybrid interaction. The loss of interaction with Rps26 in the C62Y or C84S alleles suggests that Upf1's N-

terminus mediates interaction with Rps26. The domain encompassing the K436E mutation in hUpf1 has been demonstrated to form a rigid association with the CH domain (Clerici et al., 2009), which could explain the partial loss of interaction in the K436E mutation. Interestingly, neither the C62Y nor the C84S mutations affect the association of Upf1 with polysomes or 40S ribosomal subunits (Figure 2.4.B) (Atkin et al., 1997), suggesting that Upf1:40S association may be a multivalent interaction involving multiple interacting epitopes.

Upf1 N-terminus is required for its interaction with Rps26

Mutations in the Upf1 N-terminus completely disrupted its interaction with Rps26 (Figure 2.8.B). However, the ability of two different Upf1 proteins with C-terminal amino acid substitutions (DE572AA or RR793AA) to retain interaction with Rps26 does not rule out the possibility that the Upf1 C-terminus also interacts with Rps26. To define more precisely the domain(s) of Upf1 that mediate interaction with Rps26, we further tested the interactions of a series of previously characterized N- and C-terminal Upf1 truncations (Figure 2.8.A) (He et al., 1997). We first tested Upf1(1-289), which harbors only the first 289 amino acid residues of Upf1, and Upf1(290-971), which lacks the first 289 amino acids of Upf1. Upf1(1-289), which includes the CH domain but lacks the helicase domains of Upf1, still showed interaction with Rps26 (Figure 2.8.C). Upf1(290-971), on the other hand, failed to show any interaction with Rps26 (Figure 2.8.C), confirming that the C-terminal domains of Upf1 are not important for binding to Rps26. To further narrow down the minimal interaction domain on Upf1, we

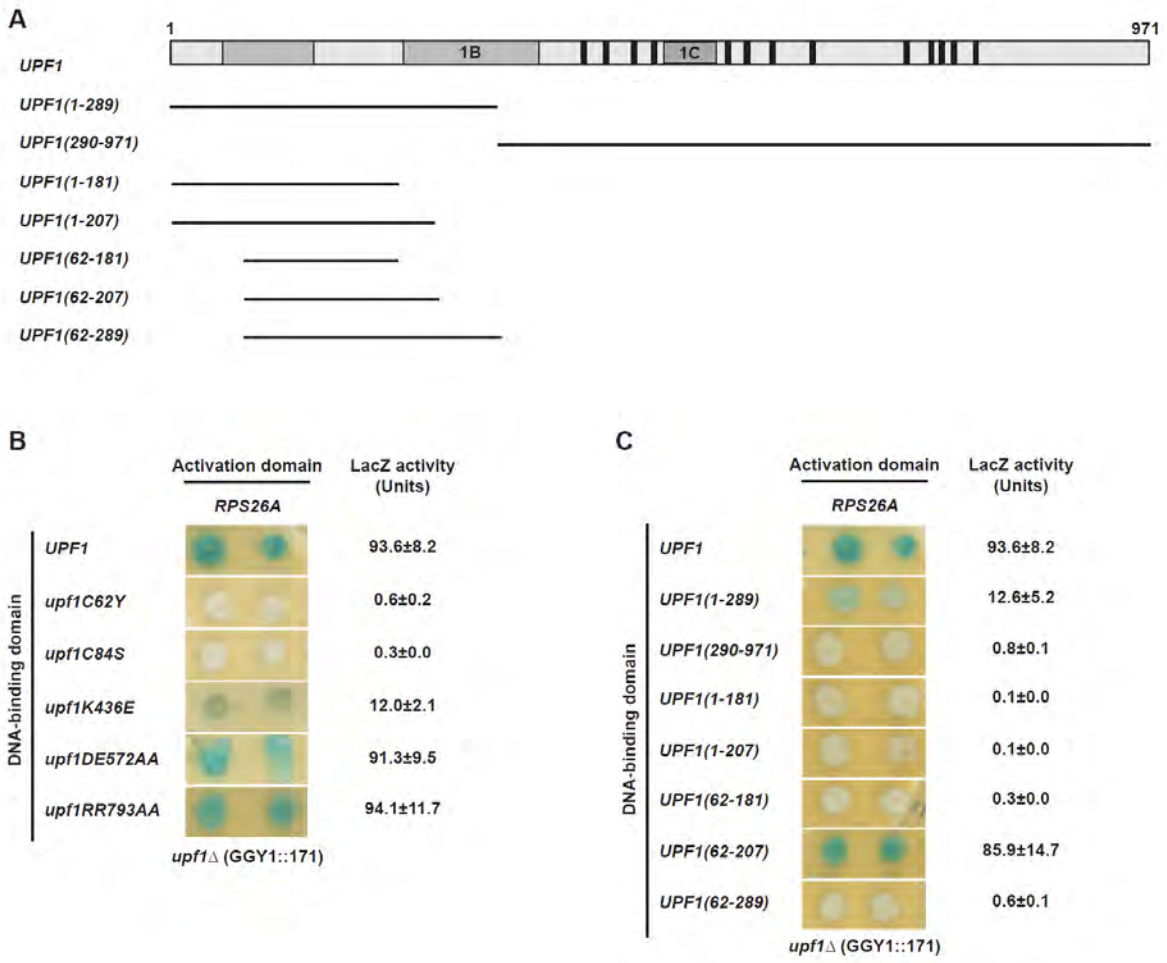

Figure 2.8 – The CH domain of Upf1 mediates interaction with Rps26.

(A) Schematic representation of Upf1 fragments tested for interaction with Rps26. (B, C) Two-hybrid assays were performed in the GGY1::171 *upf1Δ* strain to prevent any effects of possible oligomerization with endogenous Upf1 protein. Interaction of Rps26 with either full-length Upf1 mutant alleles (B) or indicated truncations of Upf1 (C) are shown. Values for β-galatosidase assays represent mean ± standard deviation for three independent experiments performed on cultures from independent transformants.

tested N- and C-terminal truncations of the Upf1(1-289) fragment. Since residues 62 and 84 were found to be important for Rps26 interaction (Figure 2.8.B), fragments tested spanned residues 1-181, 1-207, 62-181, 62-207, and 62-289 (Figure 2.8.A). The shortest Upf1 fragment that still retained the ability to interact with Rps26 was comprised of residues 62-207 (Figure 2.8.C). Interestingly, the interaction of Upf1(1-289) with Rps26 was weaker than that observed with either full-length Upf1, or the shortest Upf1(62-207) fragment.

Rps26 interacts with Upf1 *in vitro*

Two-hybrid interactions can be bridged (Bartel et al., 1993; Bartel and Fields, 1995; He et al., 1997), so we sought to determine whether Upf1:Rps26 interaction could be confirmed biochemically, using an *in vitro* binding assay. Purified yeast FLAG-Upf1 (Figure 2.9.A) and lysates from *E. coli* expressing recombinant His-tagged Rps26 (Figure 2.9.B) were incubated and subjected to immunoprecipitation using anti-FLAG beads. An *E. coli* strain not expressing any His-tagged protein was used as a control for background binding. Analysis of the immunoprecipitates showed co-immunoprecipitation of His-Rps26 with FLAG-Upf1 and not with FLAG beads alone (Figure 2.9.C, compare lanes 8 and 12). This *in vitro* data, in addition to the two-hybrid analyses, demonstrates that Upf1 association with the 40S subunit is mediated at least in part by a direct interaction with 40S ribosomal protein Rps26 and does not involve any endogenous yeast protein bridging the interaction.

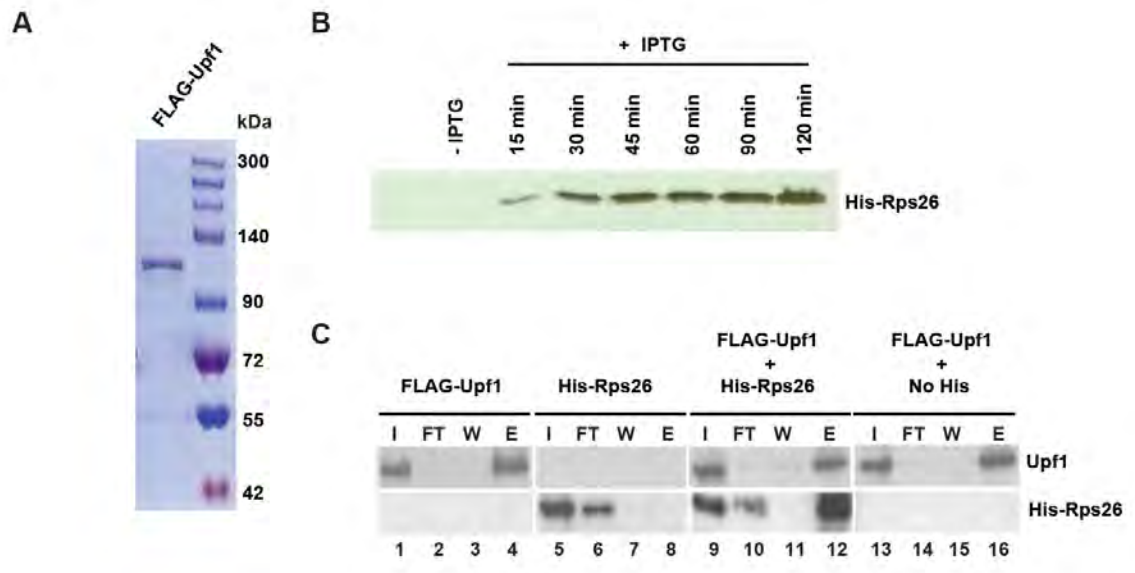

Figure 2.9 – Upf1 interacts with Rps26 *in vitro*. *In vitro* binding assays were performed with *E. coli* BL21(DE3) cells expressing His-Rps26.

(A) Coomassie-stained SDS-PAGE gel showing purity of yeast FLAG-Upf1. (B) Time course of His-Rps26 expression after IPTG induction in *E. coli* BL21(DE3) cells. (C) Western blot analyses of anti-FLAG immunoprecipitation assays utilized anti-His and anti-Upf1 antibodies on input (I), flowthrough (FT), wash (W), and eluate (E) fractions.

Discussion

Upf1 plays a central role in triggering NMD as well as in promoting several processes ancillary to this quality control pathway, including translational repression, dissociation of the translating mRNP, degradation of the nascent polypeptide, and inhibition of pre-mRNA splicing (Kervestin and Jacobson, 2012). Accordingly, the platform from which Upf1 launches these diverse activities is of considerable interest. Notwithstanding disagreement about the involvement of all termination events or just those which are premature, several models suggest that an early event in NMD is the interaction of Upf1 with the release factors localized at the A site of a terminating ribosome (Kervestin and Jacobson, 2012). The implication of such models is that Upf1, and perhaps the other Upfs, should be associated with ribosomes during at least one phase of their functional lifetimes. This notion was supported by early experiments demonstrating polysomal localization of the Upfs (Atkin et al., 1995; Atkin et al., 1997; Peltz et al., 1993a), as well as by more recent studies which have localized Upf1 to the SURF complex (Yamashita et al., 2009) or to purified 40S ribosomal subunits (Ghosh et al., 2010). To understand the mechanistic basis for Upf1's association with the termination complex, we have pursued details of its mode of interaction with yeast ribosomes.

Using affinity purification of tagged ribosomal subunits, we demonstrate here that Upf1 is specifically immunoprecipitated with tagged 40S ribosomal subunits and not 60S subunits (Figure 2.2), consistent with our previous results (Ghosh et al., 2010). The significant enrichment of *Upf1* in ribosomal pulldowns

of micrococcal nuclease-treated lysates, as well as the failure to detect poly(A)-binding protein (Pab1) in these pulldowns indicates that ribosome association of Upf1 is likely mediated by a direct interaction with the 40S subunit and not through residual ribosome-associated mRNA. Importantly, this conclusion is reinforced by the observation that the association of Upf1 with the 40S ribosome is sufficiently stable to resist either high salt-induced or puromycin-triggered ribosomal dissociation (Figure 2.4). Stable association of Upf1 with the 40S subunit appears to be modulated by ATP, and independent of the simultaneous presence of Upf2 or Upf3, or translation termination factors eRF1 and eRF3 (Figures 2.5 and 2.6).

The demonstration of specific Upf1 association with the 40S subunit led us to screen for Upf1:40S ribosomal protein interactions, an experimental approach that identified Rps26 as a strong interacting partner of Upf1 (Figures 2.7 and 2.9). The interaction between Upf1 and Rps26 was observed to be specific, direct, and independent of the other Upf factors (Figures 2.7 and 2.9). Consistent with the latter result, the association of Upf1 with purified subunits was also found to be independent of Upf2 and/or Upf3 (Figure 2.5). Two-hybrid analyses that exploited different *upf1* alleles showed that the RR793AA RNA-binding mutant had no effect on Upf1:Rps26 interaction, whereas single point mutations in the CH-domain abrogated the ability of Upf1 to interact with Rps26 completely (Figure 2.8.B). The requirement for a functional Upf1 N-terminal CH-domain in Upf1:Rps26 interaction was further evident from deletion analyses which showed that only those Upf1 fragments containing the CH-domain could interact with

Rps26 (Figure 2.8.C). Interestingly, although the C62Y and C84S mutation in the CH-domain of Upf1 abolished the Upf1:Rps26 interaction, these mutations did not significantly affect Upf1's association with the 40S ribosomal subunit. This observation suggests that Upf1 ribosomal association is likely mediated through multiple interaction epitopes. In support of this idea, we found Upf1 also interacts with Rps6, Rps9, Rps10, and Rps13 (Fig. 2.7).

The K436E mutation in the *UPF1* ATP-binding domain also manifested impaired Upf1:Rps26 interaction, although not to the extent seen with the CH domain mutants (Figure 2.8.C). X-ray crystallographic analysis of hUpf1 has demonstrated a strong association between the CH-domain (encompassing residues C62 and C84) and domain 1A (encompassing residues K436 and DE572), suggesting that Upf1 may adopt a folded conformation that allows these domains to not only interact with each other, but with Rps26 as well. Interestingly, we noted that the interaction between the DE752AA ATP hydrolysis mutant of Upf1 with Rps26 was not affected in the two-hybrid assay, whereas association of this mutant protein with the purified 40S subunits was lost (Figure 2.4). The lack of complete correspondence between the mutations that affect two-hybrid interaction and co-purification with 40S subunits must take into account the differences between the two assays. Whereas co-purification demands stable association with the subunit subsequent to treatment with high salt or puromycin, the two-hybrid assay is capable of registering a transient binding event that may be a precursor, for example, to the post-puromycin state. The former may have a readily detectable two-hybrid interaction (e.g., Rps26)

whereas the latter may not. The possibility that Upf1 association with a translating mRNP involves complex mechanisms has been highlighted in recent studies. Cryo-EM structures of the EJC-UPF complex have positioned Upf1 on the 3' side of the EJC (Melero et al., 2012), contradictory to the current notion of Upf1 localization at the 5' side that is closer to the premature termination codon. It has also been reported that hUPF1 binds directly to mRNA, with binding varying as a function of mRNA 3'-UTR length (Hogg and Goff, 2010; Kurosaki and Maquat, 2013).

Rps26 is positioned on the solvent side of the 40S platform and is a crucial component of the 40S ribosome-binding site for mRNA (Sharifulin et al., 2012). Available structural data show that the binding site of eIF3 on the 40S subunit overlaps with Rps26 as well as the other Upf1-interacting ribosomal proteins (Figure 2.10). This observation is of interest because temperature-sensitive lesions in the Prt1 subunit of eIF3 (eIF3b) antagonize NMD in yeast (Welch and Jacobson, 1999), and phosphorylated Upf1 interacts with eIF3 and inhibits translation initiation in mammalian NMD (Isken and Maquat, 2008). eIF3 has been implicated in efficient ribosome recycling after translation termination (Pisarev et al., 2007b) and *upf1Δ* extracts have been shown to be defective in efficient ribosome recycling from a nonsense-containing mRNA (Ghosh et al., 2010). Collectively, these observations suggest a possible role for Upf1:eIF3 interaction in promoting ribosome dissociation and/or recycling from premature termination events.

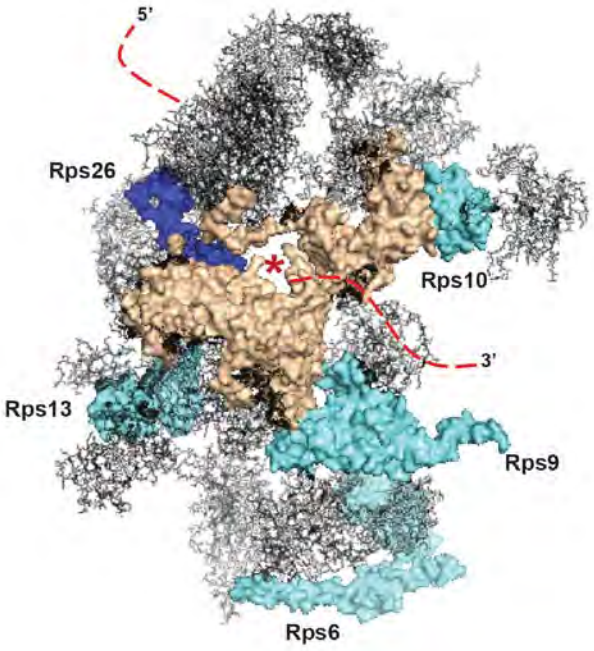

Figure 2.10 – Map of Upf1-interacting ribosomal proteins and eIF3 binding site on the solvent-side view of *S. cerevisiae* 40S subunit.

The image created using PyMol (www.pymol.org) is based on a Protein Data Bank entry (accession number 3U5C) (Ben-Shem et al., 2011) showing ribosomal proteins. Ribosomal proteins interacting with Upf1 are highlighted using different shades of blue (dark blue denoting strong interaction and light blue representing weak interaction in the two-hybrid assay). The eIF3 binding site is highlighted in wheat (Kouba et al., 2012). The asterisk denotes the mRNA entry channel and the mRNA is represented using a dotted line.

Chapter III

Yeast Upf1 associates with ribosomes translating mRNA coding sequences upstream of normal termination codons

Contributions for this chapter

Robin Ganesan performed the affinity purifications of Upf1-bound 80S ribosomes from total 80S ribosome samples that I provided. The construction of sequencing libraries from RNA fragments that I had prepared, and Illumina sequencing of these libraries, were both carried out at Beijing Genomics Institute (BGI). Data analysis was done in collaboration with Dr. Richard Baker (UMass Medical School) and Jill Moore (UMass Medical School). Mass spectrometry sample preparation and data analysis was done by Robin Ganesan and John Leszyk (Proteomics and Mass Spectrometry Facility, UMass Medical School). The negative-stain electron microscopy (EM) analysis was done by Gregory Hendricks (Electron Microscopy Core Facility, UMass Medical School).

Summary

Although NMD has been extensively studied in multiple eukaryotes, many unresolved questions about this quality control process remain to be addressed. In particular, we have yet to understand the mechanism by which Upf1, the central NMD regulator, selectively targets PTC-containing messenger ribonucleoproteins (mRNPs). Here, we determined the timing of Upf1 binding to ribosomes during translation. Employing a selective ribosome profiling approach, we identified mRNA sequences protected by Upf1-bound ribosomes. While recent studies in metazoans suggested translation-independent interactions of Upf1 with mRNA 3'-UTRs, we find that Upf1 engages with actively translating ribosomes, specifically with ribosomes in the coding regions upstream of normal termination codons. Such association is not limited to NMD substrates. Together, our results suggest that Upf1 not only triggers rapid decay of nonsense-containing mRNAs, that initiation of this process may well depend on the selective recruitment of factors downstream of Upf1 function during premature translation termination.

Introduction

Nonsense-mediated mRNA decay (NMD) is a cytoplasmic surveillance mechanism that degrades mRNA transcripts that contain premature termination codons (PTCs) (Kervestin and Jacobson, 2012). Transcriptome-wide studies using microarray or RNA-Seq analysis of yeast, fly, and human cells have revealed that NMD regulates 5-20% of cellular transcripts. These include aberrant transcripts as well as many apparently wild-type mRNAs, suggesting that NMD has a regulatory function beyond mRNA surveillance (He et al., 2003; Mendell et al., 2004; Ramani et al., 2009; Tani et al., 2012). The destabilization of nonsense-containing mRNAs requires ongoing translation as well as the conserved Upf1, -2, and -3 proteins in all eukaryotes and the Smg1 to Smg9 proteins in metazoans (Kervestin and Jacobson, 2012; Schoenberg and Maquat, 2012).

Upf1, the key regulator of NMD, has been extensively characterized. Upf1 belongs to helicase superfamily I (SF1), with two RecA-like domains in tandem at its C-terminus. Upf1 possesses ATP-dependent RNA binding, as well as RNA-dependent ATPase and 5' to 3' RNA helicase activities, all of which are essential for triggering NMD (Clerici et al., 2009; Czaplinski et al., 1998; Wang et al., 2001). An N-terminal cysteine- and histidine-rich Zn^{2+}-finger domain (CH domain) of Upf1 interacts with a C-terminal region of Upf2, which in turn binds to Upf3, to form an NMD-activating complex (He et al., 1997). Overexpression of Upf1 can compensate for mutations in Upf2 and Upf3, but not *vice versa* (Maderazo et al., 2000) and the maximal *in vitro* activation of the Upf1 ATPase

and helicase activities requires both Upf2 and Upf3 (Chamieh et al., 2008). These observations imply that Upf1 is the key effector of NMD, whereas Upf2 and Upf3 are likely to be regulators of Upf1 function. Upf1 lacking its ATPase activity is defective in association with the 40S ribosomal subunit in yeast (Min et al., 2013). Upf1 ATPase mutants also fail to promote the disassembly of the poorly dissociable premature termination complex subsequent to peptide hydrolysis, as well as translocation along the mRNA in a 5′-to-3′ direction (Franks et al., 2010; Melero et al., 2012; Shigeoka et al., 2012).

The mechanism by which nonsense-containing mRNAs are recognized and selectively targeted by NMD remains to be determined. Some current models of NMD activation by premature termination postulate that an inappropriate mRNP structure neighboring the PTC allows the recruitment of Upf1 to mRNA substrates (Kervestin and Jacobson, 2012). However, the basis for the specific targeting of Upf1 to NMD substrates and many aspects of the mechanism of action of Upf1 are unknown. For example, it is not clear whether Upf1 interacts with all mRNAs or only a specific subset, such as prematurely terminating mRNAs. RNA-immunoprecipitation approaches have been used to address this problem, namely the co-purification of reporter mRNAs with Upf1 (Hogg and Goff, 2010; Kurosaki and Maquat, 2013) or the identification of mRNAs using either microarray analysis or deep sequencing after Upf1-immunoprecipitation (Decourty et al., 2014; Johansson et al., 2007; Kurosaki et al., 2014). These studies indicate that Upf1 preferentially associates with NMD-targeted mRNAs, and long 3′-UTRs make transcripts sensitive to NMD. In

addition, Upf1 is thought to preferentially target mRNA 3'-UTRs and such association may be independent of mRNA translation (Hogg and Goff, 2010). However, recent studies suggest that the nature of Upf1-mRNA interaction is much more complex than previously thought. In contrast to the proposed selective recruitment of Upf1 to NMD substrates, there is evidence that Upf1 binds to numerous mRNAs, regardless of their PTC-status (Gregersen et al., 2014; Hurt et al., 2013; Zund et al., 2013). Upf1 was reported to bind to mRNA 3'-UTRs, including those of PTC-free mRNAs, and also to long noncoding RNAs (Gregersen et al., 2014; Hurt et al., 2013) . Strikingly, upon translation inhibition, the distribution of Upf1 was seen to shift toward coding sequences (CDS), implying that the recruitment of Upf1 to coding regions of transcripts is translation-dependent. Although non-discriminatory binding of Upf1 to numerous mRNAs is controversial, these results strongly suggest that Upf1 binds to ribosome-associated mRNAs.

However, it is unknown whether Upf1 binds directly to mRNAs or ribosomes. Upf1 co-localizes with polyribosomes, 80S ribosomes, and 40S ribosomal subunits (Atkin et al., 1995; Ghosh et al., 2010; Mangus and Jacobson, 1999; Min et al., 2013) and interacts with the release factors eRF1 and eRF3 (Czaplinski et al., 1998; Kashima et al., 2006; Singh et al., 2008) and with a specific ribosomal protein, Rps26 (Min et al., 2013). The fact that translation controls NMD activation highlights the need for studying mRNA sequences protected by Upf1-bound ribosomes, instead of mRNAs bound by Upf1.

However, the timing and open reading frame (ORF) location of Upf1 association with translating ribosomes remain obscure. To map the transcriptome positions of ribosomes when they associate with Upf1, we employed the selective ribosome profiling approach (Becker et al., 2013) to identify mRNA sequences associated with Upf1-bound ribosomes in the budding yeast *Saccharomyces cerevisiae*. Ribosome profiling is a powerful technique to monitor when proteins of interest are engaged with ribosomes on translated mRNAs at a genome-wide level (Ingolia, 2014). We combined this method with an affinity purification strategy in which epitope-tagged Upf1 was used to selectively purify Upf1-bound ribosomes from total ribosomes. Next, we isolated mRNA fragments bound by Upf1-enriched ribosomes and subjected those fragments to analysis by deep sequencing. Our results reveal a novel specificity of Upf1 binding in the coding regions upstream of the normal termination codons of most mRNAs.

Results

Affinity purification of Upf1-associated 80S ribosomes

Using selective ribosomal profiling, we analyzed the mRNA fragments protected by translating ribosomes harboring bound Upf1, thus determining the extent and open reading frame (ORF) position of Upf1:80S association. A schematic for the procedure for affinity purification of Upf1-bound ribosomes from the total translatome is shown in Figure 3.1. Given the lower intracellular abundance of Upf1 (~6900 molecules/cell) compared to that of ribosomes (~200,000 molecules/cell), we generated a yeast strain expressing high-copy 6XHis-tagged Upf1 for purifying 80S ribosomes with bound Upf1.

Although often used in ribosome profiling experiments, cycloheximide (CHX) treatment of cells inhibits the recovery of ribosomes at termination codons (Amrani et al., 2004; Ingolia et al., 2011). In order to capture all populations of ribosomes engaged in translation, cycloheximide was omitted during our sample preparation. RNase-treated extracts were subjected to sucrose gradient sedimentation to minimize the contamination of free mRNPs and the fractions corresponding to the 80S ribosome peak resulting from the disruption of polyribosomes were collected for affinity purification (Figure 3.2). Upf1 has been shown to co-sediment with polysomes and 80S ribosomes (Atkin et al., 1995; Mangus and Jacobson, 1999). Nonetheless, we checked for the co-sedimentation pattern of Upf1 with 80S ribosomes, and found that Upf1 was abundant in samples comprising the 80S ribosome peak (Figure 3.3). Next, Upf1-associated ribosomes were enriched from the total ribosome population in this

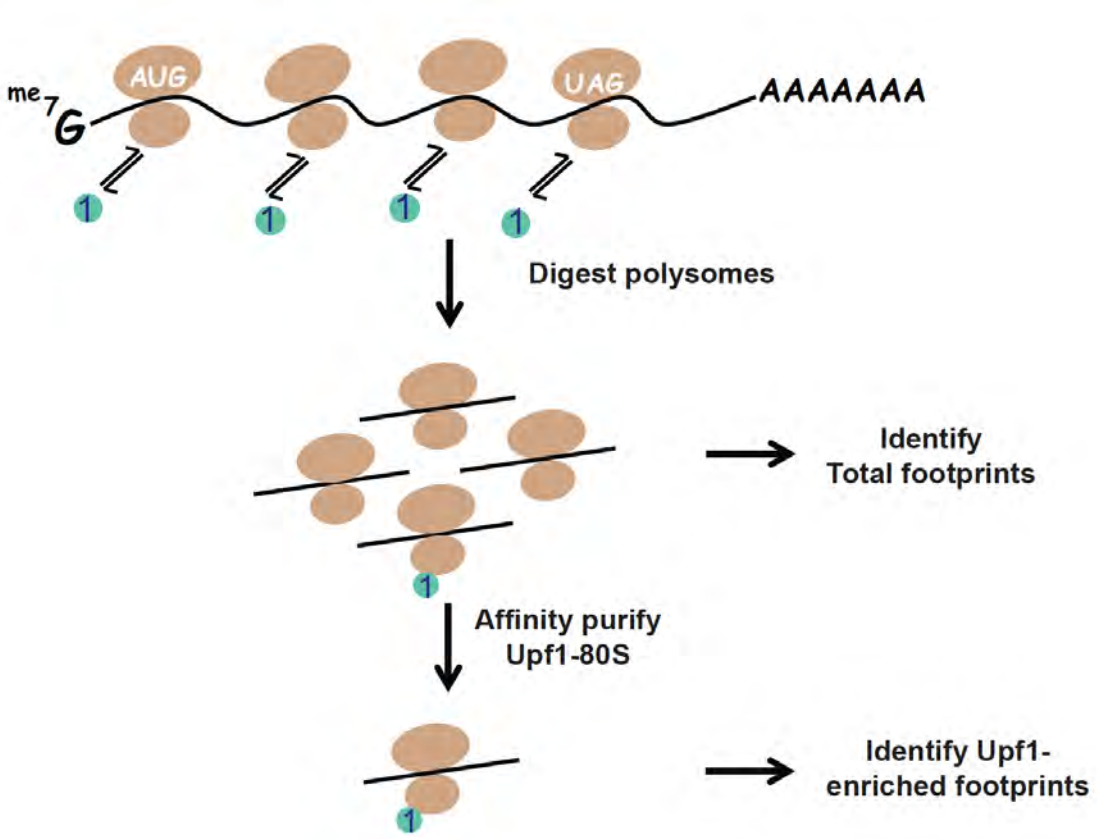

Figure 3.1 – Schematic of the procedures used for selective ribosome profiling of Upf1-bound ribosomes.

Cells expressing epitope-tagged Upf1 are harvested at mid-log phase and cryogenically lysed. Polysomes are then digested with RNase I to yield footprint-containing monosomes. Digested monosomes are separated from other debris by sucrose gradient centrifugation and Upf1-bound 80S complexes are then affinity-purified on Talon (cobalt) resin. mRNA footprint fragments derived from all monosomes and those enriched through affinity purification are then cloned for deep sequencing analysis.

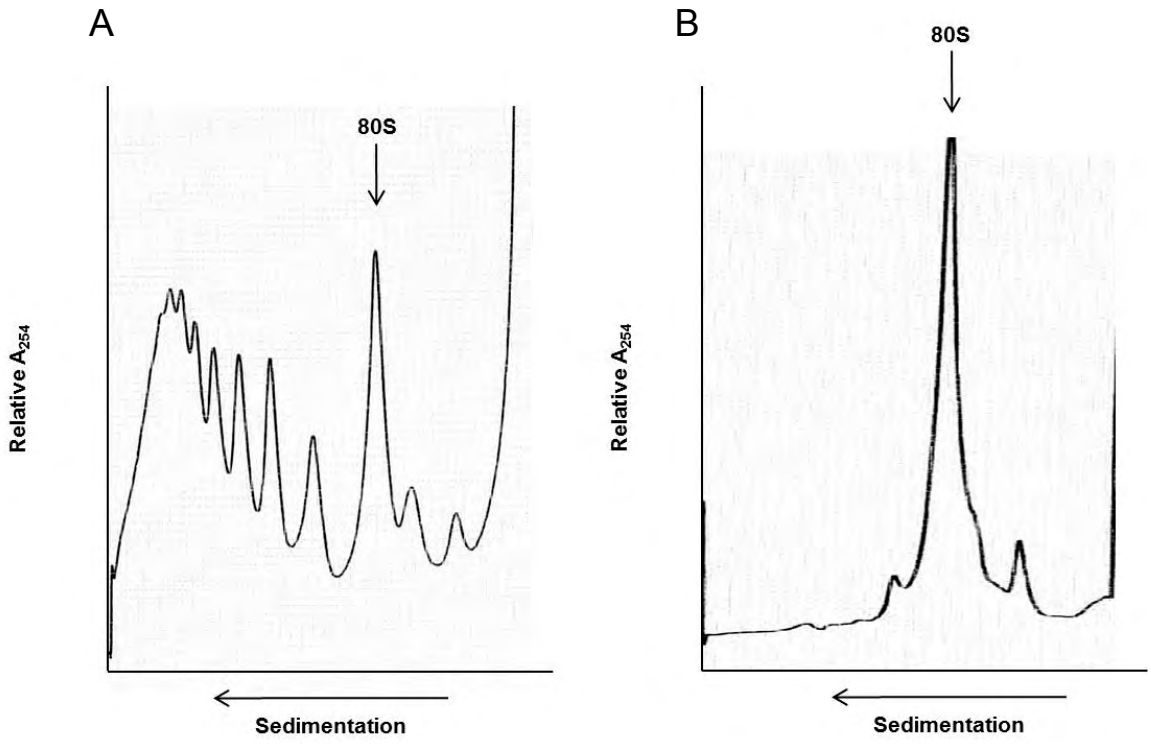

Figure 3.2 – Enrichment of 80S ribosomes after RNase I treatment.

Cytoplasmic extracts without (A) or with (B) RNase I treatment were fractionated on 7-47% sucrose gradients. The A_{254} traces of the ribosome profiles are shown, with the 80S peak indicated by an arrow.

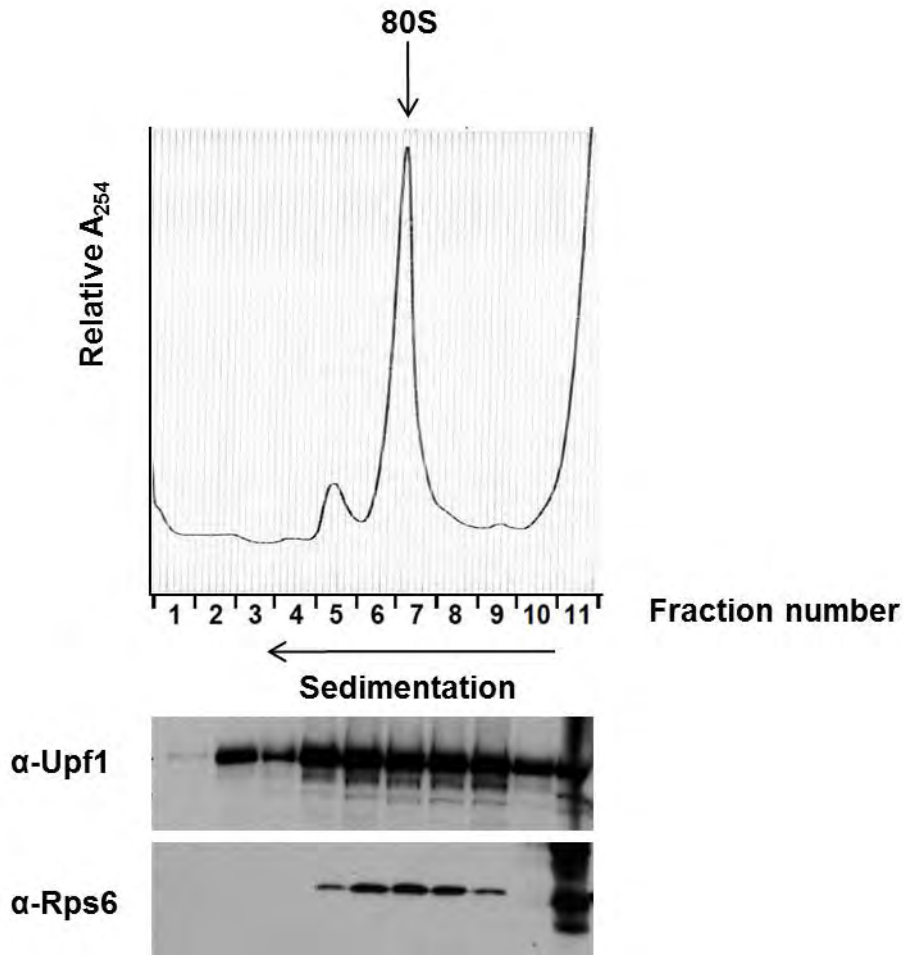

Figure 3.3 – Upf1 co-sediments with 80S ribosomes.

Cytoplasmic extracts treated with RNase I were fractionated on 7-47% sucrose gradients. The A_{254} traces of the ribosome profiles are shown, with the 80S peak indicated by an arrow. Fractions were precipitated with TCA, and subjected to SDS-PAGE, followed by western blot analysis for Upf1 and Rps6.

peak using cobalt-based affinity chromatography.

Western blotting revealed that the affinity-purification protocol enriched substantially for ribosomes bound by Upf1 (Figure 3.4.A; compare Lane 1 and 5). Mass spectrometric analyses indicated that, pre-purification, 80S ribosomes from cells overexpressing Upf1 contain approximately 1 Upf1 molecule per 42.8 ribosomal protein molecules. After purification, the ratio is 1 Upf1 per 2.0 ribosomal protein molecules (22.8-fold increase) (Table 3.1; compare Column 2 and 3), suggesting that approximately half of the affinity-purified 80S ribosomes contained bound Upf1. Further, negative-stain electron microscopy (EM) detected ample amounts of 80S ribosomes in affinity-purified samples (Figure 3.4.B). Collectively, these results indicate the efficient recovery of Upf1-associated ribosomes.

Deep sequencing of ribosome-protected fragments derived from Upf1-associated 80S ribosomes

Deep sequencing libraries were prepared from ribosome-protected mRNA fragments (RPFs) from total or Upf1-bound ribosomes. mRNA fragments derived from total RNA of the same cells was also subjected to deep sequencing analysis. Additional Ribo-Seq and mRNA-Seq libraries were also generated in three very similar but non-identical experiments (Table B.1). All libraries were sequenced on an Illumina-HiSeq 2000 and the sequence data was analyzed through a workflow of bioinformatics tools shown in Figure 3.5. Basic statistical analyses for sequencing libraries and supplementary data are in Appendix B.

Protein	Total	Upf1-bound	Fold change
UPF1_YEAST	1.0	1.0	-
RL10_YEAST	35.1	1.8	19.5
RL15A_YEAST	41.2	1.6	25.7
RL19A_YEAST	42.3	1.1	38.5
RL6B_YEAST	40.8	2.2	18.5
RS18A_YEAST	62.1	2.8	22.2
RS24A_YEAST	36.0	1.6	22.5
RS7B_YEAST	26.2	1.6	16.4
RS26A_YEAST	25.3	1.2	21.1
Average (All ribosomal proteins)	42.8	2.0	21.4

Table 3.1 – Affinity-purified 80S ribosomes are highly enriched for Upf1. Mass spectrometry analysis of Upf1 and ribosomal proteins before (Total ribosomes) and after (Upf1-bound ribosomes) affinity purification. The quantitation report was generated in Mascot Distiller by averaging intensities of spectra, where Upf1 content in each column was normalized to 1. Selected individual ribosomal proteins and the average of all ribosomal proteins are shown.

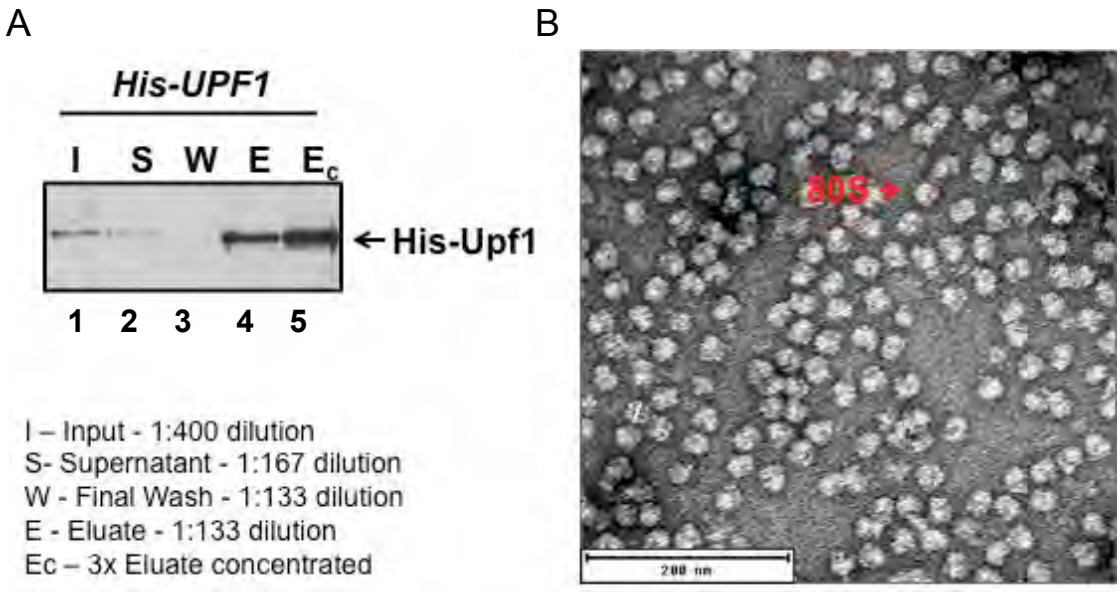

Figure 3.4 – Upf1-bound 80S ribosomes are purified efficiently by using 6xHis-tagged Upf1.

(A) RNase I-digested ribosomes from yeast cells overexpressing His-Upf1 were affinity-purified on cobalt resin. Input (I), supernatant (S), eluate (E), and concentrated eluate (Ec) fractions were subjected to western blotting with anti-Upf1 antibodies. Different amounts of each sample were loaded for SDS-PAGE analysis as indicated. (B) Negative-stain EM image of affinity-purified 80S ribosomes. Scale bar: 200 nm.

Figure 3.5 – Pipeline for analysis of RNA-Seq reads.

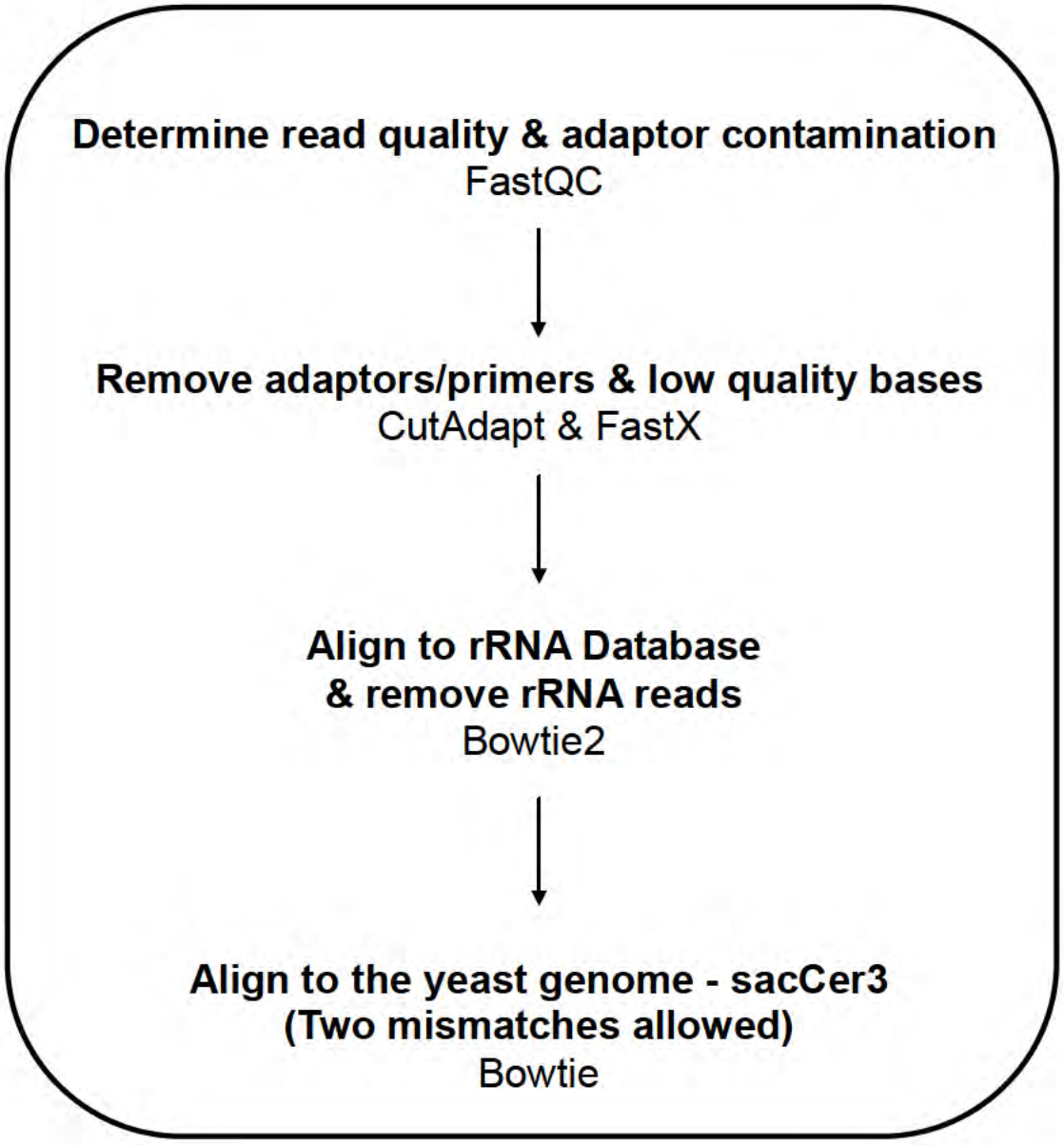

Figure 3.5 – Pipeline for analysis of RNA-Seq reads.

The pipeline shows the steps from input to output of each of the tools used within the data analysis pipeline: FastQC to check the quality control for high throughput read sequence, Cutadapt and FastX to remove adapters, Bowtie2 for alignment and generation a compact format for storing large nucleotide sequence alignments.

More than 4,900 yeast genes were sufficiently represented in our Ribo-Seq libraries to provide reliable measurements of their translational status (Table B.3). The reproducibility of our data was assessed by comparing wild-type libraries with or without rRNA depletion (r = 0.94 for Total-Ribo-Seq libraries and r = 0.89 Upf1-Ribo-Seq libraries) (Figure 3.6). Given the minimal differences observed between experiments done, downstream analyses were presented here with the rRNA-depleted wild-type library, due to its greater read depth.

The reliability of our ribosome profiling approach was tested by analyzing ribosome occupancy on individual transcripts by visualizing specific transcripts with the Integrated Genome Viewer (IGV). As shown in Figure 3.7, individual normal mRNAs, such as those encoded by the *PGK1 and ACT1* genes, manifested ribosome-protected fragments throughout the respective ORFs. Our yeast strains contain multiple nonsense alleles with known PTC positions, and ribosome-protected fragments were present near the beginnings of representative mRNAs analyzed in the Total-Ribo-Seq library, suggesting that the presence of premature stop codons halted ribosomal progression (Figure 3.7). These results are consistent with the notion that nonsense mutations cause premature translation termination.

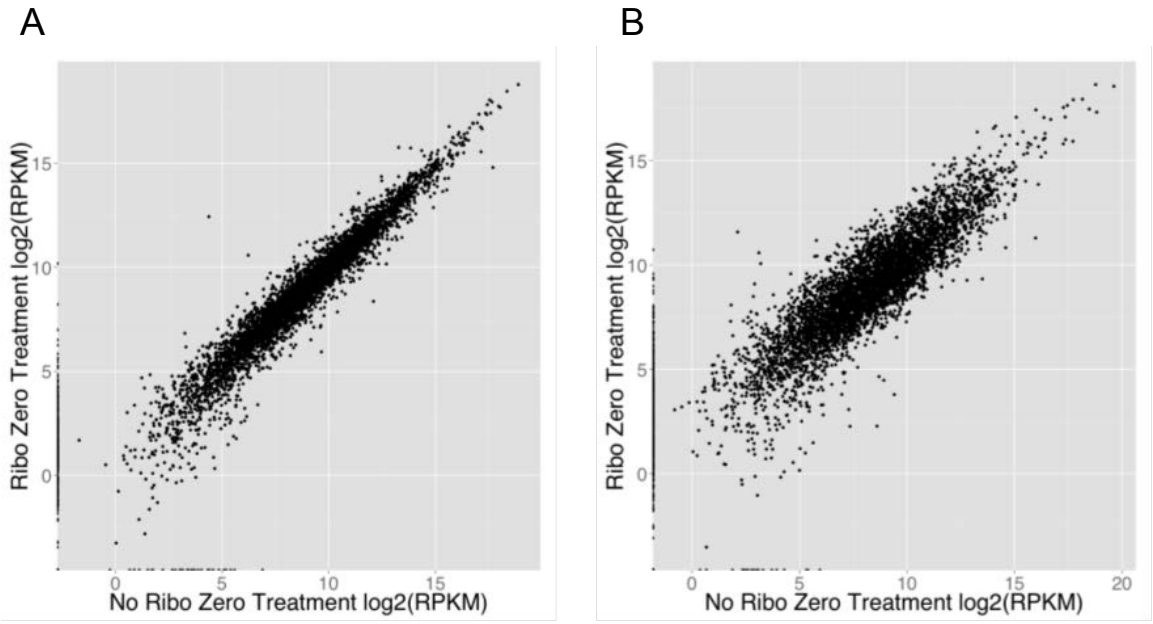

Figure 3.6 – Datasets from two independent experiments manifest good correlation.

Scatter plots showing the relative differences between wild-type libraries with or without rRNA depletion. Spearman correlations were computed using log2 RPKM values (RPKM = reads per kilobase per million total reads). (A) Total-Ribo-Seq libraries (Spearman r = 0.94), and (B) Upf1-Ribo-Seq libraries (Spearman r = 0.89)

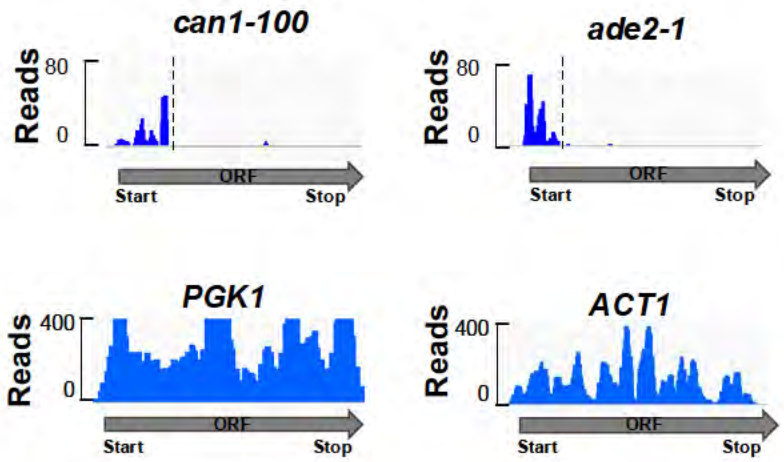

Figure 3.7 – Premature stop codons halt ribosomal progression.

Coverage density maps were generated on the IGV browser for total ribosomes from nonsense-containing mRNAs (Top) and normal mRNAs (Bottom). Read counts in total ribosomes are in blue. Dashed lines indicate positions of known premature stop codons.

Increased Upf1 occupancy of ribosomes positioned near the 3'- ends of open reading frames

To determine whether Upf1 has preferred binding sites on translating ribosomes, we performed a metagene analysis by measuring the median read coverage across each mRNA with an ORF length of greater than 250 nt. Ribosome-protected fragments from the total translatome were evenly distributed across the open reading frames of all mRNAs, except for peaks at the ORF beginnings and ends that correspond to translational start and stop sites, respectively. These results were consistently obtained in all four data sets (Figure 3.8) and thus likely represent the intrinsic ribosome distribution in the absence of any drug treatment. Peaks of ribosome footprints on transcripts at initiation and termination sites imply that translation is rate-limiting at these steps, compared to elongation. These findings are consistent with previous studies, which showed enhanced footprints at initiation codons and at termination sites (Ingolia et al., 2011).

Next, we compared the read coverage in total ribosomes with that for Upf1-bound ribosomes and identified windows where read coverage was different between Total-Ribo-Seq and Upf1-Ribo-Seq libraries (Figure 3.9; compare red lines and blue lines). Based on current models of NMD activation, we hypothesized that the majority of Upf1 binding events would take place near PTCs. However, we observed a completely different pattern, i.e., the relative absence of Upf1 association with ribosomes located in the 5' regions of ORFs (Figure 3.9.A), followed by a continuous increase of Upf1:ribosome association

Figure 3.8 – Total ribosomes are evenly distributed throughout the ORFs.

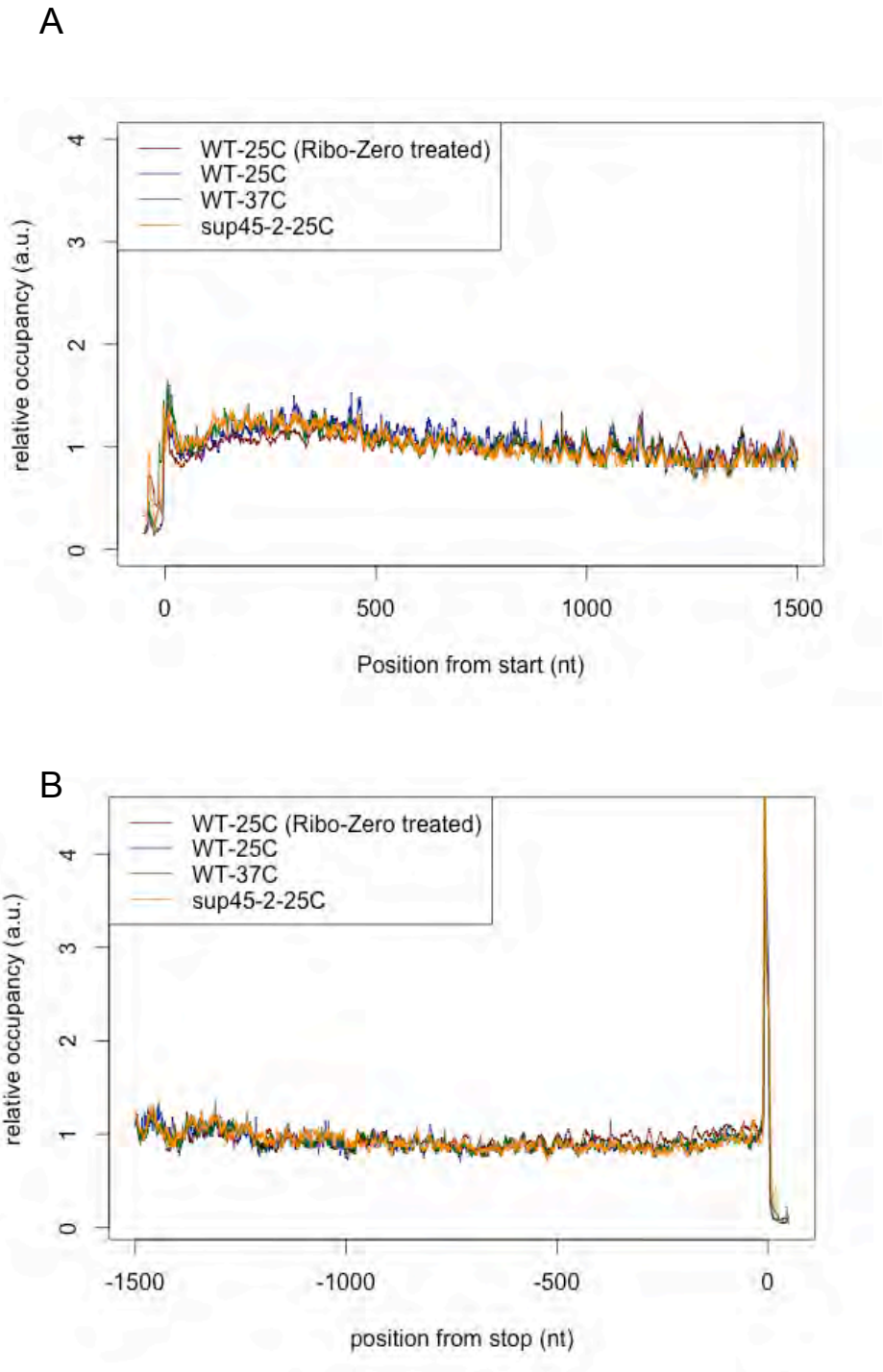

Figure 3.8 – Total ribosomes are evenly distributed throughout the ORFs. Metagene analyses of ribosome density were derived for mRNAs (with ORF length of greater than 250 nt) aligned from their start (A) or stop codon (B) and averaged across them. RPF counts from four independent experiments are shown in indicated colors.

a.u. = arbitrary units

Numbers of mRNAs analyzed are shown in Table B.3.

Detailed descriptions for WT-25C (Ribo-Zero Treated), WT-25C, WT-37C, and sup45-2-25C are shown in Table B.2.

Figure 3.9 – Upf1-bound 80S ribosomes are enriched at the 3'-ends of ORFs (and depleted at the 5'ends).

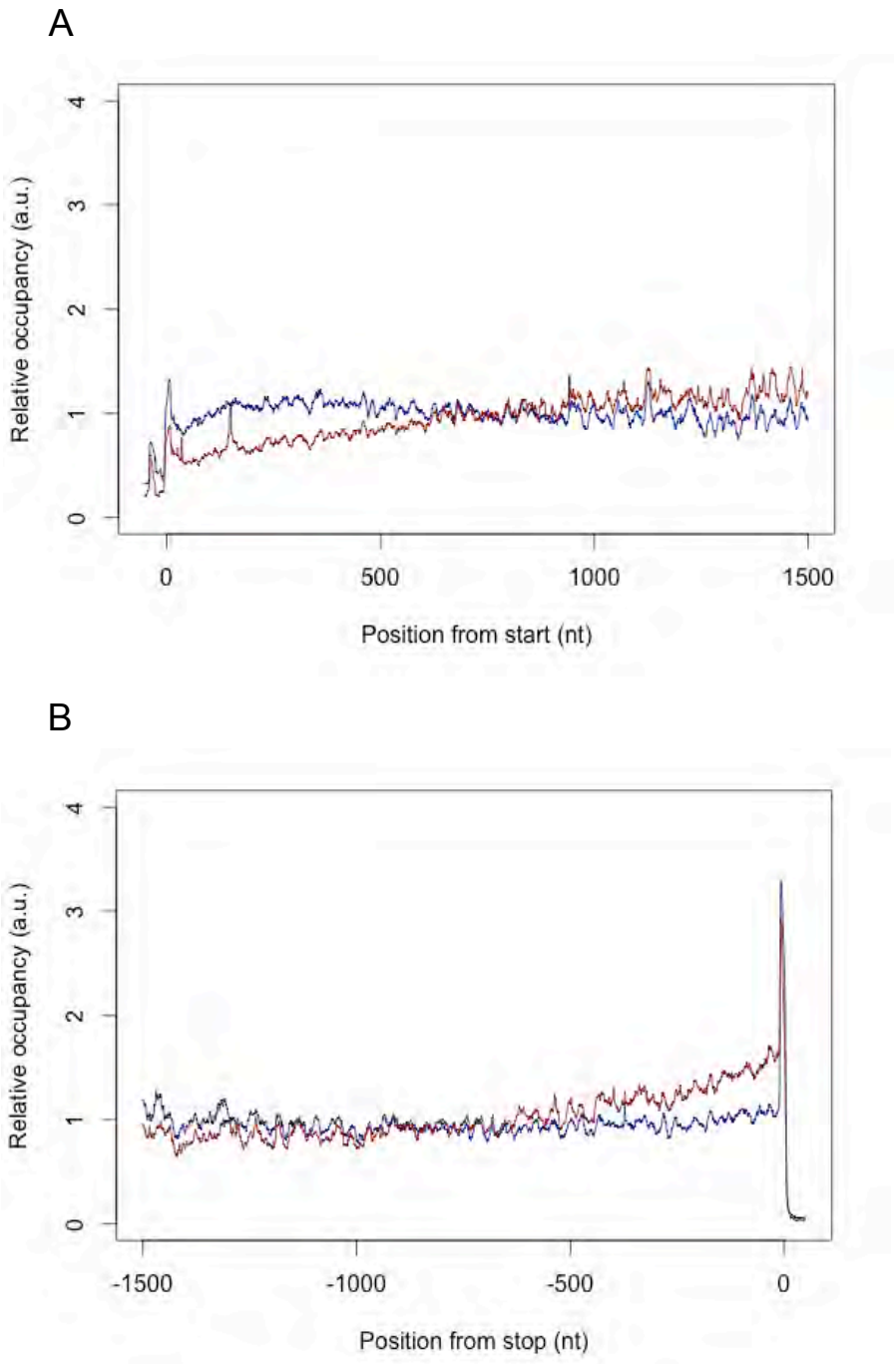

Figure 3.9 – Upf1-bound 80S ribosomes are enriched at the 3'-ends of ORFs (and depleted at the 5'ends).

Metagene analyses of ribosome density were derived for mRNAs (with ORF length greater than 250 nt) aligned from their start (A) or stop codon (B) and averaged across them. Upf1-footprint counts are shown in red and total footprint counts in blue.

a.u. = arbitrary units

Number of mRNAs analyzed shown in Table B.3.

toward the 3′ ends of ORFs (Figure 3.9.B). These results indicate that: (i) Upf1 binds to ribosomes associated with most mRNAs, not just a subset of mRNAs, and (ii) this association is not restricted to ribosomes poised at termination codons. Both observations suggest that the region encompassed by several hundred nucleotides upstream of termination codons may be a “window” in which factors associated with termination begin to assemble a termination-competent mRNP, and that pre-associated Upf1 is most likely activated for NMD function at a PTC. Further support for these conclusions came from observing the same result in all four data sets (Figure B.2).

To further define the relative ribosome position in a given mRNA, we implemented a new metric, namely the relative ribosome position (RRP). RRP is defined as the distance from the initiation codon, expressed as a fraction of ORF length, at which a given percentage of reads (ribosome-protected fragments) occur, e.g., rr50 is the location where 50% of the total reads mapped to that gene have been counted (starting from the initiation codon). A low RRP value would indicate that ribosomes are located disproportionately early on the mRNA because the majority of reads to skew toward the first-half of an ORF (Figure 3.10). Using these definitions, we performed genome wide RRP analysis and showed that rr-values of Upf1-bound ribosomes were higher than those of total ribosomes, indicating Upf1’s bias towards the 3’-ends of ORFs (Figure 3.11). For example, the rr50 of Upf1-Ribo-Seq samples is 0.75, compared to 0.5 for that of Total-Ribo-Seq (Figure 3.11; compare solid blue line and dashed blue line). These results from RRP analyses

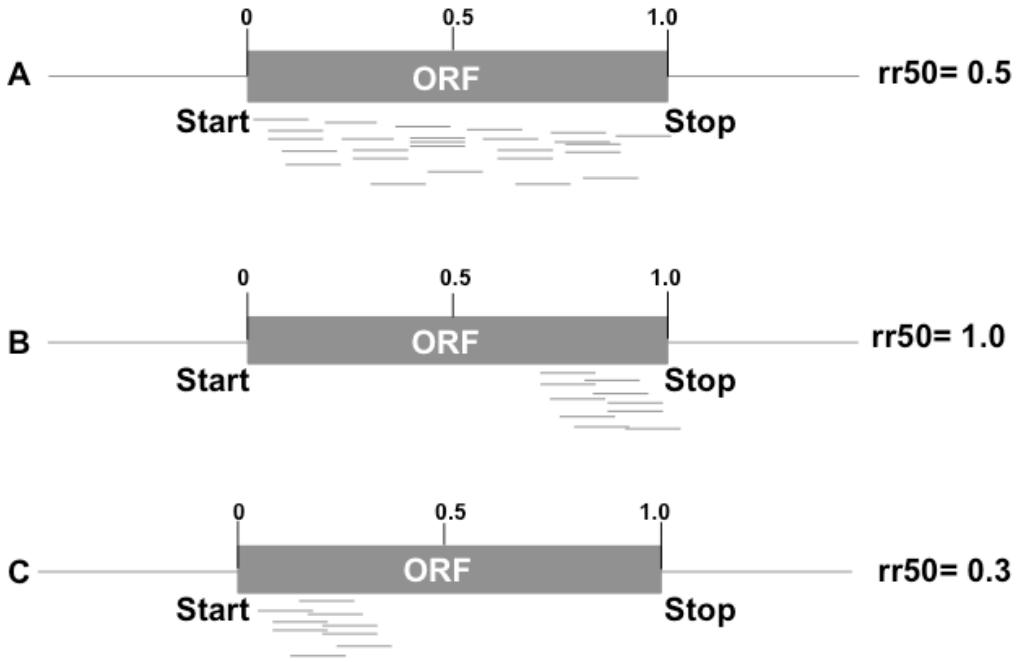

Figure 3.10 – A new analytical tool: RRP (Relative Ribosome Position). Ribosome-protected fragments (RPFs) are uniformly distributed in a "normal" mRNA (A), or largely localized near the 3'end of a mRNA (B), or mainly present near the 5' end of a mRNA (C). Hypothetical rr50 values are indicated.

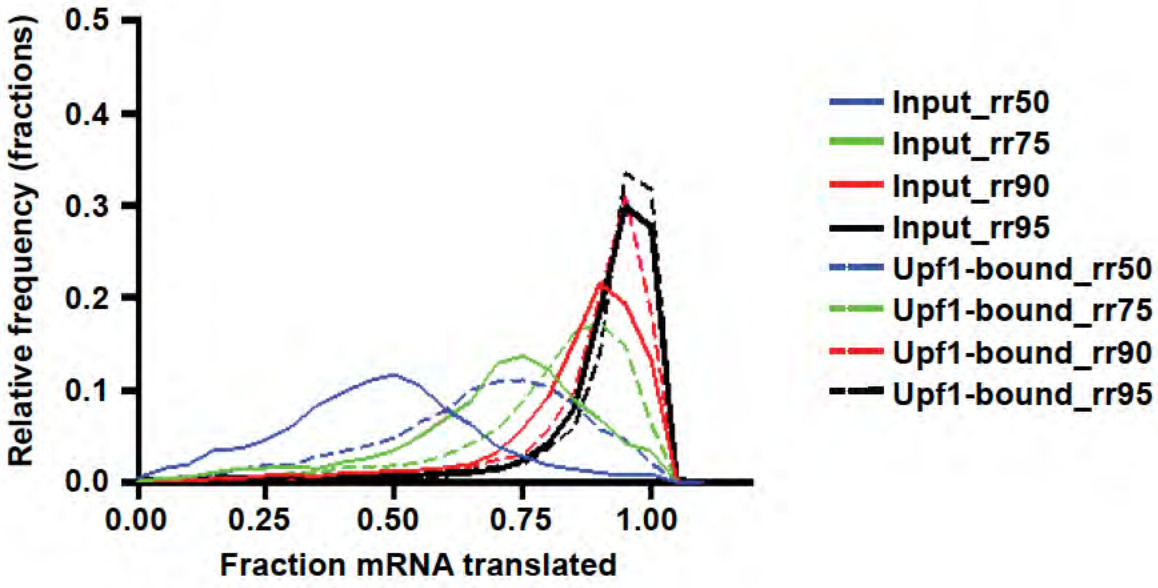

Figure 3.11 – Upf1 is preferentially associated with ribosomes near the 3'-ends of ORFs.

Calculated values of rrp50, rrp75, rrp90, rrp95, and rrp100 were plotted into a frequency distribution curve to show the distributions of relative ribosome positions (RRP) for mRNAs in the wild-type Total-Ribo-Seq library (solid lines) and the Upf1-Ribo-Seq library (dashed lines).

also suggest that Upf1 binding appeared to favor ORF 3′-ends. Again, these observations were consistent in all Upf1-Ribo-Seq libraries (Figure B.3).

These conclusions were tested further by analyzing Upf1 occupancy of ribosomes associated with specific transcripts. As shown in Figure 3.12, individual normal mRNAs, such as those encoded by the *PGK1, ACT1, RSA4, and GLR1* genes, manifested enrichment for Upf1-associated ribosomes near the 3'-ends of coding regions, consistent with results from both computational analyses. In addition, previous studies show that NMD targets have shorter ORF lengths, but long 3'-UTR lengths (Decourty et al., 2014). We found that these NMD-inducing features did not change the binding pattern of Upf1 binding to translating ribosomes (Figure 3.13 and 3.14). Collectively, all these results suggested that the distribution of Upf1-associated ribosomes is skewed towards 3'-ends of most mRNA ORFs, possibly reflecting the stable interaction of Upf1 with ribosomes near the 3' ends of ORFs in any given mRNA.

Upf1-enriched mRNAs show lower ribosome occupancy

To determine whether Upf1 has a bias for a specific subset of translationally active transcripts, we compared reads from Upf1-associated ribosomes to those obtained from total ribosomes. Transcripts were considered enriched in Upf1-associated ribosomes if RPF densities showed at least a 2-fold difference between Total-Ribo-Seq and Upf1-Ribo-Seq libraries. These analyses revealed that 1630 transcripts were enriched with Upf1-bound ribosomes. Since NMD is a translation-dependent pathway, we next examined the relationship

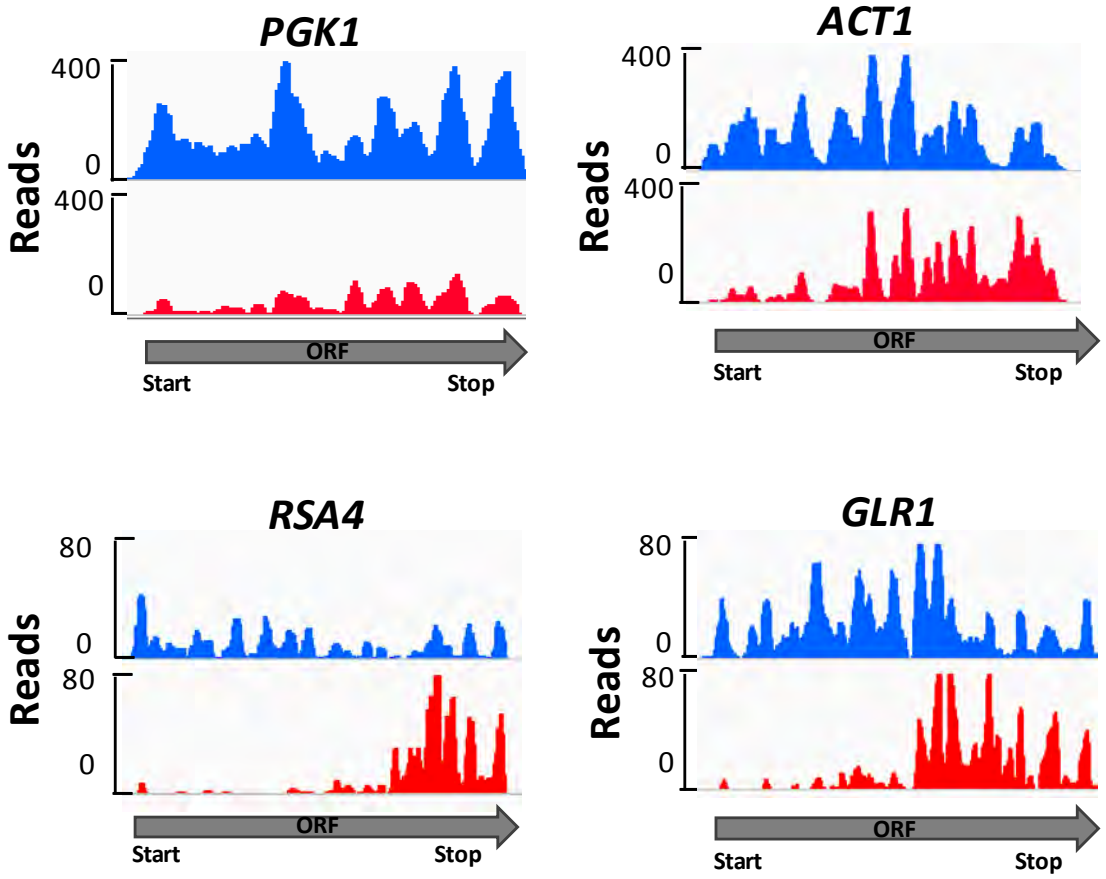

Figure 3.12 – Upf1-bound ribosomes are distributed toward the 3'-ends of normal mRNAs.

Coverage density maps were generated on the IGV browser for selected mRNAs. Read counts in Upf1-bound ribosomes are shown in red and compared to total ribosomes in blue.

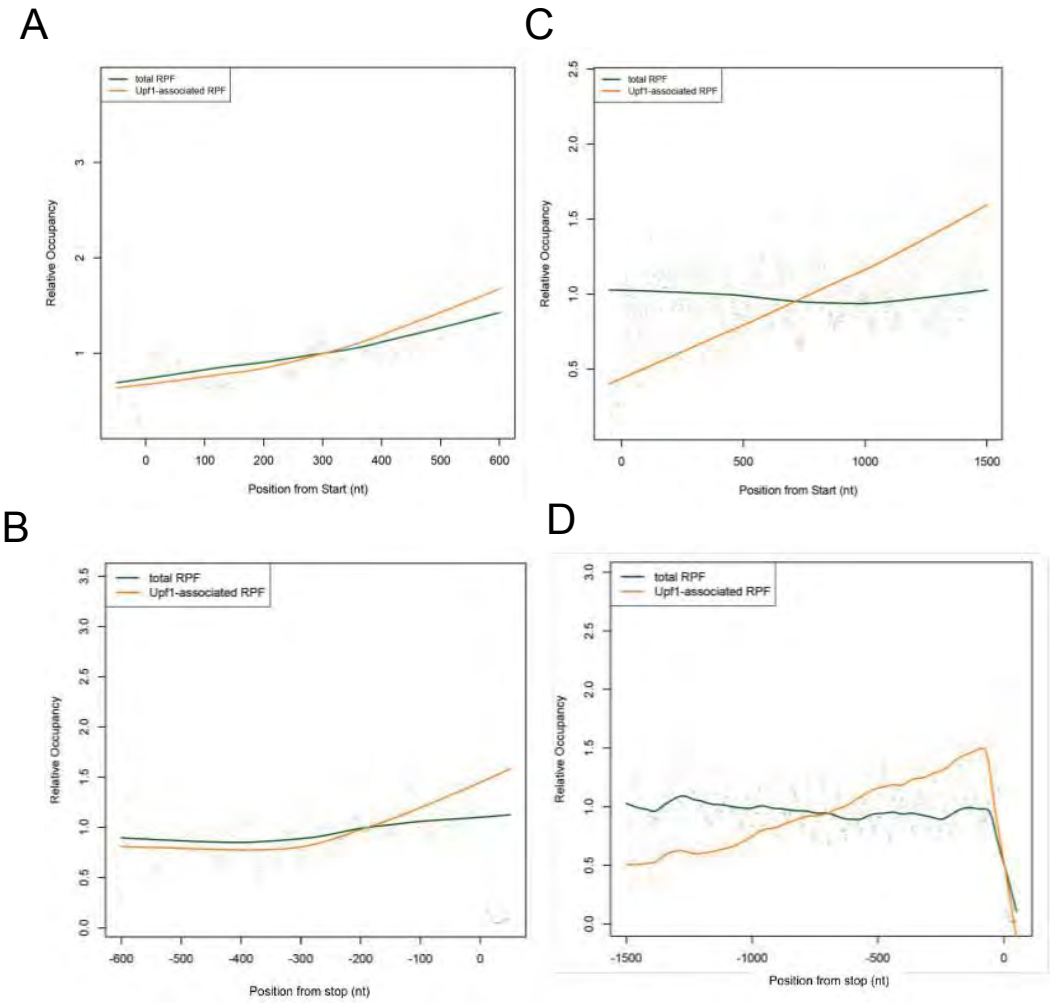

Figure 3.13 – Upf1-bias towards 3' ends of ORFs is not ORF-length dependent.

Metagene analyses of ribosome density were derived for mRNAs with ORF length between 400-600 nt (total 693 mRNAs) and 1300-1600 nt (total 744 mRNAs) aligned from their start (A,C) or stop codon (B,D) and averaged across them. Upf1-footprint counts are shown in orange and total footprint counts in green.

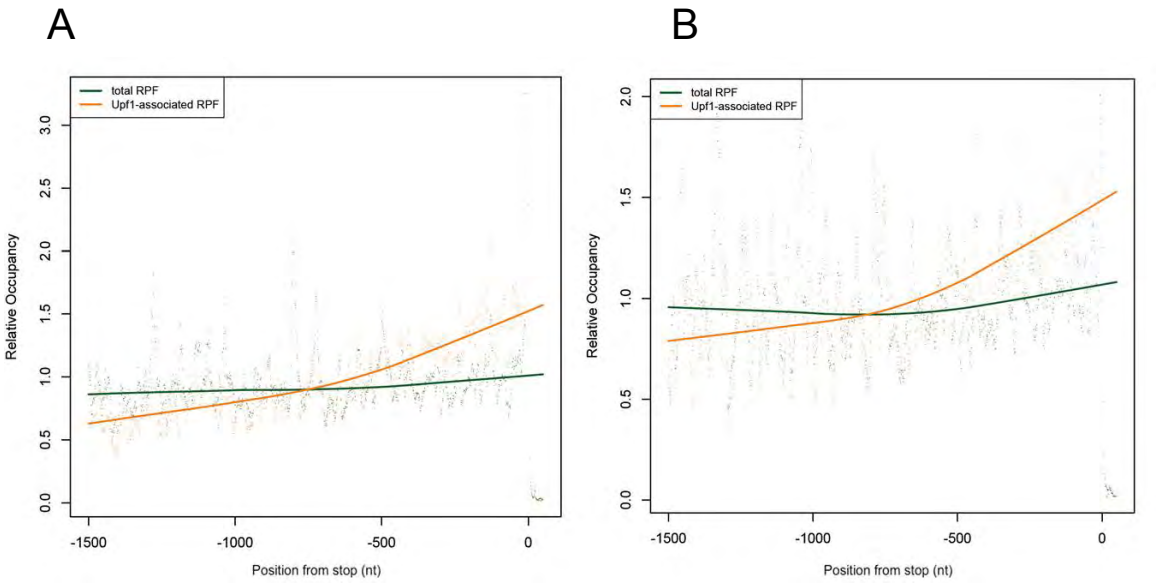

Figure 3.14 – Upf1-bias towards 3' ends of ORFs is not governed by the 3'-UTR length.

Metagene analyses of ribosome density were derived for mRNAs with short UTRs (A) and long UTRs (B) aligned from their stop codon and averaged across them. Upf1-footprint counts are shown in orange and total footprint counts in green.

The Long-UTR group is defined as mRNAs with 3'-UTR lengths greater than 250 nt (406 mRNAs).

The Short-UTR group is defined as mRNAs with 3'-UTR lengths of less than 50 nt (638 mRNAs).

between the enrichment of Upf1 binding and translation efficiency (TE), which is the extent of footprint recovery normalized to underlying mRNA abundance. We calculated TE (which is also referred to as ribosomal occupancy) by dividing the ribosome footprint density of the ORF by the mRNA-Seq read density of the same region (Ingolia et al., 2009). Of the 1630 putative targets that were enriched more than 2-fold in the Upf1-Ribo-Seq dataset, about half of the mRNAs have low ribosomal occupancy (852 out of 1630), indicating that Upf1-enriched transcripts have fewer associated ribosomes than non-enriched targets.

Several earlier studies suggest that Upf1 specifically associates with *bona fide* NMD substrates (He et al., 2003; Johansson et al., 2007; Johns et al., 2007; Kurosaki and Maquat, 2013). To determine whether the transcripts enriched in the Upf1-Ribo-Seq approach represent direct substrates of the NMD pathway, we compared the transcripts which showed >2-fold increases in our Upf1-Ribo-Seq dataset with two datasets of previously characterized putative NMD targets, which were identified as co-purified mRNAs following Upf1-TAP pull-down (Johansson et al., 2007) or mRNAs of significantly increased abundance in *upf1Δ* cells (He et al., 2003). These comparisons revealed poor overlaps, with at best only about 15% of the Upf1-Ribo-Seq enriched transcripts detected in both Upf1-TAP pull-downs and *upf1Δ* cells (Figure 3.15). We suspect that this discrepancy may be due to technical differences in sample preparation. While Upf1-RiboSeq experiments enriched for the translationally active population of transcripts, the Upf1-TAP experiments could recover mRNPs at all stages of NMD, including final stages in which Upf1 may no longer be ribosome-associated. Interestingly,

of 589 NMD-regulated transcripts that were identified from Upf1-TAP pull-downs (Johansson et al., 2007) and 680 from u*pf1Δ* cells (He et al., 2003), 219 (46%) and 296 (62%) respectively had low ribosome occupancy in our profiling experiments, providing further evidence that translation of NMD-sensitive transcripts may be significantly reduced.

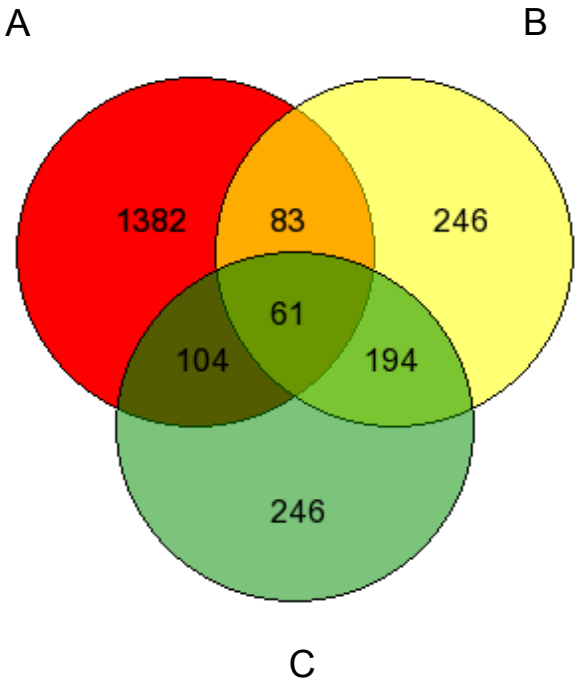

Figure 3.15 – Upf1-enriched transcripts from Ribo-Seq experiments compared to NMD substrates identified in previous studies.

The Venn diagram depicts the overlap of (A) transcripts ≥2-fold enriched for Upf1 in the Upf1-Ribo-Seq library, (B) transcripts with ≥2-fold enrichment in Upf1-TAP pulldowns (Johansson et al., 2007), and (C) transcripts that increase ≥2-fold in *upf1Δ* cells (He et al., 2003).

Discussion

To address the timing and ORF location of Upf1 association with translating ribosomes, we undertook a genome-wide assessment of Upf1:ribosome interaction and obtained results supporting a novel stochastic model of Upf1 dynamics during translation. By mapping the ORF positions associated with Upf1 binding sites on translating ribosomes, we found that most translationally active transcripts are targeted by Upf1 (Table B.3). The stable binding of Upf1 to most translating mRNAs is consistent with published studies in mammalian cells (Gregersen et al., 2014; Hurt et al., 2013; Kurosaki and Maquat, 2013) which showed that Upf1 binds promiscuously to mRNA coding regions and 3′-UTRs in a translation-dependent manner.

Our results indicate that the binding of Upf1 to mRNA-associated ribosomes is biased towards ribosomes translating the 3'-ends of ORFs. Upf1-associated ribosomes were relatively absent in ORF 5' regions, and their enrichment in the 3'-ends of ORFs extended to hundreds of nucleotides upstream of the normal termination codon (Figure 3.9.B). These results suggest that: (i) Upf1 transiently binds to ribosomes translating most mRNAs, including non-NMD targets, and (ii) ribosomes in transit across a large region upstream of termination codons accommodate more stable Upf1 binding, possibly because of concurrent ribosome association or interaction with additional factors. Interestingly, this pre-termination region is reminiscent of the position-dependence of NMD activation (Figure 3.16). In *S. cerevisiae,* PTCs in approximately the 5' half to two-thirds of ORFs promote mRNA destabilization,

while PTCs near the 3'-ends of ORFs have little or no effect on mRNA stability (Peltz and Jacobson, 1993; Yun and Sherman, 1995). These observations lead us to speculate that termination is not actually commenced spontaneously at a stop codon, but occurs as a series of events in which an early phase is the assembly of a termination-competent mRNP near the end of the process of elongation. It should be noted, however, that our data might be biased by the utilization of an overexpressed *UPF1* allele for affinity-purification of Upf1-bound ribosomes.

We observed that about half of Upf1-enriched transcripts have low ribosome occupancy, suggesting that Upf1-targeted mRNAs have low translation initiation rates or higher rates of ribosome stalling or spontaneous dissociation. These findings are consistent with previous studies showing that Upf1 association with a nonsense-containing mRNA leads to decreased translation efficiency (Isken et al., 2008; Muhlrad and Parker, 1999b) and to the targeting of nonsense-containing mRNAs to cytosolic P-bodies (Durand et al., 2007; Fillman and Lykke-Andersen, 2005; Sheth and Parker, 2006; Stalder and Muhlemann, 2009).

Our results lead us to propose a stochastic binding model for Upf1 interaction with the 40S subunits of translating ribosomes. This binding may be inefficient or otherwise impaired for ribosomes elongating in the 5' halves of ORFs, but is somehow enhanced or stabilized as ribosomes progress closer to normal termination codons. Since normal termination codons do not stimulate NMD there must be a feature of premature translation termination that

distinguishes NMD targets from normal transcripts. For example, the selective activation of NMD at PTCs may require the functional activation of ribosome-bound Upf1 by the recruitment of other NMD-activating factors such as Upf2 and Upf3, i.e., it may be the latter factors whose ribosome association is really PTC specific. Evidence supporting this model includes: (i) the distribution of Upf1 across polysomal fractions with or without Upf2 and/or Upf3 depletion (Atkin et al., 1997; Min et al., 2013), i.e., Upf2 and Upf3 are not involved in the initial recruitment of Upf1 to translating ribosomes, and (ii) Upf2 and Upf3 have been shown to activate the ATP-dependent RNA helicase activity or RNA-dependent ATPase activity of Upf1 *in vitro*.

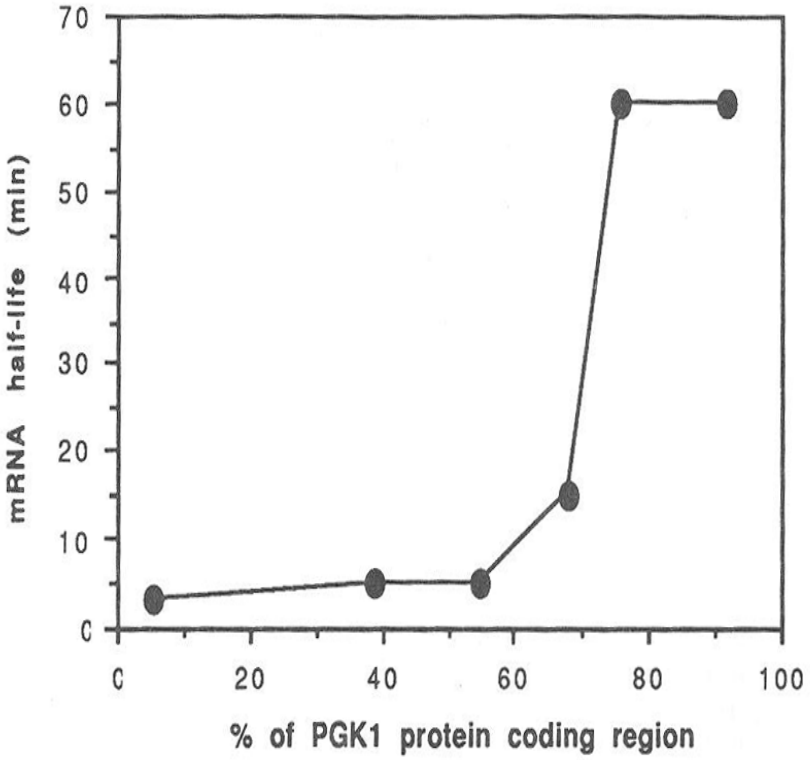

Figure 3.16 – Position effect of nonsense codons on mRNA stability on nonsense-containing mRNAs in yeast.

Locations of termination codons in the *PGK1* mRNA versus mRNA half-life measured in wild-type cells. This observation has been confirmed in the *PGK1, CYC1, HIS4,* and *Matα1* mRNAs (Peltz et al., 1993a; Yun and Sherman, 1995). From Peltz and Jacobson, 1993b.

CHAPTER IV

General Discussion

Studies in multiple model organisms over the past 20 years have led to the identification and characterization of the major regulatory factors in the NMD pathway and have provided considerable insights into the nature of NMD substrates and the initiation of their decay. But our understanding of the underlying molecular mechanism of NMD is not complete. We have yet to understand the recruitment of these factors to NMD substrates or the different steps involved in NMD activation. My thesis work presents results that advance our understanding of how the central NMD regulator Upf1 associates with its target mRNAs. In particular, I have focused on understanding the target of Upf1 binding to ribosomes, and the timing of that interaction on actively translating ribosomes. My experiments provide insight into the mechanisms involved in discriminating NMD substrates from non-substrates, and point out limitations of current models, and lead to a new model for NMD activation.

Direct interaction of Upf1 with ribosomes

Work done in Chapter II of my thesis attempted to answer the question of how Upf1 is targeted to translating mRNPs. We localized Upf1 to the 40S subunit, identified a specific Upf1-interacting ribosomal protein, and obtained evidence for additional Upf1:40S interactions. Upf1 is specifically immunoprecipitated with tagged 40S ribosomal subunits and not 60S subunits

(Figure 2.2). Such association is likely mediated by a direct interaction between Upf1 and the 40S subunit, but not through mRNA (Figure 2.3). Upf1:40S association is sufficiently stable to resist either high salt-induced or puromycin-triggered ribosomal dissociation (Figure 2.4). Further we determined that the ATP hydrolysis activity of Upf1 is required for the association of Upf1 with 40S subunits (Figure 2.4). Importantly, stable association of Upf1 with the 40S subunit is independent of Upf2 or Upf3, or translation termination factors eRF1 and eRF3 (Figures 2.5 and 2.6).

According to some current NMD activation models (cited in Chapter I), Upf1 is thought to be selectively recruited to NMD-targeted mRNAs during translation, most likely through interactions with the release factors eRF1 and eRF3 located on prematurely terminating ribosomes. Experiments done in yeast and mammalian cells have indicated that Upf1 association with a prematurely terminating ribosome may be attributable to direct interactions with the release factors, eRF1 and eRF3 (Czaplinski et al., 1998; Ivanov et al., 2008; Kashima et al., 2006; Singh et al., 2008). However, our data indicate that stable Upf1:40S association can occur independently of concurrent release factor binding to the ribosome (Figure 2.6) although our results do not rule out the possibility that Upf1's initial association with the 40S subunits depends on the presence of the release factors.

Our findings for direct binding of Upf1 to ribosomes are consistent with previous studies showing that NMD requires ongoing translation and that the majority of yeast and human Upf1 is associated with polyribosomes, 80S

ribosomes, and 40S ribosomal subunits (Atkin et al., 1995; Ghosh et al., 2010; Min et al., 2013; Pal et al., 2001). Additional links between NMD and translation came from studies demonstrating that drugs or mutations that inhibit translation also inhibit mRNA decay (Beelman and Parker, 1994; Jacobson and Peltz, 1996; Parker and Jacobson, 1990) and that initiation of the decay of nonsense-containing mRNAs occurs while those transcripts are associated with polyribosomes (Hu et al., 2010; Zhang et al., 1997). Taken together, our current results and those in the literature lead me to propose that Upf1 is most likely associated with translationally active mRNAs via direct interaction with ribosomes.

Two recent reports raise challenges to the notion of translation-dependent recruitment of Upf1 to mRNPs (Hogg and Goff, 2010; Zünd et al., 2013). Hogg and Goff demonstrated that Upf1 binding to mRNAs occurred in a 3'-UTR length-dependent manner, even when translation was inhibited, and a CLIP study from the Muhlemann lab reported that Upf1 targets the 3'-UTRs of both NMD-sensitive and NMD-insensitive transcripts. Upon translation inhibition with puromycin or cycloheximide, the relative distribution of Upf1 in the latter study was seen to shift to mRNA coding sequences (CDS) (Zund et al., 2013). Based on these results, the authors suggested that Upf1 may target most mRNAs preceding their translation, only to be displaced from the CDS by elongating ribosomes. The discrepancies between these results and my own might be due to technical limitations in the Zund et al. studies, such as underestimating Upf1 association with ribosomes by size selection against large ribosomal complexes

during sample preparation, or by discarding rRNA reads during data analysis. Another possible cause for the discrepancies between these results and my own might be that two distinct populations of Upf1 were being analyzed. Upf1 co-sediments with both polysomal mRNPs and free mRNPs (Mangus and Jacobson 1999). These results raise the possibility that Upf1 appears to exist in two distinct populations, one of which is associated with translating ribosomes and another with free cytoplasmic mRNP particles.

Upf1 associates with elongating and terminating ribosomes

Work done in Chapter III of this thesis attempted to determine when during translation Upf1 associates with ribosomes, and whether such association is unique to NMD substrates. We demonstrated that Upf1 binds to ribosomes that are translating mRNAs, including non-NMD targets, and identified an ORF region where stable Upf1:ribosome association occurs. We detected a relative dearth of Upf1 association with ribosomes located in the 5' regions of ORFs (Figure 3.9.A), and a continuous increase of Upf1:ribosome association toward the 3′ ends of ORFs (Figure 3.9.B). Importantly, Upf1:ribosome association favored a 3'-ORF region that encompassed hundreds of nucleotides upstream of the normal termination codon (Figure 3.9.B). Such association was not dependent on NMD-inducing features such as long 3'-UTRs or ORF lengths (Figures 3.13 and 3.14).

Our findings are in disagreement with models implying that Upf1 is selectively recruited to NMD substrates undergoing premature termination (Kervestin and Jacobson, 2012). Our findings also contradict results from RNA-

immunoprecipitation experiments demonstrating that Upf1 preferentially associates with NMD-targeted mRNAs in yeast, worms and mammals (Johansson et al., 2007; Johns et al., 2007; Kurosaki and Maquat, 2013). It should be noted, however, that our data might be biased by the utilization of an overexpressed *UPF1* allele for affinity-purification of Upf1-bound ribosomes. Nonetheless, I speculate that this discrepancy could be reconciled by two explanations. First, while our ribosome profiling experiments enriched for the translationally active population of transcripts, RIP experiments could recover mRNPs at all stages of NMD, including final stages in which Upf1 may no longer be ribosome-associated. Second, binding of Upf1 to mRNAs does not necessarily indicate that such mRNAs would be targeted by NMD. For example, the selective activation of NMD at PTCs may require the functional activation of ribosome-bound Upf1 by the recruitment of other NMD-activating factors such as Upf2 and Upf3.

A stochastic binding model for Upf1 interaction with the 40S subunits of translating ribosomes

Collectively, our results lead us to propose a stochastic binding model in which Upf1 routinely associates with ribosomes of all translationally active mRNAs and a ribosomal encounter with a PTC stabilizes this association, activates Upf1, and triggers the onset of NMD. As shown in Figure 4.1, I propose that during normal translation termination, Upf1 associates transiently with elongating ribosomes on all translating mRNAs via 40S subunit interaction. Such

association becomes stable or enhanced near the end of the ORF (or a pre-termination region, which couples elongation and termination steps). This region might comprise signals or stabilizing factors that accommodate more stable Upf1 binding. Another possibility is that ribosome dynamics in this region might be slow due to the local context of mRNP nature, allowing the stable binding of Upf1. During premature translation termination, Upf1 association with translating ribosomes becomes stable near PTCs, most likely due to an atypical conformation for a prematurely terminating ribosome (Figure 4.2). Ribosome-bound Upf1 could then recruit Upf2 and Upf3 to prematurely terminating ribosomes, subsequently activating the Upf1's ATPase activity to promote the dissociation and recycling of the terminating ribosome. After the release of the 60S subunit and the deacylated tRNA from the terminating mRNP, Upf1 could remain bound with the 40S subunit to the mRNA, and promote translation reinitiation and ribosome recycling or/and recruit the mRNA degradation machinery for rapid mRNA decay.

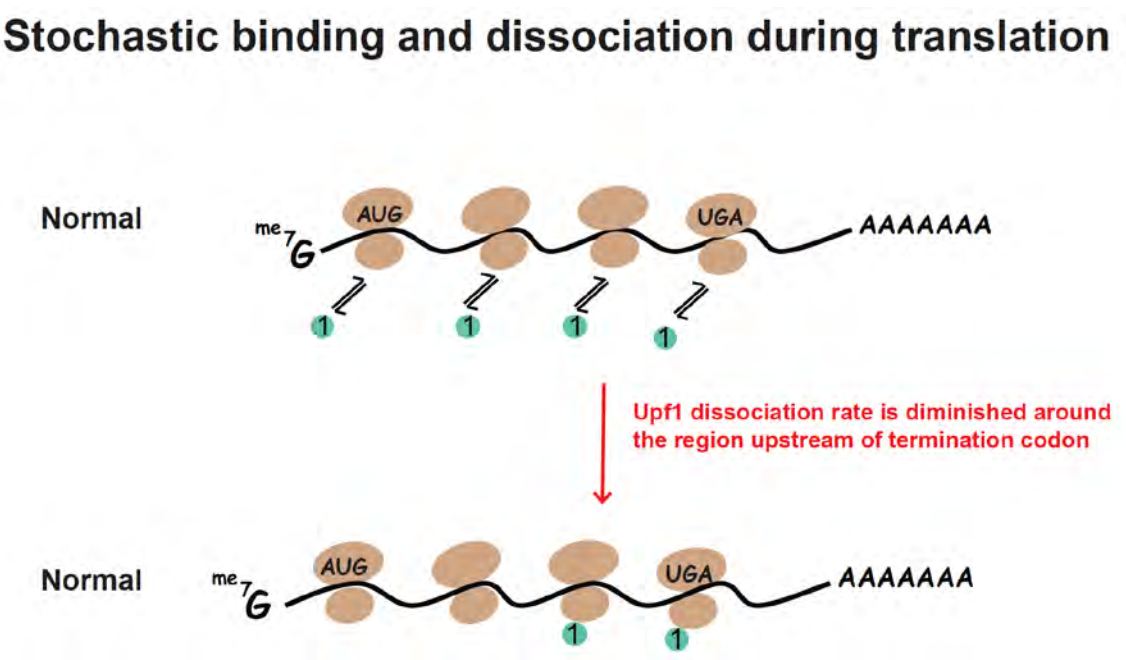

Figure 4.1: Stochastic binding of Upf1 during normal translation termination. Upf1 may associate routinely with elongating ribosomes on all translating mRNAs. In this model, Upf1:ribosome association becomes stable near pre-termination region.

Shaded brown ovals= ribosomal subunits; Black line= mRNA; 1 represents Upf1.

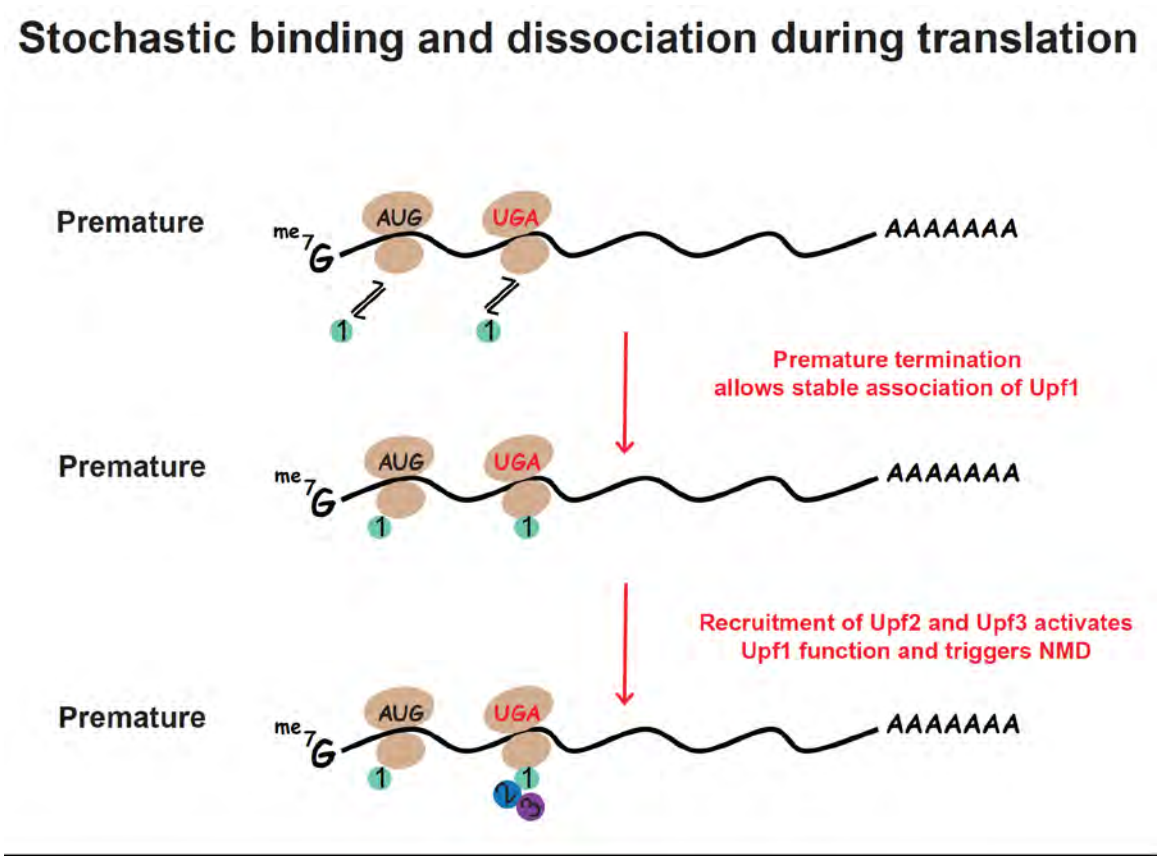

Figure 4.2: Binding of Upf1 is stabilized during premature translation termination. In this model, Upf1:ribosome association becomes stable near PTCs and the recruitment of Upf2 and Upf3 at prematurely terminating ribosomes triggers NMD.

Shaded brown ovals=ribosomal subunits; Black line=mRNA; 1,2, and 3 represent Upf1,Upf2, and Upf3, respectively.

Future directions

NMD requires the functions of the core Upf factors, yet the timing and the location of the association of these factors with terminating ribosomes are only beginning to be understood. To gain a better understanding of how Upfs are targeted to mRNPs and how Upf1 functional activation governs NMD, several key questions need to be addressed.

1. Do Upf2 and/or Upf3 manifest the same patterns and timing of ribosomal association as Upf1 or is their binding specificity suggestive of a role in targeting PTC-containing mRNAs?
2. Does functional activation of ribosome-bound Upf1 at a PTC depend on the presence of Upf2 and/or Upf3?
3. What parameters, e.g., sequence features or distance from a particular site, dictate Upf1 distribution near termination codons?
4. Do the eRFs and/or Pab1 manifest the same termination region association as Upf1? If so, is there other evidence for the formation of a “pre-termination complex”?

APPENDIX A

Cryo-EM structures of 40S ribosomal subunits and 80S ribosomes harboring bound Upf1

Contributions to this appendix

Robin Ganesan performed the affinity purifications of Upf1-bound 80S ribosomes and 40S subunits from total ribosome samples that I provided. Cryo-EM and data analysis was done in collaboration with the Spahn lab (Dr. Christian Spahn, Dr. Tatyana Budkevich, and Dr. Elmar Behrmann) from the Institute of Medical Physics and Biophysics, Charité-Universitätsmedizin, Berlin, Germany.

Introduction

Nonsense-mediated mRNA decay (NMD) is a cytoplasmic surveillance mechanism that degrades mRNA transcripts that contain PTCs (Kervestin and Jacobson 2012). Factors that regulate NMD in the yeast *Saccharomyces cerevisiae* include the highly conserved but non-essential proteins, Upf1, Upf2, and Upf3. Upf1, the key regulator of NMD, belongs to helicase superfamily I (SF1), with two RecA-like domains in tandem at its C-terminus (Kervestin and Jacobson 2012). Purified Upf1 has RNA-binding, as well as RNA-dependent ATPase and RNA helicase activities, both of which are required for NMD activity (Czaplinski et al., 1998; Clerici et al., 2009). An N-terminal Zn^{2+}-finger-like domain in Upf1 interacts with a C-terminal domain of Upf2, an acidic protein with multiple MIF4G (middle portion of eIF4G) domains. In turn, a MIF4G domain in the C-terminal half of Upf2 interacts with Upf3, a basic protein with an RNA binding domain (RBD) (Bhattacharay 2000; He et al., 1996; 1997). *In vitro* binding assays indicated that both human and yeast Upf1 interact with Upf3 via Upf2 (Chamieh et al., 2008; He et al., 1997). Overexpression of Upf1 can compensate for mutations in Upf2 and Upf3, but not *vice* versa (Maderazo et al., 2000) and the maximal *in vitro* activation of the Upf1 ATPase and helicase activities requires both Upf2 and Upf3 (Chamieh et al., 2008). These observations imply that Upf1 is the key effector of NMD, whereas Upf2 and Upf3 are likely to be regulators of Upf1 function.

In addition to the presence of NMD factors, ongoing translation has been found to be a prerequisite for nonsense-mediated decay. Consistent with this

requirement, Upf proteins and mRNA decay intermediates are associated with polysomes (Atkins et al., 1995; 1997; Mangus and Jacobson 1999; Zhang et al., 1997; Hu et al., 2010). Upf1 interacts with the release factors, eRF1 and eRF3 (Czaplinski et al., 1998; Ivanov et al., 2008; Kashima et al., 2006). In human cells, Upf1 associates with eRF-bound ribosomes forming the SURF (Smg-1-Upf1-Release Factors) complex (Kashima et al., 2006; Yamshita et al., 2009). Previous studies from our lab indicate that Upf1 associates preferentially with 40S subunits, but not with 60S subunits (Ghosh et al., 2010; Min et al., 2013). We also identified a specific Upf1-interacting ribosomal protein, Rps26 of the 40S subunit, and such interaction depends on the Upf1 CH domain (Chapter II).

In light of the known ribosome structure and the size of Upf1, interaction with Rps26 was not consistent with models of concurrent stable Upf1 interaction with the release factors (Min et al., 2013; Kervestin and Jacobson 2012). Given the fact that Upf1 interacts with factors involved in translation such as eIF3 subunits, release factors, and other 40S subunit proteins (Min et al., 2013; Isken et al., 2008), as well as the dynamic alterations of ribosome structure during the elongation cycle (Scheres 2010), there may be multiple Upf1 binding sites on the ribosome as a consequence of distinct steps in Upf1 function (Fu and Frank 2007). To gain structural insights into the topography and heterogeneity of Upf1 association with the 40S subunit or 80S ribosome, we employed multiparticle cryoelectron microscopy (cryo-EM), to localize the 40S and 80S binding sites for Upf1.

Results and Discussion

For purification of 40S subunits and 80S ribosomes, we employed the ribosomal purification protocols used in CHAPTER II and CHAPTER III, respectively. High-salt washed 40S ribosomal subunits were purified without prior puromycin release from cells harboring wild-type *UPF1* and RNase I-digested 80S ribosomes were purified by sucrose gradient sedimentation from cells harboring a *upf1* C62Y allele (mutation in the N-terminal CH domain) that precluded Upf1:Upf2 interaction to reduce sample heterogeneity (See APPENDIX C for methods). To obtain ribosome preparations highly enriched for Upf1, we utilized the same affinity-based purification procedure described in CHAPTER III (using a strain over-expressing His-tagged Upf1 and Co^{2+}-based affinity chromatography). Upf1-enriched samples, along with unpurified ribosomes and 80S ribosomes and 40S subunits ribosomes from a *upf1Δ* control strain, were frozen and sent to the Spahn lab for Cryo-EM analysis (Loerke and Spahn 2010).

Cryo-EM was used to reconstruct 40S subunits associated with wild-type Upf1 and 80S ribosomes associated with mutant Upf1 C62Y. We used computational sorting (see APPENDIX C for methods) to obtain electron density maps for these ribosomal complexes associated with Upf1 (Figure A.1) at a magnification of ~42,000. The analysis of subunits associated with WT Upf1 led to the localization of Upf1 to a density proximal to the mRNA entry site (Figure A.1.A). Analyses of mutant Upf1 associated with 80S ribosomes identified two striking features when compared to control structures of 80S ribosomes (Figure

A.1.B): (i) an extra density on the head of the small 40S subunit that is close to the same location seen in our WT Upf1-associated 40S samples, and (ii) a pronounced P-protein stalk. The latter is usually very flexible and generally observed only upon ligand binding (Scheres 2010; Leschziner and Nogales 2007), and presumably seen here as a consequence of Upf1 binding. The novel density observed on the head of the 40S subunit is smaller than that expected for the known size of Upf1, indicating that it likely represents the most stable region of interaction, or a primary binding site for Upf1 on the 80S ribosome. Both the 40S and 80S Upf1-associated structures await further high resolution structures (that will be obtained when the Spahn lab commences use of its own direct electron detector) and analyses of the consequences of additional *upf* mutations.

In summary, to gain insight into possible Upf1 functions other than the stimulation of mRNA decay we initiated high resolution analyses of Upf1 positioning on the ribosome by cryo-EM. We localized a Upf1-binding position on ribosomes near the mRNA entry channel (Figure A.1). Upf1 positioned near the mRNA entry channel may somehow influence subunit interaction, and a conformation shift upon Upf1 ATPase activation may promote dissociation of post-terminating mRNPs of PTC-containing mRNAs.

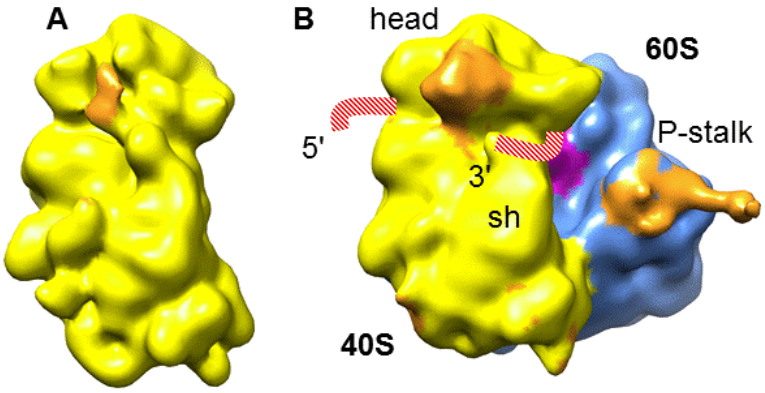

Figure A.1. Reconstructions of WT and mutant Upf1 bound to yeast 40S ribosomal subunits and 80S ribosomes. Upf1-associated 40S subunits (A) and Upf1 C62Y-associated 80S ribosomes (B) were purified and subjected to cryo-EM and image reconstruction. Densities shown in orange on the head of the 40S (yellow) and the P-stalk region of the 60S (blue) are not detected in conventional 40S or 80S samples. The shaded red line schematically approximates the mRNA track and the pink density inside of the 80S is the A-site tRNA. Sh=shoulder, a landmark for 40S topography. Magnification = 42,000x.

APPENDIX B

SUPPLEMENTARY DATA FOR CHAPTER III

Table B.1 – Description of sequencing libraries

Sample	Strain background	Growth condition	Library Description	Ribo-Zero Treatment (RZ)
WT 25°C (+RZ) Total Ribo-Seq	Wild-type	25°C	Total ribosomes	Ribo-Zero-treated
WT 25°C (+RZ) Upf1 Ribo-Seq	Wild-type	25°C	Upf1-enriched ribosomes	Ribo-Zero-treated
WT 25°C (+RZ) mRNA-Seq	Wild-type)	25°C	mRNA-seq	Ribo-Zero-treated
WT 25°C Total Ribo-Seq	Wild-type	25°C	Total ribosomes	no treatment
WT 25°C Upf1 Ribo-Seq	Wild-type	25°C	Upf1-enriched ribosomes	no treatment
WT 25°C mRNA-Seq	Wild-type	25°C	mRNA-seq	no treatment
WT 37°C Total Ribo-Seq	Wild-type	Temperature shift for 30 min at 37°C	Total ribosomes	no treatment
WT 37°C Upf1 Ribo-Seq	Wild-type	Temperature shift for 30 min at 37°C	Upf1-enriched ribosomes	no treatment
WT 37°C mRNA-Seq	Wild-type	Temperature shift for 30 min at 37°C	mRNA-seq	no treatment
sup45-2 25°C Total Ribo-Seq	*sup45-2*	25°C	Total ribosomes	no treatment
sup45-2 25°C Upf1 Ribo-Seq	*sup45-2*	25°C	Upf1-enriched ribosomes	no treatment
sup45-2 25°C mRNA-Seq	*sup45-2*	25°C	mRNA-seq	no treatment

Table B.2 – High-throughput sequencing statistics

Sample	# of reads	rRNA reads	Uniquely-mapped reads	Multi-mapped reads
WT 25°C (+RZ) Total Ribo-Seq	38,651,726	1,990,332 (5.1%)	25,788,665 (67%)	9,880,453 (25.6%)
WT 25°C (+RZ) Upf1 Ribo-Seq	38,189,844	2,236,064 (5.9%)	21,629,480 (57%)	5,752,224 (15.1%)
WT 25°C (+RZ) mRNA-Seq	38,372,050	7,349,319 (19.2%)	7,345,863 (19%)	19,003,276 (49.5%)
WT 25°C Total Ribo-Seq	32380744	27,971,204 (86.4%)	2,784,172 (9%)	1,287,171 (4%)
WT 25°C Upf1 Ribo-Seq	32454417	27,176,422 (83.7%)	1,902,839 (6%)	527,284 (2%)
WT 25°C mRNA-Seq	32264272	29,535,314 (91.5%)	1,190,774 (4%)	750,255 (4%)
WT 37°C Total Ribo-Seq	32,406,539	26,741,498 (82.5%)	3,993,082 (12%)	1,323,506 (1%)
WT 37°C Upf1 Ribo-Seq	32,466,636	28,494,922 (87.8%)	1,358,107 (4%)	357,653 (2%)
WT 37°C mRNA-Seq	31,828,603	30,127,321 (94.7%)	938,129 (3%)	428,721 (1%)
sup45-2 25°C Total Ribo-Seq	47,151,534	34,140,166 (72.4%)	8,950,331 (19%)	3,808,964 (8.1%)
sup45-2 25°C Upf1 Ribo-Seq	58,374,039	37,470,026 (64.2%)	9,296,973 (16%)	1,657,163 (2.8%)
sup45-2 25°C mRNA-Seq	55,365,468	49,355,990 (89.1%)	2,071,670 (4%)	1,551,896 (2.8%)

Table B.3 – Number of genes detected in each data set (RPKM ≥10)

Sample	# of genes	# of genes (≥ 250nt)
WT 25°C Ribo-Zero treatment	5237	4967
WT 25°C	4925	4761
WT 37°C	5019	4781
sup45-2 25°C	5122	4775

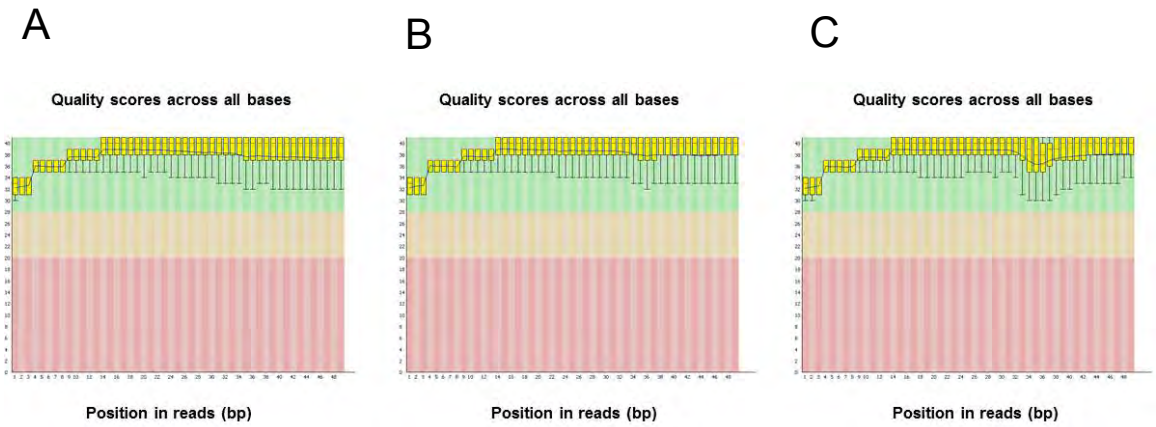

Figure B.1 – Assessment of the quality of sequence reads by FastQC analysis of wild-type 25°C libraries. The graphs for the libraries for (**A)** Total-Ribo-Seq (**B**) Upf1-Ribo-Seq, and (**C**) mRNA-Seq are illustrated by Box-Whisker plots. The y-axis represents the quality scores; bases of good quality in green, bases of average quality in orange, and bases of poor quality in red. The quality scores of reads from this data set were high with most of the reads distributed in the green area.

Similar results were observed in all four data sets (data not shown).

A

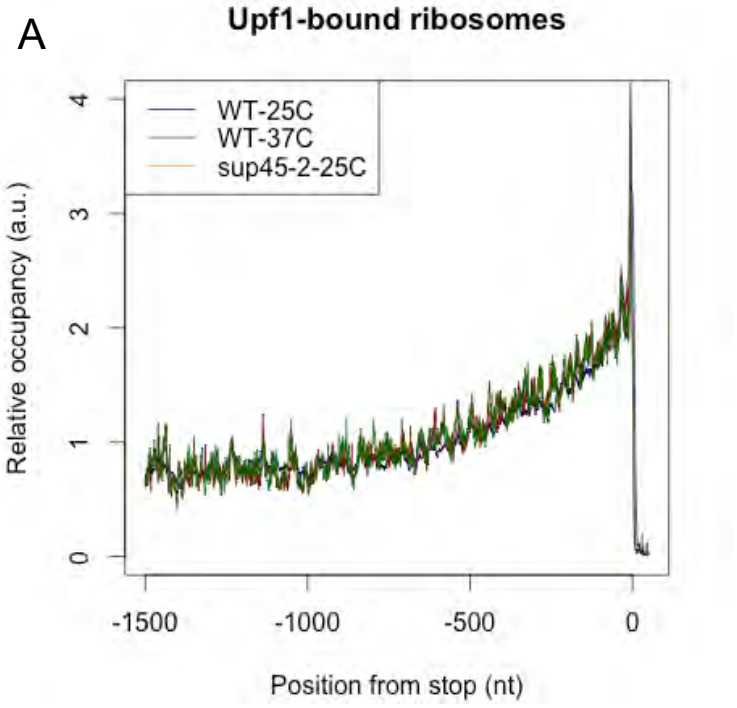
Upf1-bound ribosomes
WT-25C
WT-37C
sup45-2-25C
Relative occupancy (a.u.)
0
1
2
3
4
-1500
-1000
-500
0
Position from stop (nt)

B

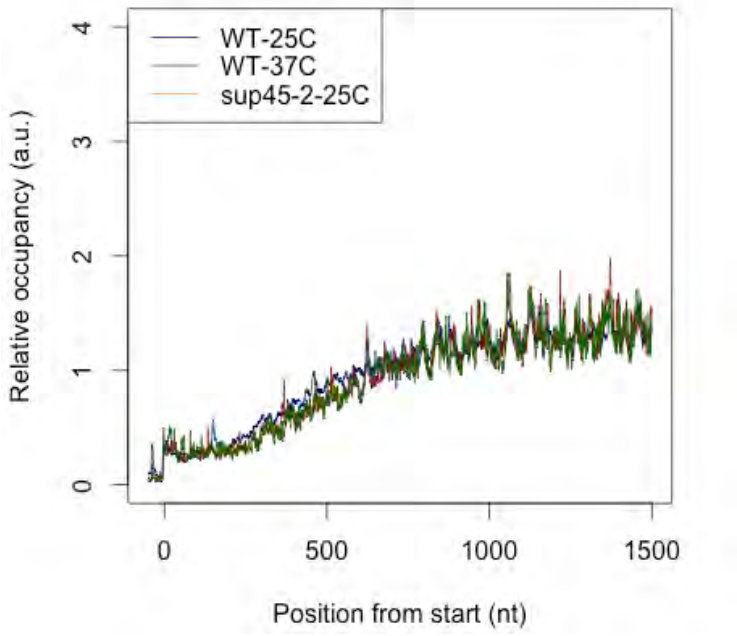
WT-25C
WT-37C
sup45-2-25C
Relative occupancy (a.u.)
0
1
2
3
4
0
500
1000
1500
Position from start (nt)

Figure B.2 – Upf1-bound 80S ribosomes are enriched at the 3'-ends of ORFs (and depleted at the 5'ends).

Metagene analyses of ribosome density were derived for mRNAs (with ORF length greater than 250 nt) aligned from their start (A) or stop codon (B) and averaged across them. RPF counts fromthree independent experiments are shown in indicated colors.

a.u. = arbitrary units

Number of mRNAs analyzed shown in Table B.3.

A

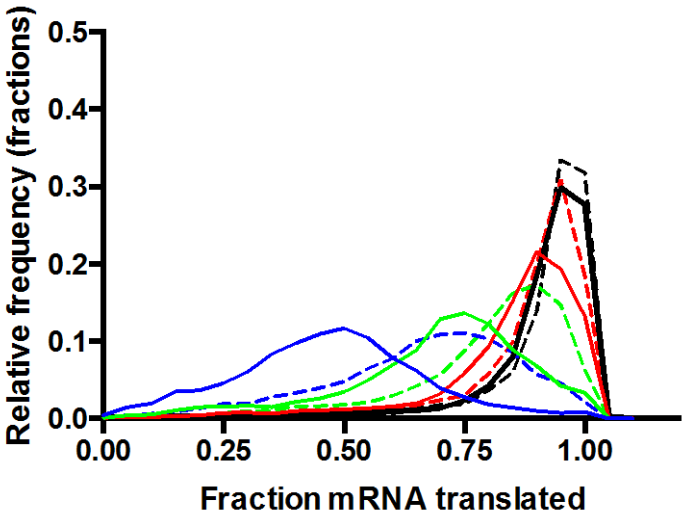
Relative frequency (fractions)
0.5
0.4
0.3
0.2
0.1
0.0
0.00
0.25
0.50
0.75
1.00
Fraction mRNA translated

B

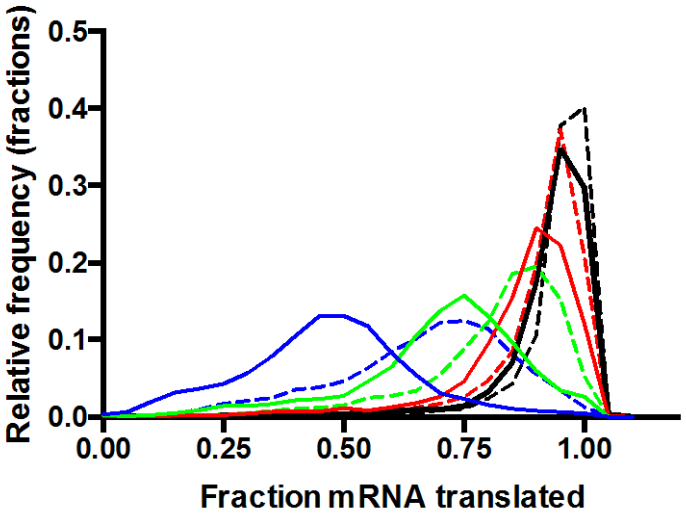
Relative frequency (fractions)
0.5
0.4
0.3
0.2
0.1
0.0
0.00
0.25
0.50
0.75
1.00
Fraction mRNA translated

C

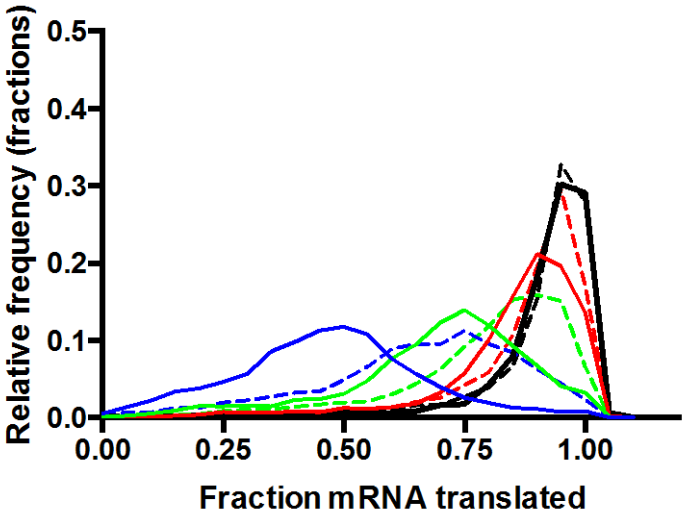
Relative frequency (fractions)
0.5
0.4
0.3
0.2
0.1
0.0
0.00
0.25
0.50
0.75
1.00
Fraction mRNA translated

Figure B.3 – Upf1 is preferentially associated with ribosomes near the 3'-ends of ORFs.

Calculated values of rrp50, rrp75, rrp90, rrp95, and rrp100 were plotted into frequency distribution curves to show the relative distributions of relative ribosome positions (RRP) for mRNAs in (A) wild-type 25°C, (B) wild-type 37°C, and (C) sup45-2 25°C.

Solid lines and dashed lines represent total and Upf1-bound ribosomes respectively.

APPENDIX C

MATERIALS AND METHODS

CHAPTER II

Construction of yeast strains with epitope-tagged ribosomal proteins

The chromosomal *RPL25* and *RPS13* genes were tagged with HA and c-Myc tags by homologous recombination at their 3' ends using a single step PCR-mediated technique (Longtine et al., 1998). The oligonucleotide primers NA193 and NA194 were used for tagging *RPL25* and oligonucleotide primers NA191 and NA192 were used for tagging *RPS13* (Table C.1).

Plasmid construction

His-tagged ribosomal fusion proteins were constructed by PCR amplification using oligonucleotides listed in Table C.2 and yeast genomic DNA as template. The PCR products were digested with *Nde*I/*Bam*HI and sub-cloned into the pET15b vector (Novagen).

Affinity purification of ribosomes and western blot analysis

Cell-free extracts were prepared as described previously (He et al., 2008). Extracts (15 A_{260}) from cells expressing c-Myc tagged *RPL25* or HA-tagged *RPS13* were mixed with an equal volume of Buffer A (100 mM Tris-HCl, pH 7.5, 24 mM $Mg(OAc)_2$, 1 mM DTT, 1 mM PMSF, 50U/mL RNasin (Roche)) and with

30ul of anti-HA or anti-c-MYC agarose slurry (Pierce).These mixtures were applied to spin columns, which were then incubated at 4°C for 2 h, with gentle rocking. The columns were subjected to pulse centrifugation and the respective flowthrough fractions were collected. The columns containing epitope-tagged ribosomal proteins were then washed three times with 0.8 mL of Buffer W (100 mM Tris-HCl, pH 7.5, 24 mM $Mg(OAc)_2$, 1 mM DTT, 100 mM PMSF, 50U/mL RNAsin (Roche), protease inhibitor cocktail (Roche), 0.1% NP40), and were eluted with 2X non-reducing sample buffer (Pierce) at 100°C on a heat block for 5 min. The eluted proteins were collected by pulse centrifugation, and 2 µl of β-mercaptoethanol was added for SDS-PAGE analysis. For micrococcal nuclease treatment, 50 units of micrococcal nuclease (S7 nuclease, Roche) was preincubated with extract for 10 min at 25°C and digestion was then terminated by adding 100 mM of EGTA. Puromycin (1 mM, Sigma) pre-treatment of extracts was performed for 15 min at 4°C and 10 min at 37°C. Aliquots of the initial extract as well as the supernatant and eluate of immunoprecipitations were subjected to SDS-PAGE analysis followed by western blotting using anti-Upf1 (1:5000, (Belk et al., 1999), anti-c-Myc (1:5000, Sigma), or anti-HA (1:5000, Sigma) antibody.

Purification of ribosomal subunits

Cytoplasmic extracts were prepared as described previously with the omission of cycloheximide and inclusion of high salt (0.5 M KCl) (Mangus and Jacobson, 1999). Extracts (20 A_{260}) were centrifuged at 120,000 *g* for 10 h at 4°C on 34 mL

15%–40% sucrose gradients containing 10mM Tris-HCl, pH 7.4, 10 mM $MgCl_2$, 30 mM NH_4Cl, and 1mM DTT. The gradients were scanned at A_{254} and the resulting absorbance profiles were used to determine the positions of the ribosomal fractions. Fractions corresponding to the 40S and 60S peaks were concentrated separately in Amicon Ultra-15 100K NMWL filters (EMD Millipore). The concentrated samples were diluted with Buffer E (10 mM Tris-HCl, pH 7.4, 10 mM KCl, 1 mM $MgCl_2$) and reconcentrated as before. The subunits were aliquotted and stored at −80°C. Concentrations of 40S and 60S subunits were determined by spectrophotometry, using 1 A_{260} = 50 nM for 40S and 1 A_{260} = 25 nM for 60S subunits (Matasova et al., 1991). The integrity and the quality of purified 40S and 60S subunits were determined by SDS-PAGE analysis followed by western blotting using anti-Rps6 (1:5000, Cell Signaling) and analysis of rRNA on denaturing agarose gels.

Yeast two-hybrid screening

Full-length yeast *UPF1* and mutant derivatives of the gene, all fused to the DNA binding domain of transcriptional activator *GAL4* (He et al., 1996; He and Jacobson, 1995), were used as bait against a two-hybrid library of ribosomal proteins fused to the *GAL4* activation domain (Valasek et al., 2003). The *UPF1-GAL4* (DNA-binding domain) and *RPS-GAL4* (activation domain) constructs were co-transformed into the two-hybrid tester strain GGY1::171 (Table 1). Transformants were incubated for 3-5 days at 30°C and qualitative and quantitative β-galactosidase activity was assayed as described previously (He et al., 1996).

In vitro binding assay

E. coli BL21 (DE3) cells (New England BioLabs Inc.) were transformed with pET-His-Rps26 and protein expression was induced by addition of isopropyl-b-D-thiogalactopyranoside (IPTG) to a final concentration of 0.4 mM. Cells expressing the His-Rps26 fusion protein were lysed in Talon Xtractor Buffer (Clontech Laboratories Inc.). The lysate was centrifuged to remove cell debris, and the supernatant was incubated with purified yeast FLAG-Upf1 (a kind gift from S. Kervestin) for 1 h at 4^{o}C. Binding was followed by incubation with FLAG beads (Sigma) for 4 h at 4^{o}C. After extensive washing in Talon Wash Buffer (Clontech Laboratories Inc.), FLAG-Upf1 was eluted with 3XFLAG peptide and samples were analyzed on SDS-PAGE followed by western blotting using anti-His (1:7000; Maine Biotechnology) or anti-Upf1 (1:5000) antibody (Belk et al., 1999).

Table C.1 – Yeast strains used in this study

Strains	Genotype	Source
MBS	MATa ade2-1 his3-11,15 leu2-3,112 trp1-1 ura3-1 can1-100 [rho+] L-o, M-o	Amrani et al, 2004
NAY101	MATa ade2-1 his3-11,15 leu2-3,112 trp1-1 ura3-1 can1-100 [rho+] L-o, M-o, upf1 :: HIS3	Amrani et al, 2004
NAY215	MATa ade2-1 his3-11,15 leu2-3,112 trp1-1 ura3-1 can1-100 [rho+] L-o, M-o, RPL25-MYC	This study
NAY217	MATa ade2-1 his3-11,15 leu2-3,112 trp1-1 ura3-1 can1-100 [rho+] L-o, M-o, upf1 :: HIS3, RPL25-MYC	This study
NAY223	MATa ade2-1 his3-11,15 leu2-3,112 trp1-1 ura3-1 can1-100 [rho+] L-o, M-o, RPS13-HA	This study
NAY225	MATa ade2-1 his3-11,15 leu2-3,112 trp1-1 ura3-1 can1-100 [rho+] L-o, M-o, upf1 :: HIS3, RPS13-HA	This study

Table C.2 – Oligonucleotides used in this study

NA191	CTACGATGCTTTGGACATTGCTAACAGAATCGGTTACATTCGGATCCCCGGGTTAATTAA
NA192	GAAAAATTTAAAAATAATATTAAATTTATTAATTAAACCAATTAGAGAATTCGAGCTCGTTTAAAC
NA193	CCAAACTGGAAGTACGAATCCGCCACTGCCTCCGCTTTGGTCAACCGGATCCCCGGGTTAATTAA
NA194	CAAAATATACATATAAAATAATGAAATAAATGATTTAAACACTGAATTCGAGCTCGTTTAAAC

CHAPTER III

Plasmid construction

Plasmids harboring 6xHis-Upf1 were generated by PCR and standard molecular cloning techniques (from 5′ to 3′: the TPI1 promoter, followed by an N-terminal 6× Histidine tag fused in-frame with the UPF1 gene). Oligonucleotides containing restriction sites were used for PCR amplification, and the resulting fragments were inserted into yEplac112 after digestion of the respective restriction sites.

Cells and treatments

Yeast strains were grown on -trp minimal medium overnight at 25°C, with shaking, and inoculated into large cultures with fresh -trp medium at an initial OD_{600} = 0.025 and then incubated at 30°C with shaking until the OD_{600} reached 0.6-0.8. Cells were harvested by vacuum filtration on 80 um filters (Millipore). Cells were scraped off the filter with a chilled spatula, resuspended in lysis buffer (10 mM Tris, pH 7.4, 100 mM NaCl, 30 mM $MgCl_2$, 1 mM DTT, 1 mM PMSF, 200 ug/ml Heparin), and dripped into liquid N_2. Frozen cell pellets were cryogenically ground at 10Hz for 15min in a mixer mill (Retsch). Frozen cell powder was thawed on ice and centrifuged for 10 min at 5000 rpm. The supernatant was centrifuged at 13,000 RPM for 10 min at 4°C. Absorbance at 260 nm was measured and 1 OD_{260} unit was treated with 0.15 ul of RNase I (100 Units/ul of Ambion) for 1 hr at room temperature with rotating. 5 ul of

Superase-In (20 U/ul; Ambion AM2694) was added to the RNase I-treated samples and subjected to sucrose gradient centrifugation (see below).

Ribosome isolation

Lysates prepared as above were loaded on 34 ml 10-50% sucrose gradients, prepared in low-salt polysome buffer (0.5 M Tris acetate pH 7.4, 0.5 M NH_4Cl, 0.12 M $MgCl_2$, 10 mM DTT), and centrifuged at 28,000 rpm in an SW-28 Ti rotor for 3.15 hr at 4°C. Sucrose gradient fractions containing 80S ribosomes (monosomes) were collected and concentrated with 100 kDa Amicon filter units (Millipore) to a volume of about 500-1000 ml. The retentate was exchanged with ribosome storage buffer (10 mM Tris, pH 7.4, 50 mM KCl, 50 mM NaCl, 10 mM $MgCl_2$, 1 mM DTT, 10 mg/ml Heparin), and saved in aliquots at -80°C.

Affinity purification of Upf1-bound ribosomes

Ribosomes (0.05 pmol) were incubated with 50 µl of magnetic Dynabeads (Invitrogen, 10103D) pre-equilibrated with Buffer A (50mM Tris 7.4, 1M NaCl, 1% NP40, 0.1% SDS, 0.5% NaDOC, and 50x protease inhibitor cocktail [Roche]) for 10 min at 4°C. The magnetic beads were washed five times in Buffer A. His-Upf1-associated mRNP complexes were eluted with Buffer A supplemented with 100 mM imidazole (pH 7.0) by incubating for 10 min at 4°C. The eluted His-Upf1-80S samples were combined and concentrated by centrifugation through 100 µl sucrose cushions (50 mM Tris, pH 7.0, 500 mM KOA, 25 mM $Mg[OAc]_2$, 5 mM β-

mercaptoethanol, 1 M sucrose, protease inhibitor, RNase inhibitor) at 50,000 rpm for 180 min in a TLS 55 rotor at 4°C. The resulting pellet was dissolved in 30 ul of Buffer B (20 mM HEPES, pH 7.0, 100 mM KCl, 1.5 mM $MgCl_2$, 1 mM DTT, 0.5 mM spermidine, 0.05% Nikkol, 0.5% protease inhibitor, and 0.1 U/ml RNAsin) for 1 hr on a rotating shaker at 4°C. Aliquots of concentrated Upf1-associated ribosomes were flash frozen in liquid nitrogen and stored at −80°C.

Mass spectrometry

After affinity purification, Upf1-eniriched ribosomes were subjected to 8% SDS-PAGE analysis. Gels were silver stained using ProteoSilver Silver Stain Kit (Sigma, PROTSIL1-1KT) and processed for mass spectrometry (MS) analysis. Destained gel bands were denatured, reduced with dithiothreitol, and alkylated with iodoacetamide, and subjected to in-gel trypsin digestion. The resulting peptides were subjected to Liquid Chromatography/Tandem MS Analysis (LC-MS) on a Thermo LTQ. Protein identification was performed with the Mascot Server (version 2.4; Matrix Sciences, Ltd.) using the UniProt index of *Saccharomyces cerevisiae.* Quantitation was performed using Mascot Distiller (version 2.4; Matrix Science, Inc.).

RNA isolation and sequencing library preparation

RNA was purified by hot acid phenol extraction, precipitated by ethanol with glycogen (Ambion) as a coprecipitant, and resuspended in 10 µL of 10 mM Tris, pH 8, and analyzed on 15% TBE-Urea polyacrylamide gels (Invitrogen). The bands around 25–34 nt were excised, and RNA was eluted in 300 µL of an elution buffer (20 mM Tris, pH 7.0, 2 mM EDTA, 0.5 M ammonium acetate) overnight at room temperature. Gel particles were eliminated using a spin-X 0.22 mm column (Corning Costar), followed by precipitation and resuspension in 10 µL of 10 mM Tris, pH 8. For rRNA-depleted samples, gel-purified small RNA fragments were depleted of rRNA using Ribo-Zero Magnetic Gold Kit (Epicenter, MRZY1306). Both ends of small mRNA fragments were modified as follows: The

3’ ends of mRNA fragments were dephosphorylated by addition of 10 U of T4 Polynucleotide Kinase (PNK) in 1x PNK buffer (New England Biolabs, MS2018) for 60 min at 37°C, and the reaction mixture was inactivated for 5 min at 80°C. The 5’ends of mRNA fragments were phosphorylated by addition of 10 U of T4 PNK in 1x PNK buffer with 2mM ATP (New England Biolabs, MS2018) for 60 min at at 37°C. End-cured small mRNA fragments were used as starting material in Illumina Tru-Seq Small RNA Sample Preparation Kit (Illumina, RS-200-0012). After reverse transcription, sequencing adapters were ligated onto both ends of a DNA molecule. Ligated cDNA fragments were size-selected for 250-bp by gel electrophoresis. Libraries were subjected to amplification using 14-16 PCR cycles, and sequenced on an Illumina HiSeq 2000.

mRNA sequencing library construction

mRNA-Seq libraries were prepared in two ways; (i) total RNA was prepared with SDS/hot acid phenol and chloroform. mRNA was purified from total RNA using oligo-dT-coated magnetic beads (Dynabeads mRNA purification kit) (Invitrogen, 610-06). mRNA was fragmented in alkaline solution [2 mM EDTA, 100 mM Na_2CO3 (pH 9.2)], the fragments were loaded onto a 15% TBE urea gel, and the 25- to 34-nt region was cut from the gel. Further steps in library preparation were identical to those used for ribosomal footprints. (ii) total RNA was prepared with SDS/hot acid phenol and chloroform and fragmented in alkaline solution [2 mM EDTA, 100 mM Na_2CO3 (pH 9.2)]. The total RNA fragments were loaded onto a 15% TBE urea gel, and the 25- to 34-nt region

was cut from the gel. Gel-purified small RNA fragments were depleted of rRNA using Ribo-Zero Magnetic Gold Kit (Epicenter, MRZY1306). Further steps in library preparation were identical to those used for ribosomal footprints.

Bioinformatics analysis

Data analyses, including calculation of read density, RPKM (reads per kilobase per million total reads) for mRNAs, metagene analysis, and RRP (relative ribosome position), were performed using custom Perl or Python scripts (see below for computational methods). Read densities were visualized using the Integrative Genomics Viewer (IGV).

Footprint alignment

Sequencing was performed by BGI, and "cleaned" sequences between 15 and 45 nt in length were provided in fasta and/or fastq format. Low-quality read filtering and adaptor trimming was performed as part of the standard BGI data processing pipeline. The yeast S288C reference sequence (release R64-1-1) and the corresponding rna_genomic.fasta files were downloaded from SGD (yeastgenome.org). Sequence libraries were filtered to rRNA by aligning to rna_genomic.fasta using bowtie2. Unaligned sequences were then aligned to the genome using Bowtie (version 1), allowing two mismatches. Only uniquely aligned reads were included in further downstream analysis. However, when we used multi-mapped alignments (i.e., sequences that matched to multiple places in the genome), there was no apparent difference in downstream analysis.

Translation efficiency (or Ribosome occupancy)

Translation efficiency is defined as $\log_2$[(Footprints RPKM/mRNA RPKM) If a gene had a $\log_2$ (TE change) above 1.0 it was considered up-regulated and, if below 1.0, as down-regulated.

Comparison with previously published data

Ribo-Seq and RNA-Seq data for yeast cells in the absence of drug treatment or with cycloheximide were downloaded from the Gene Expression Omnibus (Accession number: GSE52968, Guydosh et al., 2013; GSE33671, Smith et al., 2014). All sequencing data were processed as above for data generated in this study. For NMD substrate lists, we used mRNAs identified in microarray studies of *upf1*Δ cells (Feng et al., 2003) or Upf1-TAP IP (Johannsson et al., 2007), focusing on those mRNAs manifesting twofold or larger increases relative to controls.

Computational Methods

Data processing followed the scheme of Becker et al. [Selective ribosome profiling as a tool for studying the interaction of chaperones and targeting factors with nascent polypeptide chains and ribosomes (2013) Nat. Protocols **8**, 2212–2239] and utilized the Python scripts included as Supplementary Materials in their publication. The scripts were downloaded and modified to run as standalone Python code. Custom Perl programs (“wrappers”) were written to call the respective Python scripts for each yeast chromosome and aggregate the

output. The Python scripts, their general description, and the Perl wrappers are given in Table C.3. Additional Perl programs were written for cases specific to our needs.

Steps in the data processing were as follows:

1) Sequence data preprocessing. Sequencing was performed by BGI, and "cleaned" sequences between 15 and 45 nt in length were provided in fasta and/or fastq format. Low-quality read filtering and adaptor trimming were performed as part of the standard BGI data processing pipeline.

2) Alignment. The yeast S288C reference sequence (release R64-1-1; sacCer3) and the corresponding rna_genomic.fasta file were downloaded from SGD (yeastgenome.org). Sequence libraries were filtered to remove sequences corresponding to RNA genes (primarily rRNA) by aligning to rna_genomic.fasta using bowtie2 version 2.1.0 with default parameters. Unaligned sequences were then aligned to the genome using Bowtie version 0.0.19, allowing two mismatches and retaining only unique alignments (-v2 -m1). Alignments were output in default bowtie format. Both alignment runs were performed on the UMass Green High Performance Computing Cluster (GHPCC).

3) Center-weighted read density files. The center_weighting_v1.0.pl Perl program was run to call supp_note_2.py and generate a directory of center-weighted read density files, one for each chromosome and strand. All read lengths were included in the analysis. Additionally, total read counts for each

chromosome were calculated (supp_note_3.py) and written to a file included in the output directory for use in downstream analyses. [Note: By including all read lengths, some as short as 15 bases, the offset for center-weighting is 7 bases. For long reads, this results in dividing the density over many bases, thus increasing the "fuzziness" of the mapping, e.g., for a 28-base read, the density would be allocated to bases 8-21 (1/14 for each base). If analysis were restricted to reads ≥ 27 bases (offset of 13), the density for a 28-base read would be allocated only to bases 14-15 (0.5 to each).]

4) Normalized read density. The normalize_reads_v1.0.pl Perl program was run to call supp_note_6.py and generate a directory of center-weighted read density files with values normalized to reads per million total mapped reads (RPM). For visualization in the Integrated Genomics Viewer (IGV), the normalized read density files were converted to a single file in WIG format using the Perl program make_genomic_wig.pl. For faster loading, WIG files were subsequently converted to tdf format using IGV Tools. [Note: Since the input read density files are already normalized to RPM, the "Normalize Coverage Data" option should be left unchecked in the IGV Preferences ("Tracks" tab).]

5) Genomic feature directories. The parse_features_v1.1.pl Perl program was used to obtain a directory of genomic feature files, one for each chromosome and strand. Input to the program is a tab-delimited file of genomic features (e.g., genes, UTRs) with feature ID, start, end, strand (+/-) on each line.

Coordinates are 1-based relative to the top strand (i.e., start < end). Data for sacCer3 genes are downloaded from the UCSC Table Browser. [Note: Coordinates downloaded from UCSC are 0-based half open (0-based start, 1-based end) and must be converted to 1-based fully closed (1-based start, 1-based end) for input to parse_features_v1.1.pl.]

6) Read density per gene (or other feature). The read_density_per_gene.pl Perl program was run to call supp_note_4.py and calculate read density per gene or other feature. Inputs are a directory of center-weighted read densities (step 3) and a directory of feature files (step 5). Output is a directory of read densities per feature files, one for each chromosome/strand.

7) Feature RPKM. The compare_gene_expression.pl Perl program was used to call supp_note_5.py and summarize read density per feature data. Input is a pair of read density per gene/feature directories (step 6). Output is a single file aggregating the results, expressed as reads per kilobase per million reads (RPKM), for each of the two input directories.

8) Metagene analysis. The Perl programs genomic_meta_init.pl and genomic_meta.pl were used to call supp_note_12.py and supp_note_13.py to calculate meta-gene values (relative ribosome occupancy averaged over all genes) measured from the initiator or terminator codons, respectively. The following filtering criteria were used for meta-gene calculations; genes with

greater than 10 RPKM and an ORF length of at least 250 nt. Programs output the results as tab-delimited text (coordinate, value), which can be plotted using R or other statistical software (Excel, Prism).

9) Relative ribosome position. Relative ribosome position (RRP) is a metric we devised to identify prematurely terminating mRNA's. RRP is defined as the distance from the initiation codon, expressed as fraction of gene length, at which a given percentage of ribosome protected fragments (reads) occur, e.g., rrp50 is the location where 50% of the total reads mapped to that gene have been counted (starting from the initiator ATG). A low RRP value would indicate that ribosomes are located disproportionately early on the mRNA because premature termination results in the majority of reads skewing towards the 5' end of the mRNA.

The Perl program find_PTC_v1.1.pl takes as input a directory of center-weighted read densities and a genomic feature directory (e.g., ORF's) and calculates values of rrp50, rrp75, rrp90, rrp95, and rrp100 for each feature. The initial implementation of the program excluded genes <500 bp in length, although this is easily changed.

Table C.3 – Computer programs used for data processing

Python script	Function	Wrapper program
supp_note_2.py	Center Weighting	center_weighting_v1.0.pl
supp_note_3.py	Total reads	center_weighting_v1.0.pl
supp_note_4.py	Read density per gene	read_density_per_gene.pl
supp_note_5.py	Compare gene expression levels	compare_gene_expression.pl
supp_note_6.py	RPM-normalized read densities	normalize_reads_v1.0.pl
supp_note_12.py	Meta-gene analysis from start codon	genomic_meta_init.pl
supp_note_13.py	Meta-gene analysis from stop codon	genomic_meta.pl
Additional data processing		
	Separates genomic feature file by chromosome/strand	parse_features_v1.1.pl
	Generates single WIG file from directory of center-weighted read density files	make_genomic_wig.pl
	Calculates relative ribosome position (RRP)	find_PTC_v1.1.pl

Appendix A

Cryo-electron microscopy and image processing

A drop of a solution (~30 pmol/ml) of the ribosomal complexes is applied to a copper cryo-EM grid coated with a holey carbon film, blotted, immediately plunged into liquid ethane, and then super-cooled with liquid nitrogen. (Shock freezing prevents the formation of ice crystals, leading to a thin layer of vitreous ice that surrounds the macromolecular complexes.) Preparation of grids is facilitated by use of a semi-automated plunge-freezer (Vitrobot®, FEI). Small data sets (500 to 1,500 micrographs) were collected for initial structure determination using a Tecnai Spirit microscope, providing an assessment of sample quality (homogeneity, presence of the ligands). Digital image processing using the SPIDER/WEB software packages (Frank et al., 1996) was employed to determine macromolecular structures.

BIBILOGRAPHY

Algire, M.A., Maag, D., Savio, P., Acker, M.G., Tarun, S.Z., Jr., Sachs, A.B., Asano, K., Nielsen, K.H., Olsen, D.S., Phan, L.*, et al.* (2002). Development and characterization of a reconstituted yeast translation initiation system. RNA *8*, 382-397.

Alkalaeva, E.Z., Pisarev, A.V., Frolova, L.Y., Kisselev, L.L., and Pestova, T.V. (2006). In vitro reconstitution of eukaryotic translation reveals cooperativity between release factors eRF1 and eRF3. Cell *125*, 1125-1136.

Amrani, N., Dong, S., He, F., Ganesan, R., Ghosh, S., Kervestin, S., Li, C., Mangus, D.A., Spatrick, P., and Jacobson, A. (2006a). Aberrant termination triggers nonsense-mediated mRNA decay. Biochem. Soc. Trans. *34 (part 1)*, 39-42.

Amrani, N., Ganesan, R., Kervestin, S., Mangus, D.A., Ghosh, S., and Jacobson, A. (2004). A *faux* 3'-UTR promotes aberrant termination and triggers nonsense-mediated mRNA decay. Nature *432*, 112-118.

Amrani, N., Sachs, M.S., and Jacobson, A. (2006b). Early nonsense: mRNA decay solves a translational problem. Nat. Rev. Mol. Cell. Biol. *7*, 415-425.

Arribere, J.A., and Gilbert, W.V. (2013). Roles for transcript leaders in translation and mRNA decay revealed by transcript leader sequencing. Genome Res *23*, 977-987.

Atkin, A.L., Altamura, N., Leeds, P., and Culbertson, M.R. (1995). The majority of yeast UPF1 co-localizes with polyribosomes in the cytoplasm. Mol. Biol. Cell *6*, 611-625.

Atkin, A.L., Schenkman, L.R., Eastham, M., Dahlseid, J.N., Lelivelt, M.J., and Culbertson, M.R. (1997). Relationship between yeast polyribosomes and Upf proteins required for nonsense mRNA decay. J. Biol. Chem. *272*, 22163-22172.

Azzam, M.E., and Algranati, I.D. (1973). Mechanism of puromycin action: fate of ribosomes after release of nascent protein chains from polysomes. Proceedings of the National Academy of Sciences of the United States of America *70*, 3866-3869.

Balistreri, G., Horvath, P., Schweingruber, C., Zund, D., McInerney, G., Merits, A., Muhlemann, O., Azzalin, C., and Helenius, A. (2014). The host nonsense-mediated mRNA decay pathway restricts Mammalian RNA virus replication. Cell Host Microbe *16*, 403-411.

Bartel, P., Chien, C.T., Sternglanz, R., and Fields, S. (1993). Elimination of false positives that arise in using the two-hybrid system. Biotechniques *14*, 920-924.

Bartel, P.L., and Fields, S. (1995). Analyzing protein-protein interactions using two-hybrid system. Methods Enzymol *254*, 241-263.

Barthelme, D., Dinkelaker, S., Albers, S.V., Londei, P., Ermler, U., and Tampe, R. (2011). Ribosome recycling depends on a mechanistic link between the FeS cluster domain and a conformational switch of the twin-ATPase ABCE1. Proc. Natl. Acad. Sci. USA *108*, 3228-3233.

Becker, A.H., Oh, E., Weissman, J.S., Kramer, G., and Bukau, B. (2013). Selective ribosome profiling as a tool for studying the interaction of chaperones and targeting factors with nascent polypeptide chains and ribosomes. Nat. Protoc. *8*, 2212-2239.

Becker, T., Franckenberg, S., Wickles, S., Shoemaker, C.J., Anger, A.M., Armache, J.P., Sieber, H., Ungewickell, C., Berninghausen, O., Daberkow, I.*, et al.* (2012). Structural basis of highly conserved ribosome recycling in eukaryotes and archaea. Nature *482*, 501-506.

Beelman, C.A., and Parker, R. (1994). Differential effects of translational inhibition in cis and in trans on the decay of the unstable yeast MFA2 mRNA. J. Biol. Chem. *269*, 9687-9692.

Behm-Ansmant, I., Gatfield, D., Rehwinkel, J., Hilgers, V., and Izaurralde, E. (2007). A conserved role for cytoplasmic poly(A)-binding protein 1 (PABPC1) in nonsense-mediated mRNA decay. EMBO J. *26*, 1591-1601.

Belgrader, P., Cheng, J., and Maquat, L.E. (1993). Evidence to implicate translation by ribosomes in the mechanism by which nonsense codons reduce the nuclear level of human triosephosphate isomerase mRNA. Proc. Natl. Acad. Sci. USA *90*, 482-486.

Belgrader, P., and Maquat, L.E. (1994). Nonsense but not missense mutations can decrease the abundance of nuclear mRNA for the mouse major urinary protein, while both types of mutations can facilitate exon skipping. Mol. Cell. Biol. *14*, 6326-6336.

Belk, J.P., He, F., and Jacobson, A. (1999). Overexpression of truncated Nmd3p inhibits protein synthesis in yeast. RNA *5*, 1055-1070.

Ben-Shem, A., Garreau de Loubresse, N., Melnikov, S., Jenner, L., Yusupova, G., and Yusupov, M. (2011). The structure of the eukaryotic ribosome at 3.0 A resolution. Science *334*, 1524-1529.

Bhattacharya, A., Czaplinski, K., Trifillis, P., He, F., Jacobson, A., and Peltz, S.W. (2000). Characterization of the biochemical properties of the human Upf1 gene product that is involved in nonsense-mediated mRNA decay. RNA *6*, 1226-1235.

Bono, F., and Gehring, N.H. (2011). Assembly, disassembly and recycling: the dynamics of exon junction complexes. RNA Biol *8*, 24-29.

Bruno, Ivone G., Karam, R., Huang, L., Bhardwaj, A., Lou, Chih H., Shum, Eleen Y., Song, H.-W., Corbett, Mark A., Gifford, Wesley D., Gecz, J.*, et al.* (2011). Identification of a MicroRNA that Activates Gene Expression by Repressing Nonsense-Mediated RNA Decay. Molecular Cell *42*, 500-510.

Buchwald, G., Ebert, J., Basquin, C., Sauliere, J., Jayachandran, U., Bono, F., Le Hir, H., and Conti, E. (2010). Insights into the recruitment of the NMD machinery from the crystal structure of a core EJC-UPF3b complex. Proc. Natl. Acad. Sci. USA *107*, 10050-10055.

Buhler, M., Steiner, S., Mohn, F., Paillusson, A., and Muhlemann, O. (2006). EJC-independent degradation of nonsense immunoglobulin μ mRNA depends on 3'-UTR length. Nature Struct. Mol. Biol. *13*, 462-464.

Chakrabarti, S., Bonneau, F., Schussler, S., Eppinger, E., and Conti, E. (2014). Phospho-dependent and phospho-independent interactions of the helicase UPF1 with the NMD factors SMG5-SMG7 and SMG6. Nucleic acids research *42*, 9447-9460.

Chakrabarti, S., Jayachandran, U., Bonneau, F., Fiorini, F., Basquin, C., Domcke, S., Le Hir, H., and Conti, E. (2011). Molecular mechanisms for the

RNA-dependent ATPase activity of Upf1 and its regulation by Upf2. Mol. Cell *41*, 693-703.

Chamieh, H., Ballut, L., Bonneau, F., and Le Hir, H. (2008). NMD factors UPF2 and UPF3 bridge UPF1 to the exon junction complex and stimulate its RNA helicase activity. Nat. Struct. Mol. Biol. *15*, 85-93.

Chan, W.K., Huang, L., Gudikote, J.P., Chang, Y.F., Imam, J.S., MacLean, J.A., 2nd, and Wilkinson, M.F. (2007). An alternative branch of the nonsense-mediated decay pathway. EMBO J. *26*, 1820-1830.

Chang, J.C., and Kan, Y.W. (1979). Beta 0 thalassemia, a nonsense mutation in man. Proc. Natl. Acad. Sci. USA *76*, 2886-2889.

Chang, Y.F., Imam, J.S., and Wilkinson, M.F. (2007). The nonsense-mediated decay RNA surveillance pathway. Ann. Rev. Biochem. *76*, 51-74.

Chazal, P.E., Daguenet, E., Wendling, C., Ulryck, N., Tomasetto, C., Sargueil, B., and Le Hir, H. (2013). EJC core component MLN51 interacts with eIF3 and activates translation. Proc. Natl. Acad. Sci. USA *110*, 5903-5908.

Cheng, Z., Saito, K., Pisarev, A.V., Wada, M., Pisareva, V.P., Pestova, T.V., Gajda, M., Round, A., Kong, C., Lim, M.*, et al.* (2009). Structural insights into eRF3 and stop codon recognition by eRF1. Genes Dev. *23*, 1106-1118.

Clerici, M., Deniaud, A., Boehm, V., Gehring, N.H., Schaffitzel, C., and Cusack, S. (2014). Structural and functional analysis of the three MIF4G domains of nonsense-mediated decay factor UPF2. Nucleic Acids Res. *42*, 2673-2686.

Clerici, M., Mourao, A., Gutsche, I., Gehring, N.H., Hentze, M.W., Kulozik, A., Kadlec, J., Sattler, M., and Cusack, S. (2009). Unusual bipartite mode of interaction between the nonsense-mediated decay factors, UPF1 and UPF2. EMBO J. *28*, 2293-2306.

Cosson, B., Berkova, N., Couturier, A., Chabelskaya, S., Philippe, M., and Zhouravleva, G. (2002). Poly(A)-binding protein and eRF3 are associated *in vivo* in human and *Xenopus* cells. Biol. Cell *94*, 205-216.

Cui, Y., Dinman, J.D., and Peltz, S.W. (1996). Mof4-1 is an allele of the UPF1/IFS2 gene which affects both mRNA turnover and -1 ribosomal frameshifting efficiency. The EMBO journal *15*, 5726-5736.

Culbertson, M.R., and Leeds, P.F. (2003). Looking at mRNA decay pathways through the window of molecular evolution. Current opinion in genetics & development *13*, 207-214.

Culbertson, M.R., Underbrink, K.M., and Fink, G.R. (1980). Frameshift suppression *Saccharomyces cerevisiae*. Genetic properties of group II suppressors. Genetics *95*, 833-853.

Czaplinski, K., Ruiz-Echevarria, M.J., Paushkin, S.V., Han, X., Weng, Y., Perlick, H.A., Dietz, H.C., Ter-Avanesyan, M.D., and Peltz, S.W. (1998). The surveillance complex interacts with the translation release factors to enhance termination and degrade aberrant mRNAs. Genes Dev. *12*, 1665-1677.

Czaplinski, K., Weng, Y., Hagan, K.W., and Peltz, S.W. (1995). Purification and characterization of the Upf1 protein: a factor involved in translation and mRNA degradation. RNA *1*, 610-623.

Das, B., Guo, Z., Russo, P., Chartrand, P., and Sherman, F. (2000). The role of nuclear cap binding protein Cbc1p of yeast in mRNA termination and degradation. Mol. Cell. Biol. *20*, 2827-2838.

Decourty, L., Doyen, A., Malabat, C., Frachon, E., Rispal, D., Seraphin, B., Feuerbach, F., Jacquier, A., and Saveanu, C. (2014). Long open reading frame transcripts escape nonsense-mediated mRNA decay in yeast. Cell Rep *6*, 593-598.

Dunn, J.G., Foo, C.K., Belletier, N.G., Gavis, E.R., and Weissman, J.S. (2013). Ribosome profiling reveals pervasive and regulated stop codon readthrough in Drosophila melanogaster. eLife *2*, e01179.

Durand, S., Cougot, N., Mahuteau-Betzer, F., Nguyen, C.H., Grierson, D.S., Bertrand, E., Tazi, J., and Lejeune, F. (2007). Inhibition of nonsense-mediated mRNA decay (NMD) by a new chemical molecule reveals the dynamic of NMD factors in P-bodies. J. Cell. Biol. *178*, 1145-1160.

Eberle, A.B., Lykke-Andersen, S., Muhlemann, O., and Jensen, T.H. (2009). SMG6 promotes endonucleolytic cleavage of nonsense mRNA in human cells. Nat. Struct. Mol. Biol. *16*, 49-55.

Eberle, A.B., Stalder, L., Mathys, H., Orozco, R.Z., and Muhlemann, O. (2008). Posttranscriptional gene regulation by spatial rearrangement of the 3' untranslated region. PLoS Biol. *6*, e92.

Fairman-Williams, M.E., Guenther, U.P., and Jankowsky, E. (2010). SF1 and SF2 helicases: family matters. Curr Opin Struct Biol *20*, 313-324.

Fatscher, T., Boehm, V., Weiche, B., and Gehring, N.H. (2014). The interaction of cytoplasmic poly(A)-binding protein with eukaryotic initiation factor 4G suppresses nonsense-mediated mRNA decay. RNA *20*, 1579-1592.

Ferraiuolo, M.A., Lee, C.S., Ler, L.W., Hsu, J.L., Costa-Mattioli, M., Luo, M.J., Reed, R., and Sonenberg, N. (2004). A nuclear translation-like factor eIF4AIII is recruited to the mRNA during splicing and functions in nonsense-mediated decay. Proceedings of the National Academy of Sciences of the United States of America *101*, 4118-4123.

Fillman, C., and Lykke-Andersen, J. (2005). RNA decapping inside and outside of processing bodies. Current opinion in cell biology *17*, 326-331.

Franks, T.M., Singh, G., and Lykke-Andersen, J. (2010). Upf1 ATPase-dependent mRNP disassembly is required for completion of nonsense- mediated mRNA decay. Cell *143*, 938-950.

Frolova, L., Le Goff, X., Zhouravleva, G., Davydova, E., Philippe, M., and Kisselev, L. (1996). Eukaryotic polypeptide chain release factor eRF3 is an eRF1- and ribosome-dependent guanosine triphosphatase. RNA *2*, 334-341.

Gaba, A., Jacobson, A., and Sachs, M.S. (2005). Ribosome occupancy of the yeast *CPA1* upstream open reading frame termination codon modulates nonsense-mediated mRNA decay. Mol. Cell *20*, 449-460.

Gatfield, D., Unterholzner, L., Ciccarelli, F.D., Bork, P., and Izaurralde, E. (2003). Nonsense-mediated mRNA decay in *Drosophila*: at the intersection of the yeast and mammalian pathways. EMBO J. *22*, 3960-3970.

Ge, Y., and Porse, B.T. (2014). The functional consequences of intron retention: Alternative splicing coupled to NMD as a regulator of gene expression. BioEssays *36*, 236-243.

Gehring, N.H., Kunz, J.B., Neu-Yilik, G., Breit, S., Viegas, M.H., Hentze, M.W., and Kulozik, A.E. (2005). Exon-junction complex components specify distinct routes of nonsense-mediated mRNA decay with differential cofactor requirements. Mol. Cell *20*, 65-75.

Gehring, N.H., Neu-Yilik, G., Schell, T., Hentze, M.W., and Kulozik, A.E. (2003). Y14 and hUpf3b form an NMD-activating complex. Mol. Cell *11*, 939-949.

Ghosh, S., Ganesan, R., Amrani, N., and Jacobson, A. (2010). Translational competence of ribosomes released from a premature termination codon is modulated by NMD factors. RNA *16*, 1832-1847.

Glavan, F., Behm-Ansmant, I., Izaurralde, E., and Conti, E. (2006). Structures of the PIN domains of SMG6 and SMG5 reveal a nuclease within the mRNA surveillance complex. EMBO J. *25*, 5117-5125.

Gloggnitzer, J., Akimcheva, S., Srinivasan, A., Kusenda, B., Riehs, N., Stampfl, H., Bautor, J., Dekrout, B., Jonak, C., Jiménez-Gómez, J.M.*, et al.* (2014). Nonsense-mediated mRNA decay modulates immune receptor levels to regulate plant antibacterial defense. Cell Host and Microbe *16*, 376-390.

Gong, C., Kim, Y.K., Woeller, C.F., Tang, Y., and Maquat, L.E. (2009). SMD and NMD are competitive pathways that contribute to myogenesis: effects on PAX3 and myogenin mRNAs. Genes & development *23*, 54-66.

Goodenough, E., Robinson, T.M., Zook, M.B., Flanigan, K.M., Atkins, J.F., Howard, M.T., and Eisenlohr, L.C. (2014). Cryptic MHC class I-binding peptides are revealed by aminoglycoside-induced stop codon read-through into the 3' UTR. Proc. Natl. Acad. Sci. USA *111*, 5670-5675.

Gozalbo, D., and Hohmann, S. (1990). Nonsense suppressors partially revert the decrease of the mRNA level of a nonsense mutant allele in yeast. Curr. Genet. *17*, 77-79.

Gregersen, L.H., Schueler, M., Munschauer, M., Mastrobuoni, G., Chen, W., Kempa, S., Dieterich, C., and Landthaler, M. (2014). MOV10 Is a 5' to 3' RNA Helicase Contributing to UPF1 mRNA Target Degradation by Translocation along 3' UTRs. Molecular Cell *54*, 573-585.

Grimson, A., O'Connor, S., Newman, C.L., and Anderson, P. (2004). SMG-1 is a phosphatidylinositol kinase-related protein kinase required for nonsense-mediated mRNA Decay in Caenorhabditis elegans. Mol. Cell. Biol. *24*, 7483-7490.

Guan, Q., Zheng, W., Tang, S., Liu, X., Zinkel, R.A., Tsui, K.W., Yandell, B.S., and Culbertson, M.R. (2006). Impact of nonsense-mediated mRNA decay on the global expression profile of budding yeast. PLoS Genet. *2*, e203.

Hagan, K.W., Ruiz-Echevarria, M.J., Quan, Y., and Peltz, S.W. (1995). Characterization of *cis*-acting sequences and decay intermediates involved in nonsense-mediated mRNA turnover. Mol. Cell. Biol. *15*, 809-823.

He, F., Amrani, N., Johansson, M.J.O., and Jacobson, A. (2008). Qualitative and quantitative assessment of the activity of the yeast nonsense-mediated mRNA decay pathway. In Methods Enzymol. - RNA Turnover, L. Maquat, and M. Kiledjian, eds. (San Diego: Elsevier), pp. 127-147.

He, F., Brown, A.H., and Jacobson, A. (1996). Interaction between Nmd2p and Upf1p is required for activity but not for dominant-negative inhibition of the nonsense-mediated mRNA decay pathway in yeast. RNA *2*, 153-170.

He, F., Brown, A.H., and Jacobson, A. (1997). Upf1p, Nmd2p, and Upf3p are interacting components of the yeast nonsense-mediated mRNA decay pathway. Mol. Cell. Biol. *17*, 1580-1594.

He, F., and Jacobson, A. (1995). Identification of a novel component of the nonsense-mediated mRNA decay pathway by use of an interacting protein screen. Genes Dev. *9*, 437-454.

He, F., and Jacobson, A. (2001). Upf1p, Nmd2p, and Upf3p regulate the decapping and exonucleolytic degradation of both nonsense-containing mRNAs and wild-type mRNAs. Mol. Cell. Biol. *21*, 1515-1530.

He, F., Li, X., Spatrick, P., Casillo, R., Dong, S., and Jacobson, A. (2003). Genome-wide analysis of mRNAs regulated by the nonsense-mediated and 5' to 3' mRNA decay pathways in yeast. Mol. Cell *12*, 1439-1452.

He, F., Peltz, S.W., Donahue, J.L., Rosbash, M., and Jacobson, A. (1993). Stabilization and ribosome association of unspliced pre-mRNAs in a yeast *upf1*-mutant. Proc. Natl. Acad. Sci. USA *90*, 7034-7038.

Hilleren, P., and Parker, R. (1999). mRNA surveillance in eukaryotes: kinetic proofreading of proper translation termination as assessed by mRNP domain organization? RNA *5*, 711-719.

Hodgkin, J., Papp, A., Pulak, R., Ambros, V., and Anderson, P. (1989). A new kind of informational suppression in the nematode *Caenorhabditis elegans*. Genetics *123*, 301-313.

Hogg, J.R., and Goff, S.P. (2010). Upf1 senses 3'UTR length to potentiate mRNA decay. Cell *143*, 379-389.

Hoshino, S., Imai, M., Kobayashi, T., Uchida, N., and Katada, T. (1999). The eukaryotic polypeptide chain releasing factor (eRF3/GSPT) carrying the translation termination signal to the 3'-poly(A) tail of mRNA. Direct association of erf3/GSPT with polyadenylate-binding protein. J. Biol. Chem. *274*, 16677-16680.

Hu, W., Petzold, C., Coller, J., and Baker, K.E. (2010). Nonsense-mediated mRNA decapping occurs on polyribosomes in Saccharomyces cerevisiae. Nat. Struct. Mol. Biol. *17*, 244-247.

Huang, L., Lou, C.H., Chan, W., Shum, E.Y., Shao, A., Stone, E., Karam, R., Song, H.W., and Wilkinson, M.F. (2011). RNA homeostasis governed by cell type-specific and branched feedback loops acting on NMD. Mol Cell *43*, 950-961.

Huntzinger, E., Kashima, I., Fauser, M., Sauliere, J., and Izaurralde, E. (2008). SMG6 is the catalytic endonuclease that cleaves mRNAs containing nonsense codons in metazoan. RNA *14*, 2609-2617.

Hurt, J.A., Robertson, A.D., and Burge, C.B. (2013). Global analyses of UPF1 binding and function reveal expanded scope of nonsense-mediated mRNA decay. Genome Res. *23*, 1636-1650.

Inada, T., Winstall, E., Tarun, S.Z., Jr., Yates, J.R., 3rd, Schieltz, D., and Sachs, A.B. (2002). One-step affinity purification of the yeast ribosome and its associated proteins and mRNAs. RNA *8*, 948-958.

Ingolia, N.T. (2014). Ribosome profiling: new views of translation, from single codons to genome scale. Nat. Rev. Genet. *15*, 205-213.

Ingolia, N.T., Lareau, L.F., and Weissman, J.S. (2011). Ribosome profiling of mouse embryonic stem cells reveals the complexity and dynamics of mammalian proteomes. Cell *147*, 789-802.

Isken, O., Kim, Y.K., Hosoda, N., Mayeur, G.L., Hershey, J.W., and Maquat, L.E. (2008). Upf1 phosphorylation triggers translational repression during nonsense-mediated mRNA decay. Cell *133*, 314-327.

Isken, O., and Maquat, L.E. (2007). Quality control of eukaryotic mRNA: safeguarding cells from abnormal mRNA function. Genes Dev. *21*, 1833-1856.

Isken, O., and Maquat, L.E. (2008). The multiple lives of NMD factors: balancing roles in gene and genome regulation. Nat. Rev. Genet. *9*, 699-712.

Ivanov, P.V., Gehring, N.H., Kunz, J.B., Hentze, M.W., and Kulozik, A.E. (2008). Interactions between UPF1, eRFs, PABP and the exon junction complex suggest an integrated model for mammalian NMD pathways. EMBO J. *27*, 736-747.

Jackson, R.J., Hellen, C.U., and Pestova, T.V. (2012). Termination and post-termination events in eukaryotic translation. Adv. Protein Chem. Struct. Biol. *86*, 45-93.

Jacobson, A., and Izaurralde, E. (2007). Nonsense-mediated mRNA decay: from yeast to metazoans. In Translational Control in Biology and Medicine, M.B. Mathews, N. Sonenberg, and J.W.B. Hershey, eds. (Cold Spring Harbor, NY: Cold Spring Harbor Laboratory Press), pp. 659-691.

Jacobson, A., and Peltz, S.W. (1996). Interrelationships of the pathways of mRNA decay and translation in eukaryotic cells. Annu. Rev. Biochem. *65*, 693-739.

Johansson, M.J., He, F., Spatrick, P., Li, C., and Jacobson, A. (2007). Association of yeast Upf1p with direct substrates of the NMD pathway. Proc. Natl. Acad. Sci. U S A *104*, 20872-20877.

Johns, L., Grimson, A., Kuchma, S.L., Newman, C.L., and Anderson, P. (2007). Caenorhabditis elegans SMG-2 selectively marks mRNAs containing premature translation termination codons. Mol. Cell. Biol. *27*, 5630-5638.

Joncourt, R., Eberle, A.B., Rufener, S.C., and Muhlemann, O. (2014). Eukaryotic initiation factor 4G suppresses nonsense-mediated mRNA decay by two genetically separable mechanisms. PloS one *9*, e104391.

Kadlec, J., Izaurralde, E., and Cusack, S. (2004). The structural basis for the interaction between nonsense-mediated mRNA decay factors UPF2 and UPF3. Nature Struct. Mol. Biol. *11*, 330-337.

Kashima, I., Jonas, S., Jayachandran, U., Buchwald, G., Conti, E., Lupas, A.N., and Izaurralde, E. (2010). SMG6 interacts with the exon junction complex via two conserved EJC-binding motifs (EBMs) required for nonsense-mediated mRNA decay. Genes Dev. *24*, 2440-2450.

Kashima, I., Yamashita, A., Izumi, N., Kataoka, N., Morishita, R., Hoshino, S., Ohno, M., Dreyfuss, G., and Ohno, S. (2006). Binding of a novel SMG-1-Upf1-eRF1-eRF3 complex (SURF) to the exon junction complex triggers Upf1 phosphorylation and nonsense-mediated mRNA decay. Genes Dev. *20*, 355-367.

Kebaara, B.W., and Atkin, A.L. (2009). Long 3'-UTRs target wild-type mRNAs for nonsense-mediated mRNA decay in Saccharomyces cerevisiae. Nucleic Acids Res. *37*, 2771-2778.

Keeling, K.M., Xue, X., Gunn, G., and Bedwell, D.M. (2014). Therapeutics Based on Stop Codon Readthrough. Annu. Rev. Genomics Hum. Genet. *15*, 8.1-8.24.

Kertesz, S., Kerenyi, Z., Merai, Z., Bartos, I., Palfy, T., Barta, E., and Silhavy, D. (2006). Both introns and long 3'-UTRs operate as cis-acting elements to trigger nonsense-mediated decay in plants. Nucleic Acids Res. *34*, 6147-6157.

Kervestin, S., and Jacobson, A. (2012). NMD: a multifaceted response to premature translational termination. Nat. Rev. Mol. Cell. Biol. *13*, 700-712.

Kervestin, S., Li, C., Buckingham, R., and Jacobson, A. (2012). Testing the faux-UTR model for NMD: Analysis of Upf1p and Pab1p competition for binding to eRF3/Sup35p. In Biochimie, pp. 1560-1571.

Khoshnevis, S., Gross, T., Rotte, C., Baierlein, C., Ficner, R., and Krebber, H. (2010). The iron-sulphur protein RNase L inhibitor functions in translation termination. EMBO Rep. *11*, 214-219.

Kim, V.N., Kataoka, N., and Dreyfuss, G. (2001). Role of the nonsense-mediated decay factor hUpf3 in the splicing- dependent exon-exon junction complex. Science *293*, 1832-1836.

Kouba, T., Danyi, I., Gunisova, S., Munzarova, V., Vlckova, V., Cuchalova, L., Neueder, A., Milkereit, P., and Valasek, L.S. (2012). Small ribosomal protein RPS0 stimulates translation initiation by mediating 40S-binding of eIF3 via its direct contact with the eIF3a/TIF32 subunit. PloS one *7*, e40464.

Kurihara, Y., Matsui, A., Hanada, K., Kawashima, M., Ishida, J., Morosawa, T., Tanaka, M., Kaminuma, E., Mochizuki, Y., Matsushima, A.*, et al.* (2009). Genome-wide suppression of aberrant mRNA-like noncoding RNAs by NMD in Arabidopsis. Proceedings of the National Academy of Sciences of the United States of America *106*, 2453-2458.

Kurland, C.G. (1992). Translational accuracy and the fitness of bacteria. Annu. Rev. Genet. *26*, 29-50.

Kuroha, K., Tatematsu, T., and Inada, T. (2009). Upf1 stimulates degradation of the product derived from aberrant messenger RNA containing a specific nonsense mutation by the proteasome. EMBO Rep. *10*, 1265-1271.

Kurosaki, T., Li, W., Hoque, M., Popp, M.W., Ermolenko, D.N., Tian, B., and Maquat, L.E. (2014). A post-translational regulatory switch on UPF1 controls targeted mRNA degradation. Genes Dev *28*, 1900-1916.

Kurosaki, T., and Maquat, L.E. (2013). Rules that govern UPF1 binding to mRNA 3' UTRs. Proc. Natl. Acad. Sci. USA *110*, 3357-3362.

Lasalde, C., Rivera, A.V., Leon, A.J., Gonzalez-Feliciano, J.A., Estrella, L.A., Rodriguez-Cruz, E.N., Correa, M.E., Cajigas, I.J., Bracho, D.P., Vega, I.E.*, et al.* (2014). Identification and functional analysis of novel phosphorylation sites in the RNA surveillance protein Upf1. Nucleic Acids Res. *42*, 1916-1929.

Lawford, G.R. (1969). The effect of incubation with puromycin on the dissociation of rat liver ribosomes into active subunits. Biochem Biophys Res Commun *37*, 143-150.

Le Hir, H., Moore, M.J., and Maquat, L.E. (2000). Pre-mRNA splicing alters mRNP composition: evidence for stable association of proteins at exon-exon junctions. Genes Dev. *14*, 1098-1108.

LeBlanc, J.J., and Beemon, K.L. (2004). Unspliced Rous sarcoma virus genomic RNAs are translated and subjected to nonsense-mediated mRNA decay before packaging. J. Virol. *78*, 5139-5146.

Lee, B.S., and Culbertson, M.R. (1995). Identification of an additional gene required for eukaryotic nonsense mRNA turnover. Proc. Natl. Acad. Sci. USA *92*, 10354-10358.

Leeds, P., Peltz, S.W., Jacobson, A., and Culbertson, M.R. (1991). The product of the yeast *UPF1* gene is required for rapid turnover of mRNAs containing a premature translational termination codon. Genes Dev. *5*, 2303-2314.

Leeds, P., Wood, J.M., Lee, B.S., and Culbertson, M.R. (1992). Gene products that promote mRNA turnover in *Saccharomyces cerevisiae*. Mol. Cell. Biol. *12*, 2165-2177.

Lejeune, F., and Maquat, L.E. (2005). Mechanistic links between nonsense-mediated mRNA decay and pre-mRNA splicing in mammalian cells. Curr. Opin. Cell. Biol. *17*, 309-315.

Lelivelt, M.J., and Culbertson, M.R. (1999). Yeast Upf proteins required for RNA surveillance affect global expression of the yeast transcriptome. Mol. Cell. Biol. *19*, 6710-6719.

Linde, L., and Kerem, B. (2008). Introducing sense into nonsense in treatments of human genetic diseases. Trends Genet. *24*, 552-563.

Loh, B., Jonas, S., and Izaurralde, E. (2013). The SMG5-SMG7 heterodimer directly recruits the CCR4-NOT deadenylase complex to mRNAs containing nonsense codons via interaction with POP2. Genes & development *27*, 2125-2138.

Longman, D., Plasterk, R.H., Johnstone, I.L., and Caceres, J.F. (2007). Mechanistic insights and identification of two novel factors in the C. elegans NMD pathway. Genes Dev. *21*, 1075-1085.

Longtine, M.S., McKenzie, A., 3rd, Demarini, D.J., Shah, N.G., Wach, A., Brachat, A., Philippsen, P., and Pringle, J.R. (1998). Additional modules for versatile and economical PCR-based gene deletion and modification in Saccharomyces cerevisiae. Yeast *14*, 953-961.

Losson, R., and Lacroute, F. (1979). Interference of nonsense mutations with eukaryotic messenger RNA stability. Proc. Natl. Acad. Sci. USA *76*, 5134-5137.

Lou, C.H., Shao, A., Shum, E.Y., Espinoza, J.L., Huang, L., Karam, R., and Wilkinson, M.F. (2014). Posttranscriptional control of the stem cell and neurogenic programs by the nonsense-mediated RNA decay pathway. Cell Rep *6*, 748-764.

Lykke-Andersen, J., and Bennett, E.J. (2014). Protecting the proteome: Eukaryotic cotranslational quality control pathways. Journal of Cell Biology *204*, 467-476.

Lykke-Andersen, J., Shu, M.D., and Steitz, J.A. (2000). Human Upf proteins target an mRNA for nonsense-mediated decay when bound downstream of a termination codon. Cell *103*, 1121-1131.

Lykke-Andersen, J., Shu, M.D., and Steitz, J.A. (2001). Communication of the position of exon-exon junctions to the mRNA surveillance machinery by the protein RNPS1. Science *293*, 1836-1839.

Lykke-Andersen, S., Chen, Y., Ardal, B.R., Lilje, B., Waage, J., Sandelin, A., and Jensen, T.H. (2014). Human nonsense-mediated RNA decay initiates widely by endonucleolysis and targets snoRNA host genes. Genes Dev *28*, 2498-2517.

Ma, X.M., Yoon, S.O., Richardson, C.J., Julich, K., and Blenis, J. (2008). SKAR links pre-mRNA splicing to mTOR/S6K1-mediated enhanced translation efficiency of spliced mRNAs. Cell *133*, 303-313.

Maderazo, A.B., He, F., Mangus, D.A., and Jacobson, A. (2000). Upf1p control of nonsense mRNA translation is regulated by Nmd2p and Upf3p. Mol. Cell. Biol. *20*, 4591-4603.

Mangus, D.A., and Jacobson, A. (1999). Linking mRNA turnover and translation: assessing the polyribosomal association of mRNA decay factors and degradative intermediates. Methods *17*, 28-37.

Maquat, L.E., Kinniburgh, A.J., Rachmilewitz, E.A., and Ross, J. (1981). Unstable beta-globin mRNA in mRNA-deficient beta o thalassemia. Cell *27*, 543-553.

Matasova, N.B., Myltseva, S.V., Zenkova, M.A., Graifer, D.M., Vladimirov, S.N., and Karpova, G.G. (1991). Isolation of ribosomal subunits containing intact rRNA from human placenta: estimation of functional activity of 80S ribosomes. Anal Biochem *198*, 219-223.

McGlincy, N.J., and Smith, C.W. (2008). Alternative splicing resulting in nonsense-mediated mRNA decay: what is the meaning of nonsense? Trends Biochem. Sci. *33*, 385-393.

Meaux, S., van Hoof, A., and Baker, K.E. (2008). Nonsense-mediated mRNA decay in yeast does not require PAB1 or a poly(A) tail. Mol. Cell *29*, 134-140.

Medghalchi, S.M., Frischmeyer, P.A., Mendell, J.T., Kelly, A.G., Lawler, A.M., and Dietz, H.C. (2001). Rent1, a trans-effector of nonsense-mediated mRNA decay, is essential for mammalian embryonic viability. Hum. Mol. Genet. *10*, 99-105.

Melero, R., Buchwald, G., Castano, R., Raabe, M., Gil, D., Lazaro, M., Urlaub, H., Conti, E., and Llorca, O. (2012). The cryo-EM structure of the UPF-EJC complex shows UPF1 poised toward the RNA 3' end. Nat. Struct. Mol. Biol. *19*, 498-505, S491-492.

Mendell, J.T., Sharifi, N.A., Meyers, J.L., Martinez-Murillo, F., and Dietz, H.C. (2004). Nonsense surveillance regulates expression of diverse classes of mammalian transcripts and mutes genomic noise. Nature Genet. *36*, 1073-1078.

Metzstein, M.M., and Krasnow, M.A. (2006). Functions of the nonsense-mediated mRNA decay pathway in Drosophila development. PLoS Genet. *2*, e180.

Min, E.E., Roy, B., Amrani, N., He, F., and Jacobson, A. (2013). Yeast Upf1 CH domain interacts with Rps26 of the 40S ribosomal subunit. RNA *19*, 1105-1115.

Mort, M., Ivanov, D., Cooper, D.N., and Chuzhanova, N.A. (2008). A meta-analysis of nonsense mutations causing human genetic disease. Hum. Mutation *29*, 1037-1347.

Muhlrad, D., Decker, C.J., and Parker, R. (1994). Deadenylation of the unstable mRNA encoded by the yeast *MFA2* gene leads to decapping followed by 5'-->3' digestion of the transcript. Genes Dev. *8*, 855-866.

Muhlrad, D., and Parker, R. (1999a). Aberrant mRNAs with extended 3' UTRs are substrates for rapid degradation by mRNA surveillance. RNA *5*, 1299-1307.

Muhlrad, D., and Parker, R. (1999b). Recognition of yeast mRNAs as "nonsense containing" leads to both inhibition of mRNA translation and mRNA degradation: implications for the control of mRNA decapping. Mol. Biol. Cell. *10*, 3971-3978.

Nagy, E., and Maquat, L.E. (1998). A rule for termination-codon position within intron-containing genes: when nonsense affects RNA abundance. Trends Biochem. Sci. *23*, 198-199.

Nott, A., Le Hir, H., and Moore, M.J. (2004). Splicing enhances translation in mammalian cells: an additional function of the exon junction complex. Genes Dev. *18*, 210-222.

Nyiko, T., Sonkoly, B., Merai, Z., Benkovics, A.H., and Silhavy, D. (2009). Plant upstream ORFs can trigger nonsense-mediated mRNA decay in a size-dependent manner. Plant Mol. Biol. *71*, 367-378.

Ohnishi, T., Yamashita, A., Kashima, I., Schell, T., Anders, K.R., Grimson, A., Hachiya, T., Hentze, M.W., Anderson, P., and Ohno, S. (2003a). Phosphorylation of hUPF1 induces formation of mRNA surveillance complexes containing hSMG-5 and hSMG-7. Mol Cell *12*, 1187-1200.

Ohnishi, T., Yamashita, A., Kashima, I., Schell, T., Anders, K.R., Grimson, A., Hachiya, T., Hentze, M.W., Anderson, P., and Ohno, S. (2003b). Phosphorylation of hUPF1 induces formation of mRNA surveillance complexes containing hSMG-5 and hSMG-7. Mol. Cell *12*, 1187-1200.

Okada-Katsuhata, Y., Yamashita, A., Kutsuzawa, K., Izumi, N., Hirahara, F., and Ohno, S. (2012). N- and C-terminal Upf1 phosphorylations create binding platforms for SMG-6 and SMG-5:SMG-7 during NMD. Nucleic Acids Res. *40*, 1251-1266.

Page, M.F., Carr, B., Anders, K.R., Grimson, A., and Anderson, P. (1999). *SMG-2* is a phosphorylated protein required for mRNA surveillance in *Caenorhabditis elegans* and related to Upf1p of yeast. Mol. Cell. Biol. *19*, 5943-5951.

Paillusson, A., Hirschi, N., Vallan, C., Azzalin, C.M., and Muhlemann, O. (2005). A GFP-based reporter system to monitor nonsense-mediated mRNA decay. Nucleic Acids Res. *33*, e54.

Pal, M., Ishigaki, Y., Nagy, E., and Maquat, L.E. (2001). Evidence that phosphorylation of human Upf1 protein varies with intracellular location and is mediated by a wortmannin-sensitive and rapamycin-sensitive PI 3-kinase-related kinase signaling pathway. RNA *7*, 5-15.

Palacios, I.M., Gatfield, D., St Johnston, D., and Izaurralde, E. (2004). An eIF4AIII-containing complex required for mRNA localization and nonsense-mediated mRNA decay. Nature *427*, 753-757.

Parker, R., and Jacobson, A. (1990). Translation and a 42-nucleotide segment within the coding region of the mRNA encoded by the *MAT*a1 gene are involved in promoting rapid mRNA decay in yeast. Proc. Natl. Acad. Sci. USA *87*, 2780-2784.

Peixeiro, I., Inacio, A., Barbosa, C., Silva, A.L., Liebhaber, S.A., and Romao, L. (2012). Interaction of PABPC1 with the translation initiation complex is critical to the NMD resistance of AUG-proximal nonsense mutations. Nucleic Acids Res. *40*, 1160-1173.

Peltz, S.W., Brown, A.H., and Jacobson, A. (1993a). mRNA destabilization triggered by premature translational termination depends on at least three *cis*-acting sequence elements and one *trans*-acting factor. Genes Dev. *7*, 1737-1754.

Peltz, S.W., and Jacobson, A. (1993). mRNA Turnover in *Saccharomyces cerevisiae*. (NY: Academic Press).

Peltz, S.W., Morsy, M., Welch, E.M., and Jacobson, A. (2013). Ataluren as an agent for therapeutic nonsense suppression. Ann. Rev. Med. *64*, 407-425.

Peltz, S.W., Trotta, C., He, F., Brown, A., Donahue, J.L., Welch, E., and Jacobson, A. (1993b). Identification of the *cis*-acting sequences and *trans*-acting

factors involved in nonsense-mediated mRNA decay. In Protein Synthesis and Targetting in Yeast, J.M. M. Tuite, A., and F. Sherman, ed. (Springer-Verlag), pp. 1-10.

Pisarev, A.V., Hellen, C.U., and Pestova, T.V. (2007a). Recycling of eukaryotic posttermination ribosomal complexes. Cell *131*, 286-299.

Pisarev, A.V., Skabkin, M.A., Pisareva, V.P., Skabkina, O.V., Rakotondrafara, A.M., Hentze, M.W., Hellen, C.U., and Pestova, T.V. (2010). The role of ABCE1 in eukaryotic posttermination ribosomal recycling. Mol. Cell *37*, 196-210.

Pisarev, A.V., Unbehaun, A., Hellen, C.U., and Pestova, T.V. (2007b). Assembly and analysis of eukaryotic translation initiation complexes. Methods Enzymol *430*, 147-177.

Ponting, C.P. (2000). Novel eIF4G domain homologues linking mRNA translation with nonsense-mediated mRNA decay. Trends Biochem. Sci. *25*, 423-426.

Pulak, R., and Anderson, P. (1993). mRNA surveillance by the *Caenorhabditis elegans smg* genes. Genes Dev. *7*, 1885-1897.

Quek, B.L., and Beemon, K. (2014). Retroviral strategy to stabilize viral RNA. Curr Opin Microbiol *18*, 78-82.

Rajavel, K.S., and Neufeld, E.F. (2001). Nonsense-mediated decay of human HEXA mRNA. Mol. Cell. Biol. *21*, 5512-5519.

Ramani, A.K., Nelson, A.C., Kapranov, P., Bell, I., Gingeras, T.R., and Fraser, A.G. (2009). High resolution transcriptome maps for wild-type and nonsense-mediated decay-defective Caenorhabditis elegans. Genome Biol. *10*, R101.

Riehs-Kearnan, N., Gloggnitzer, J., Dekrout, B., Jonak, C., and Riha, K. (2012). Aberrant growth and lethality of Arabidopsis deficient in nonsense-mediated RNA decay factors is caused by autoimmune-like response. Nucleic acids research *40*, 5615-5624.

Sachs, A.B., and Davis, R.W. (1989). The poly(A) binding protein is required for poly(A) shortening and 60S ribosomal subunit-dependent translation initiation. Cell *58*, 857-867.

Salas-Marco, J., and Bedwell, D.M. (2004). GTP hydrolysis by eRF3 facilitates stop codon decoding during eukaryotic translation termination. Mol. Cell. Biol. *24*, 7769-7778.

Sauliere, J., Murigneux, V., Wang, Z., Marquenet, E., Barbosa, I., Le Tonqueze, O., Audic, Y., Paillard, L., Roest Crollius, H., and Le Hir, H. (2012). CLIP-seq of eIF4AIII reveals transcriptome-wide mapping of the human exon junction complex. Nat Struct Mol Biol *19*, 1124-1131.

Schmidt, S.A., Foley, P.L., Jeong, D.H., Rymarquis, L.A., Doyle, F., Tenenbaum, S.A., Belasco, J.G., and Green, P.J. (2014). Identification of SMG6 cleavage sites and a preferred RNA cleavage motif by global analysis of endogenous NMD targets in human cells. Nucleic acids research.

Schoenberg, D.R., and Maquat, L.E. (2012). Regulation of cytoplasmic mRNA decay. Nature Rev. Genet. *13*, 246-259.

Schwartz, A.M., Komarova, T.V., Skulachev, M.V., Zvereva, A.S., Dorokhov Iu, L., and Atabekov, J.G. (2006). Stability of plant mRNAs depends on the length of the 3'-untranslated region. Biochemistry. Biokhimiia *71*, 1377-1384.

Schweingruber, C., Rufener, S.C., Zund, D., Yamashita, A., and Muhlemann, O. (2013). Nonsense-mediated mRNA decay - mechanisms of substrate mRNA recognition and degradation in mammalian cells. Biochim. Biophys. Acta *1829*, 612-623.

Serin, G., Gersappe, A., Black, J.D., Aronoff, R., and Maquat, L.E. (2001). Identification and characterization of human orthologues to *Saccharomyces cerevisiae* Upf2 protein and Upf3 protein (*Caenorhabditis elegans SMG-4*). Mol. Cell. Biol. *21*, 209-223.

Sharifulin, D., Khairulina, Y., Ivanov, A., Meschaninova, M., Ven'yaminova, A., Graifer, D., and Karpova, G. (2012). A central fragment of ribosomal protein S26 containing the eukaryote-specific motif YxxPKxYxK is a key component of the ribosomal binding site of mRNA region 5' of the E site codon. Nucleic acids research *40*, 3056-3065.

Sheth, U., and Parker, R. (2006). Targeting of aberrant mRNAs to cytoplasmic processing bodies. Cell *125*, 1095-1109.

Shibuya, T., Tange, T.O., Sonenberg, N., and Moore, M.J. (2004). eIF4AIII binds spliced mRNA in the exon junction complex and is essential for nonsense-mediated decay. Nature Struct. Mol. Biol. *11*, 346-351.

Shigeoka, T., Kato, S., Kawaichi, M., and Ishida, Y. (2012). Evidence that the Upf1-related molecular motor scans the 3'-UTR to ensure mRNA integrity. Nucleic Acids Res. *40*, 6887-6897.

Shoemaker, C.J., and Green, R. (2012). Translation drives mRNA quality control. Nat Struct Mol Biol *19*, 594-601.

Singh, G., Kucukural, A., Cenik, C., Leszyk, J.D., Shaffer, S.A., Weng, Z., and Moore, M.J. (2012). The cellular EJC interactome reveals higher-order mRNP structure and an EJC-SR protein nexus. Cell *151*, 750-764.

Singh, G., Rebbapragada, I., and Lykke-Andersen, J. (2008). A competition between stimulators and antagonists of Upf complex recruitment governs human nonsense-mediated mRNA decay. PLoS Biol. *6*, e111.

Song, H., Mugnier, P., Das, A.K., Webb, H.M., Evans, D.R., Tuite, M.F., Hemmings, B.A., and Barford, D. (2000). The crystal structure of human eukaryotic release factor eRF1--mechanism of stop codon recognition and peptidyl-tRNA hydrolysis. Cell *100*, 311-321.

Spahn, C.M., Beckmann, R., Eswar, N., Penczek, P.A., Sali, A., Blobel, G., and Frank, J. (2001). Structure of the 80S ribosome from Saccharomyces cerevisiae--tRNA-ribosome and subunit-subunit interactions. Cell *107*, 373-386.

Stalder, L., and Muhlemann, O. (2008). The meaning of nonsense. Trends Cell Biol. *18*, 315-321.

Stalder, L., and Muhlemann, O. (2009). Processing bodies are not required for mammalian nonsense-mediated mRNA decay. RNA *15*, 1265-1273.

Sun, X., and Maquat, L.E. (2000). mRNA surveillance in mammalian cells: the relationship between introns and translation termination. RNA *6*, 1-8.

Takahashi, S., Araki, Y., Ohya, Y., Sakuno, T., Hoshino, S., Kontani, K., Nishina, H., and Katada, T. (2008). Upf1 potentially serves as a RING-related E3 ubiquitin ligase via its association with Upf3 in yeast. RNA *14*, 1950-1958.

Tani, H., Imamachi, N., Salam, K.A., Mizutani, R., Ijiri, K., Irie, T., Yada, T., Suzuki, Y., and Akimitsu, N. (2012). Identification of hundreds of novel UPF1 target transcripts by direct determination of whole transcriptome stability. RNA Biol *9*, 1370-1379.

Tani, H., Torimura, M., and Akimitsu, N. (2013). The RNA degradation pathway regulates the function of GAS5 a non-coding RNA in mammalian cells. PloS one *8*, e55684.

Unterholzner, L., and Izaurralde, E. (2004). SMG7 acts as a molecular link between mRNA surveillance and mRNA decay. Mol. Cell *16*, 587-596.

Valasek, L., Mathew, A.A., Shin, B.S., Nielsen, K.H., Szamecz, B., and Hinnebusch, A.G. (2003). The yeast eIF3 subunits TIF32/a, NIP1/c, and eIF5 make critical connections with the 40S ribosome in vivo. Genes Dev *17*, 786-799.

Vilela, C., Ramirez, C.V., Linz, B., Rodrigues-Pousada, C., and McCarthy, J.E. (1999). Post-termination ribosome interactions with the 5'-UTR modulate yeast mRNA stability. EMBO J. *18*, 3139-3152.

Wang, W., Cajigas, I.J., Peltz, S.W., Wilkinson, M.F., and Gonzalez, C.I. (2006). A role for Upf2p phosphorylation in *Saccharomyces cerevisiae* nonsense-mediated mRNA decay. Mol. Cell. Biol. *26*, 3390-4000.

Wang, W., Czaplinski, K., Rao, Y., and Peltz, S.W. (2001). The role of Upf proteins in modulating the translation read-through of nonsense-containing transcripts. EMBO J. *20*, 880-890.

Weischenfeldt, J., Damgaard, I., Bryder, D., Theilgaard-Monch, K., Thoren, L.A., Nielsen, F.C., Jacobsen, S.E., Nerlov, C., and Porse, B.T. (2008). NMD is essential for hematopoietic stem and progenitor cells and for eliminating by-products of programmed DNA rearrangements. Genes Dev. *22*, 1381-1396.

Weischenfeldt, J., Waage, J., Tian, G., Zhao, J., Damgaard, I., Jakobsen, J.S., Kristiansen, K., Krogh, A., Wang, J., and Porse, B.T. (2012). Mammalian tissues defective in nonsense-mediated mRNA decay display highly aberrant splicing patterns. Genome Biol *13*, R35.

Welch, E.M., Barton, E.R., Zhuo, J., Tomizawa, Y., Friesen, W.J., Trifillis, P., Paushkin, S., Patel, M., Trotta, C.R., Hwang, S.*, et al.* (2007). PTC124 targets genetic disorders caused by nonsense mutations. Nature *447*, 87-91.

Welch, E.M., and Jacobson, A. (1999). An internal open reading frame triggers nonsense-mediated decay of the yeast SPT10 mRNA. EMBO J. *18*, 6134-6145.

Weng, Y., Czaplinski, K., and Peltz, S.W. (1996). Genetic and biochemical characterization of mutations in the ATPase and helicase regions of the Upf1 protein. Mol. Cell. Biol. *16*, 5477-5490.

Weng, Y., Czaplinski, K., and Peltz, S.W. (1998). ATP is a cofactor of the Upf1 protein that modulates its translation termination and RNA binding activities. RNA *4*, 205-214.

Wittkopp, N., Huntzinger, E., Weiler, C., Sauliere, J., Schmidt, S., Sonawane, M., and Izaurralde, E. (2009). Nonsense-mediated mRNA decay effectors are essential for zebrafish embryonic development and survival. Mol. Cell. Biol. *29*, 3517-3528.

Wittmann, J., Hol, E.M., and Jack, H.M. (2006). hUPF2 silencing identifies physiologic substrates of mammalian nonsense-mediated mRNA decay. Mol. Cell. Biol. *26*, 1272-1287.

Yamashita, A. (2013). Role of SMG-1-mediated Upf1 phosphorylation in mammalian nonsense-mediated mRNA decay. Genes Cells *18*, 161-175.

Yamashita, A., Izumi, N., Kashima, I., Ohnishi, T., Saari, B., Katsuhata, Y., Muramatsu, R., Morita, T., Iwamatsu, A., Hachiya, T.*, et al.* (2009). SMG-8 and SMG-9, two novel subunits of the SMG-1 complex, regulate remodeling of the mRNA surveillance complex during nonsense-mediated mRNA decay. Genes Dev. *23*, 1091-1105.

Yamashita, A., Ohnishi, T., Kashima, I., Taya, Y., and Ohno, S. (2001). Human SMG-1, a novel phosphatidylinositol 3-kinase-related protein kinase, associates with components of the mRNA surveillance complex and is involved in the regulation of nonsense-mediated mRNA decay. Genes Dev. *15*, 2215-2228.

Yepiskoposyan, H., Aeschimann, F., Nilsson, D., Okoniewski, M., and Muhlemann, O. (2011). Autoregulation of the nonsense-mediated mRNA decay pathway in human cells. RNA *17*, 2108-2118.

Yoine, M., Nishii, T., and Nakamura, K. (2006). Arabidopsis UPF1 RNA helicase for nonsense-mediated mRNA decay is involved in seed size control and is essential for growth. Plant & cell physiology *47*, 572-580.

Yun, D.F., and Sherman, F. (1995). Initiation of translation can occur only in a restricted region of the CYC1 mRNA of *Saccharomyces cerevisiae*. Mol. Cell. Biol. *15*, 1021-1033.

Zaher, H.S., and Green, R. (2009). Fidelity at the molecular level: lessons from protein synthesis. Cell *136*, 746-762.

Zhang, J., Sun, X., Qian, Y., LaDuca, J.P., and Maquat, L.E. (1998). At least one intron is required for the nonsense-mediated decay of triosephosphate isomerase mRNA: a possible link between nuclear splicing and cytoplasmic translation. Mol. Cell. Biol. *18*, 5272-5283.

Zhang, S., Welch, E.M., Hogan, K., Brown, A.H., Peltz, S.W., and Jacobson, A. (1997). Polysome-associated mRNAs are substrates for the nonsense-mediated mRNA decay pathway in *Saccharomyces cerevisiae*. RNA *3*, 234-244.

Zund, D., Gruber, A.R., Zavolan, M., and Muhlemann, O. (2013). Translation-dependent displacement of UPF1 from coding sequences causes its enrichment in 3' UTRs. Nat. Struct. Mol. Biol. *20*, 936-943.

Zünd, D., Gruber, A.R., Zavolan, M., and Mühlemann, O. (2013). Translation-dependent displacement of UPF1 from coding sequences causes its enrichment in 3′ UTRs. Nat Struct Mol Biol *20*, 936-943.